UNDERSTANDING SOIL MOISTURE DYNAMICS USING OBSERVATIONS AND

CLIMATE MODELS

by

HAIBIN LI

A Dissertation submitted to the

Graduate School-New Brunswick

Rutgers, The State University of New Jersey

in partial fulfillment of the requirements

for the degree of

Doctor of Philosophy

Graduate Program in Environmental Sciences

written under the direction of

Professor Alan Robock

and approved by

_____

_____

_____

_____

New Brunswick, New Jersey

[May, 2007]

ABSTRACT OF THE DISSERTATION

UNDERSTANDING SOIL MOISTURE DYNAMICS USING OBSERVATIONS AND

CLIMATE MODELS

by HAIBIN LI

Dissertation Director:

Professor Alan Robock

With the objective to improve our understanding of soil moisture and its long term changes, I analyzed and compared climate model simulations with *in situ* soil moisture observations. Three studies were conducted to investigate soil moisture variations on seasonal to interannual scales and its long term changes.

To investigate soil moisture evolutions on seasonal to interannual scales and the capacity of reanalysis systems to capture the observed characteristics, I analyzed newly updated 19 yr of Chinese soil moisture data and evaluated ERA40, NCEP/NCAR reanalysis (R-1), and NCEP/DOE reanalysis 2 (R-2). Over this region, soil moisture seasonality is in general not strong. Seasonal cycles and interannual variations exhibit considerably spatial diversity. R-2 generally exhibits improved interannual variability and better seasonal patterns of soil moisture than R-1 as a result of incorporating observed precipitation. ERA40 produces a better mean value of soil moisture for most Chinese stations and good interannual variability. In terms of temporal scale – an

indicator of anomaly persistence, R-2 has a memory about twice that of the observations for the growing season. The unrealistic long temporal scale of R-2 can be attributed to the deep layer of the land surface model, which is too thick and dominates the soil moisture variability. The analysis highlights the importance of correct soil parameters to land surface processes and points out possible directions in which the reanalysis can be continuously improved to provide more realistic soil moisture outputs.

Observations from Ukraine and Russia show significant increases in summer for the period from 1958-1999 that seem contradictory to the classic summer drying issue from early modeling studies. To see whether the latest climate models can capture the observed patterns, I calculated trends in soil moisture simulations from Intergovernmental Panel on Climate Change Fourth Assessment climate models. The upward trends in observations, which cannot be explained by precipitation and temperature changes alone, were found to be much larger than most trends in model realizations. Solar dimming is proposed to have played an important role in modulating soil moisture variations for these two regions.

Further, a series off-line sensitivity experiments with a sophisticated land surface model were conducted to investigate possible contribution from solar dimming and elevated CO_2 to the observed soil moisture trends for Ukraine and Russia. I demonstrate, by imposing a downward trend to shortwave radiation forcing to mimic the dimming, the observed soil moisture pattern can be essentially reproduced. On the other hand, the effects of elevated CO_2 are relatively small for the study period. The results support the hypothesis that solar dimming may have played an important role in regional soil moisture changes.

ACKNOWLEDGMENTS

First and foremost I want to express my deepest gratitude to my advisor and friend, Dr. Alan Robock, for the source of knowledge, guidance, and support that he has been to me through my graduate career. Otherwise, my graduate study here at Rutgers would not have been possible. His encouragement of my work and commitment to whatever projects we undertook was inspiring, and has made the time at Rutgers really enjoyable and fruitful. His influences on me not only to be a successful scientist but also to be a great man will be life-long. I could not have had a better advisor and colleague.

Sincere appreciation is due to Dr. Christopher Milly, Prof. Anthony Broccoli and Prof. Ying Fan Reinfelder for taking the time to serve on my dissertation committee and also for numerous conversations and e-mail communications we had which enlarged my sphere of understanding of the climate system in general and the hydrological cycle in particular.

I thank Dr. Konstantin Y. Vinnikov, Dr. Jared Entin and Dr. Mingquan Mu for their assistance on using the optimal averaging technique and clarifying soil moisture observation related issues. I also thank Prof. Daniel Giménez for the great course, soil physics – my first course in this subject, from which I benefited a lot and which made my dissertation work is much easier. Thanks to Prof. Ignacio Rodriguez-Iturbe for the inspiring course "eco-hydrology" and to Prof. Ming Xu for all the wonderful discussions about plant physiology that helped me to form a clearer picture of vegetation dynamics. My appreciation also goes to faculty members Dr. Georgiy Stenchikov, Dr. Dana Veron, and Dr. Christopher Weaver, in the atmospheric sciences option. Your expertise and passion make a climate layman like me dare to commit to climate studies.

iv

helps improve my oral English. I feel in debt to my fishes that bring me peace and energy during my late-night work.

Finally but most importantly, I thank my family- my wife, my parents, and my sisters, for their unconditional support and love during my course of pursuing degree in a foreign country. It is your confidence, support, patience that carry me through.

DEDICATION

To my wife, Juan

To my parents and sisters, Yingxi, Suqiong, Junying, Junyong, and Yi

TABLE OF CONTENTS

LIST OF TABLES

LIST OF FIGURES

1 Introduction

This dissertation consists of three separate studies with central objectives to improve our understanding of soil moisture climatology and its long term changes by using the newly updated *in situ* observations from the Global Soil Moisture Data Bank (GSMDB) and climate modeling results. Specifically it is intended to address the following scientific questions: 1) How does soil moisture vary on seasonal to interannual scales? 2) How has soil moisture changed for the past several decades? and 3) What are the likely reasons for such changes?

1.1 Literature Review

Soil moisture is usually defined as the water content in the soil above the water table. Its importance has long been recognized in the field of agriculture, water resources management, hydrology, and soil science. Monitoring of soil moisture, especially the occurrence of hydrologic drought (soil moisture deficiency) and flooding (soil moisture excess), is crucial for successful agriculture practices and water resources management. Variations of soil moisture modulate the water balance by affecting partition of precipitation falling on the surface into infiltration and runoff. Bioavailability of organic matters in soil, largely controlled by soil water content, is an important indicator for pest detection and control for soil microbiologists.

In the climate context, soil moisture is involved in both mass transport and energy transport. In addition to serving as source by providing moisture to the atmosphere and sink by storing precipitation from the atmosphere, soil wetness is also responsible for the partitioning of incoming radiation into sensible and latent heat. The Bowen ratio (the

ratio of sensible heat to latent heat) is generally smaller for wet surface in contrast with dry surface where more energy is released via latent heat that cools the surface. Latent heat release accounts for about half of the surface cooling that balances the heating by absorption of solar radiation [*Hartmann*, 1994]. The role of soil moisture has been recognized in climate communities, mainly due to its long meteorological memory, active role in land-atmosphere interaction and contribution to atmospheric predictability.

Meteorological memory of soil moisture

Over the ocean, the tropical atmosphere large-scale circulation and rainfall are mainly determined by the boundary conditions of sea surface temperatures and it is possible to predict large-scale circulation and rainfall over tropics provided ocean temperature can be predicted over this region [*Shukla*, 1998]. Over the continents, soil moisture is the most important component of meteorological memory, along with snow cover [*Delworth and Manabe* 1988, 1993]. Especially in the extratropics, with relative large seasonal changes, soil moisture plays a role analogous to that of the ocean [*Shukla and Mintz*, 1982]. *Delworth and Manabe* [1988] proposed that soil moisture variations in time be approximated as a first-order Markov process from an analysis of GFDL AGCM outputs. *Vinnikov et al*. [1996, 1999a, 1999b] and *Entin et al*. [2000] validated this idea by investigating soil moisture observations collected from about two hundred ground-based stations in the extratropics. They found the temporal scale of soil moisture associated with atmospheric forcing was about 1-3 months. Such memory is estimated to be much longer for drier conditions than moist environments with sufficient rainfall in warm climates [*Wu and Dickinson*, 2004]. *Eltahir* [1998] proposed that this memory be provided by the land surface through a positive feedback between soil moisture and

rainfall. Using a standard water balance method, *Koster and Suarez* [2001] further characterized that soil moisture memory in an AGCM was controlled by four distinct factors: (i) seasonality in the atmospheric forcing, such as precipitation and net radiation; (ii) the effect of evapotranspiration on reducing soil moisture persistence (memory); (iii) the analogous dependence of runoff; and (iv) correlation between initial soil moisture and the subsequent atmospheric forcing. It is expected such memory has profound implications for weather prediction that will be discussed next.

Soil moisture and atmosphere predictability

In spite of the chaotic property of our climate system [*Lorenz* 1963, 1993], climate predictability, as pointed out by Lorenz, is still possible if based on forcing by slowly changing boundary conditions (climate predictability of the second kind). As atmospheric anomalies dissipate quickly, seasonal prediction of meteorological conditions has to rely on the response of atmosphere to those components of the earth system that can be predicted months in advance [*Koster et al.*, 2000a] such as sea surface temperature (SST) and continental water storage [*Betts and Ball*, 1996]. Knowledge of slowly varying SSTs has been demonstrated capable of improving atmospheric predictions [e.g., *Lau and Nath* 1990; *Stern and Miyakoda* 1995]. Similarly, soil moisture might be a source of forecast skill for summer precipitation over midlatitude continents [*Koster et al.*, 2000a]. *Dirmeyer* [2000] found that the simulation of boreal summer precipitation and near-surface air temperature was improved with specified soil moisture boundary condition (the soil moisture in their experiment was from the Global Soil Wetness Project which was thought to be realistic in many ways). Analyzing a dozen of AGCM boreal summer simulations in the Global Land-Atmosphere Coupling

Experiment (GLACE), *Koster et al.* [2004] found that such predictability was particularly high in transition zones between dry and humid climates where soil moisture anomalies have a substantial impact on precipitation.

Land-atmosphere interaction

As the basic elements between land and atmosphere interaction, fluxes of moisture and heat (energy) from the land surface determine the overlying atmospheric conditions, such as temperature, water vapor, precipitation, cloud properties, and hence the downward radiative fluxes at the surface [*Dickinson*, 1995]. The two-way land-atmosphere interaction takes place at rather broad scales. The turbulent heat fluxes near the ground surface, closely related to planetary boundary layer (PBL) development, are strongly affected by the ability of the surface to partition net incoming radiation into sensible and latent heat [*Avissar*, 1995], which is largely dependent on moisture availability for evapotranspiration. Therefore, soil moisture plays an important role in boundary layer development [*Betts et al.*, 1993, 1994; *Li and Avissar*, 1994; *Lynn et al.*, 1995; *Quinn et al.*, 1995]. Surface heterogeneity creates favorable conditions for the development of mesoscale circulations [e.g., *McCumber and Pielke*, 1981; *Avissar and Pielke*, 1989; *Pielke et al.*, 1991; *Lynn et al.*, 1995; *Pielke*, 2001]. *Pielke et al.* [1991] demonstrated that mesoscale fluxes of heat generating from surface heterogeneity were of the same order of magnitude found for the turbulent fluxes. Large-scale atmospheric circulation model simulations indicate that changes of land-surface characteristics, for example soil parameterizations, can affect evapotranspiration, surface albedo, and convective instability [e.g., *Milly and Dunne*, 1994; *Milly*, 1997; *Koster et al.*, 2000b; *Ducharne et al.*, 2000]. *Milly* [1997] demonstrated that a 14% decrease of plant-available

water holding capacity in a bucket model was equivalent to summer dryness induced by doubling of atmospheric carbon dioxide.

Since the first land surface model [the bucket model, *Manabe* 1969] with only three prognostic variables (soil moisture, snow mass and surface temperature) and uniform prescriptions of surface parameters, there are a lot of developments in land models for the past decades. Representations of leaves, root distributions, soil types, especially stomatal conductance have been incorporated in schemes developed in 1980s, such as the Simple Biosphere Model (SiB) [*Sellers et al.*, 1986] and Biosphere-Atmosphere Transfer Scheme (BATS) [*Dickinson et al.*, 1986]. *Avissar and Pielke* [1989] advanced the mosaic approach to address the issue of parameterizations of heterogeneous surface. In comparison with the big leaf approach in earlier models, the mosaic approach approximates land heterogeneity with a mosaic of patches, each patch consisting of a single land use [*Avissar and Pielke*, 1989]. A similar approach has been implemented in GCMs [e.g., *Koster and Suarez*, 1992]. Models developed later [e.g., *Bonan et al.*, 1995; *Sellers et al.*, 1996a] incorporate the physiological effects of plants by relating photosynthesis and plant water relations. All in all, descriptions of land surface processes, including hydrology, soil respiration, and ecological responses to climate change, are becoming more realistic [*Sellers et al.*, 1997].

On the other hand, although the physical principles are essentially the same, a variety of ways exists to parameterize the land surface conditions, which may cause significant disparities in the simulated land surface climate. *Koster and Suarez* [1994] showed that the treatment of land in climate models had significant impacts on the model climate. *Robock et al.* [1995] demonstrated that the energy partitioning in a bucket model

and the Simplified SiB (SSiB) can be quite different even forced by the same observations. Such differences in energy partitioning would have large effects on simulations when coupled to GCM since two-way feedbacks between land and atmosphere do not dampen land-surface climate differences [*Irannejad et al.*, 1995]. Several international cooperated research projects have been developed to address and understand model differences. One of the excellent examples is the project for Intercomparison of Land-Surface Parameterization Schemes (PILPS) [*Henderson-Sellers et al.*, 1995a] initialized in early 1990s. PILPS aims to understand surface and near-surface processes through intercomparisons of land surface schemes (LSSs) either forced by model outputs [Phase 1: *Pitman et al.*, 1993, 1998; *Koster and Milly*, 1997] or by actual observations from different climates [Phase 2: *Henderson-Sellers et al.*, 1995a, 1996; *Chen et al.*, 1997; *Qu et al.*, 1998; *Luo et al.*, 2003a]. *Pitman and Henderson-Sellers* [1998] summarized that considerable model differences existed in the partitioning of available energy and partitioning of precipitation in phase 1 and phase 2. Similar results were found in the first phase of Atmospheric Model Intercomparison Project [AMIP 1: *Gates* 1992; *Irannejad et al.*, 1995; *Love et al.*, 1995; *Qu and Henderson-Sellers*, 1998], the Diagnostic Subproject 12 (DSP12) of PILPS. *Robock et al.* [1998] evaluated the soil moisture simulations in AMIP 1 with observations from Illinois and Former Soviet Union. They found that observed interannual variations of soil moisture were not captured by any single model and the winter soil moisture variations in high latitudes were not simulated well. *Srinivasan et al.* [2000] later analyzed revisit simulations contributed by six of the AMIP 1 participating model groups. They found that there was no systematic improvement in the revised models. In the current AMIP

[Phase 2: *Henderson-Sellers et al*., 2003], the simulation period has been extended by 7 years (from 1979–1988 to 1979–1995). This may help resolve the spin-up problem in some participating models.

Based on the review presented above, before drawing any conclusion about how soil moisture varies in the current/past climate and may change in future, we should first have a clear picture about how good model simulated soil moisture is and try to understand why models fail at some aspects, preferably compared with available observations.

Over the past several years, there are several important updates to the existing soil moisture data sets archived at GSMDB, the Chinese soil moisture (1981-1999), the Ukrainian soil moisture (1958-2004), the Mongolian data (1970-2002), the Illinois measurements (1981-2004), and data for Western Russia (1958-1999). These observations, though still limited in space and time, are invaluable for climate model evaluations and understanding of soil moisture variations at seasonal and longer scales, which is the central theme of my dissertation.

1.2 Summary of dissertation work

To attempt to partially answer the scientific questions posed at the beginning of this chapter, I conducted the following studies. I collected, quality controlled, and provided the scientific community with new soil moisture data sets. I evaluated current model simulations of soil moisture. And I improved a state-of-the-art land surface model and used it to evaluate soil moisture trends using the longest available soil moisture records.

By using newly updated 19 yr Chinese soil moisture observations, the first study evaluates soil moisture simulations from three reanalyses, namely the European Centre for Medium Range Weather Forecasting (ECMWF) 40-year reanalysis [ERA40, *Simmons and Gibson*, 2000], the National Centers for Environmental Prediction/National Center for Atmospheric Research (NCEP/NCAR) [Reanalysis 1 (R-1), *Kalnay et al.*, 1996, *Kistler et al.*, 2001], and the follow-up NCEP/Department of Energy [Reanalysis 2 (R-2), *Kanamitsu et al.*, 2002]. Specifically, I evaluate the model simulated soil moisture with respect to seasonal cycles, interannual variations and soil moisture memories at point scale. The motivation for this study comes from the contradictory facts that no operational reanalysis systems actually assimilate soil moisture but reanalysis soil moisture probably is the most widely used product for model initialization or even for model evaluation. Unfortunately, there are very limited studies devoted to identifying the potential deficiencies in reanalysis soil moisture. Subsection 2 presents the updated Chinese soil moisture for 1981-1999. Subsection 3 discusses land surface schemes used in reanalyses and the nudging techniques employed. In subsection 4, the soil moisture reanalysis is evaluated in terms of the seasonal cycle, interannual variability and temporal scale. First, how reanalysis soil moisture is rescaled to be comparable with observations is given, followed by detailed analysis. Discussions and conclusions are presented in subsection 5.

The second study is a voluntary diagnostic project intended for IPCC AR4. The model analysis activity is organized by Joint Scientific Committee /Climate Variability and Predictability (JSC/CLIVAR) Working Group on Coupled Modeling and their Coupled Model Intercomparison Project and Climate Simulation Panel. Having

recognized that no soil moisture evaluation works have been done for the previous three IPCC reports, this study is intended to provide quantitative evidences about the quality of IPCC model simulated soil moisture. Soil moisture simulations from a number of state-of-the-art climate models are evaluated by using *in situ* soil moisture measurements collected from over 140 stations or districts in mid-latitudes of the Northern Hemisphere, with respect to seasonal cycles, interannual variations and the long term soil moisture changes in summer. Subsection 2 describes the data sets used in this study, detailing the criteria for observations and model output selection, and the preprocessing techniques used to rescale observations and model output so that they are comparable. Subsection 3 presents the evaluation results for seasonal cycles and interannual variability. Seasonal trends and validation of summer drying issue are presented in subsection 4. A summary is followed in subsection 5.

The third study, a follow-up study for the second one, tests the hypothesis in the second study that solar dimming may have important contribution to soil moisture changes for Ukraine and Russia. Additionally, I investigate possible contributions from carbon fertilization effects. To understand the contributions from solar dimming and carbon fertilizations, I conduct a series offline sensitivity experiments with a sophisticated land surface model, and validate the idea by comparing the model simulations to observed soil moisture. Subsection 2 presents the experimental design, including the model developments for hydrology module and soil moisture control on photosynthesis. Subsection 3 describes the forcing data. Modeling results and analysis is presented in subsection 4. Subsection 5 gives a short discussion.

1.3 My contribution to the work

All these studies utilized soil moisture observations from the GSMDB and showed how these observations could be used to help us understand climate changes and identify model deficiencies. The first study is part of my work related to Chinese soil moisture. After updating the old Chinese soil moisture in our data bank to 19 yr homogenous data sets for 40 stations, I was looking for a research topic about how to use the data. Dr. Alan Robock, who previously evaluated ERA15, suggested I take a look at soil moisture in ERA40 and other reanalysis products to see whether I can find some interesting topics. I found the temporal scale, a very important soil moisture property, was not addressed yet for reanalysis soil moisture. So I added this aspect into my work in addition to addressing the seasonal cycles and interannual variations. My contribution to this work is to identify target reanalyses, collect soil moisture outputs, specify scientific questions and do the analysis. Dr. Pedro Viterbo provided the finer resolution ERA40 soil moisture after I identified several problems with the coarse resolution soil moisture close to the coast areas. During this study, I had numerous communications with reanalysis experts to understand the existing reanalysis problems and discussed our findings with them. The paper based on this work was published by *Journal of Hydrometeorology*.

As finishing the first study, Dr. Alan Robock noticed an advertisement in EOS soliciting voluntary diagnostic projects to analyze state-of-the-art climate model simulations for the forthcoming IPCC AR4, and recommended that it be a potential topic for another study. I also realized there was no soil moisture related evaluation work at all in previous three IPCC reports. I felt it was my responsibility as a climatologist to test

how these state-of-the-art models can reproduce the past soil moisture climate now that we have the observations in hand. Around that time, I just updated the Ukrainian soil moisture through 2004 and identified 42 yr Russian soil moisture (1958-1999) sitting in our data bank. These data sets can then be used to investigate whether summer drying really occurs in observations and in models on decadal-scale. My responsibility for this study is to collect model simulated soil moisture and other related variables (precipitation, temperature, radiation), and then to compare the model outputs with quality-controlled observations. During this project, I identified several obvious errors related to postprocessing and informed the model developers so that they could send the reprocessed correct data to PCMDI which is responsible for the data distribution and maintenance. Based on the analysis and previous work by others, Dr. Alan Robock and I proposed solar dimming may have important contribution to regional soil moisture changes for the past decades. The resulted work was accepted for publishing by *Journal of Geophysical Research – Atmospheres*.

The third study was inspired by a comment of Dr. Alan Robock for our IPCC draft paper, saying we may use an offline approach to further test the dimming hypothesis proposed in the second study. I extended the idea to include the physiological effects of CO_2 by selecting the Community Land Model (CLM3.0) that couples the stomatal-photosynthesis modules. My responsibility is to locate a good model, find reliable atmospheric forcing data sets, design the experiments, and conduct the data analysis. To ensure the quality of the forcing data we will use, I compared several forcings from different modeling groups to the observed quantities. I also reprocessed the forcings (over 50 GB in size) so that they can be used for limited-domain simulations. After

finding several problems related to model hydrology, I incorporated hydrology module improvements to CLM with the help of Dr. Gui-yue Niu who happened to work on the improvement of hydrology module with an old version of CLM (CLM2.0). I further modified the soil moisture control on photosynthesis according to several recent studies. Over 30,000 data files and 160 GB model outputs were produced as the experiments were continuously improved and modified. Prof. Robock and I summarized our findings in a journal article that was published by *Geophysical Research Letters*.

2 Evaluation of Reanalysis Soil Moisture Simulations Using Updated Chinese Soil Moisture Observations

2.1 Introduction

Our climate system is chaotic, such that a small perturbation in initial conditions may produce dramatically different weather patterns after a finite amount of time [*Lorenz* 1963, 1993], and this property of the climate system makes a precise weather forecast beyond a few weeks nearly impossible. However, as pointed out by Lorenz, climate predictability is possible if based on forcing by slowly changing boundary conditions (climate predictability of the second kind). Over the ocean, the tropical atmosphere large-scale circulation and rainfall are mainly determined by the boundary conditions of sea surface temperatures and it is possible to predict large-scale circulation and rainfall over tropics provided ocean temperature can be predicted over this region [*Shukla* 1998]. Over the continents, soil moisture is the most important component of meteorological memory, along with snow cover [*Delworth and Manabe* 1988, 1993]. Especially in the extratropics, with its large seasonal changes, the soil plays a role analogous to that of the ocean [*Shukla and Mintz*, 1982]. This idea has been validated by various studies. For example, *Durre et al.* [2000] found a memory of past precipitation existing in the interior of continents at least during summers. *Eltahir* [1998] proposed that this memory is provided by the land surface through a positive feedback between soil moisture and rainfall. GCM simulations also indicate soil moisture contributes to precipitation predictability [*Dirmeyer*, 2000], especially in transition zones between dry and humid climates [*Koster et al.*, 2000, *Koster et al.*, 2004].

Since soil moisture observations are limited both in time and space, model produced soil moisture often serves as an alternative in research work [*Robock et al.*, 2000]. Reanalyses are the most widely used substitutes, as they have the advantages of global coverage and long time series. Three most widely-known soil moisture reanalysis come from the European Centre for Medium Range Weather Forecasting (ECMWF) 40-year reanalysis [ERA40, *Simmons and Gibson*, 2000] and the National Centers for Environmental Prediction/National Center for Atmospheric Research (NCEP/NCAR) [Reanalysis 1 (R-1), *Kalnay et al.*, 1996; *Kistler et al.*, 2001] and the follow-up NCEP/Department of Energy [Reanalysis 2 (R-2), *Kanamitsu et al.*, 2002]. These reanalysis products are widely used in model initializations and climatology research. However evaluations with *in situ* observations or model intercomparisons are indispensable for a better understanding of parameterization systems and improving reanalyses. *Roads et al.* [1999] compared surface water terms in R-1 to the NCEP global spectral model, and they found the variability of surface water in R-1 is less than that in the global spectral model, mainly due to the nudging term. *Maurer et al.* [2001] evaluated the surface water characteristics in R-1 and R-2 with model simulated surface fluxes, and they reported that evapotranspiration in R-2 shows less biases than R-1. However, these works are not based on observed fluxes. Recently, *Dirmeyer et al.* [2004] compared ERA40, R-1 and R-2 along with other 5 soil moisture products with observed soil moisture. They concluded that no single product was obviously superior in all climates, and that the mean annual cycle is generally better simulated than interannual variations.

In this study, we take advantage of newly updated soil moisture observations from China to evaluate the soil moisture simulations from ERA40, R-1 and R-2. In subsection 2, we describe our updated Chinese soil moisture, which is followed by a short review of soil moisture reanalysis products in subsection 3. In subsection 4, the soil moisture reanalysis is evaluated in terms of the seasonal cycle, interannual variability and temporal scale. Subsection 5 presents discussion and conclusions.

2.2 Updated Chinese Soil Moisture for 1981-1999

The Global Soil Moisture Data Bank archived a Chinese soil moisture data set for 43 stations for 1981-1991 [*Robock et al.*, 2000]. These data sets have been extensively used to investigate the scales of soil moisture variations [e.g., *Entin et al.*, 2000; *Liu et al.*, 2001] or for land surface model evaluation and have proved to be very helpful for model improvements [e.g., *Entin et al.*, 1999]. Recently we updated the Chinese soil moisture observations through 1999. Figure 2.1 shows the distributions of the stations, which are listed in Table 2.1. Soil moisture in China was measured 3 times each month on the 8th, 18th and 28th at 11 vertical layers – 5-cm layers from 0 cm down to 10 cm and 10-cm layers from 10 cm down to 1 m. The soil moisture is originally recorded as mass percentage by the gravimetric technique, and this has two major advantages: no auxiliary calibration is necessary and relatively small errors. The soil moisture then is converted to volumetric soil moisture:

$$\theta_v = \theta_m \frac{\rho_b}{\rho_w}$$

(2.1)

where ρ_b is the bulk density of soil, ρ_w is the density of water, θ_m is the mass percent of measured soil moisture and θ_v is volumetric soil moisture. For evaluation purposes,

volumetric soil moisture usually is converted to total soil water by multiplying by the corresponding layer thickness or plant available soil moisture by subtracting the wilting level from the total. Figure 2.2 gives a sample plot of total soil moisture for the top 10 cm, 50 cm and 1 m layers for station 9 (a northern station) and station 15 (a western station). Station 9 shows greater interannual variations than station 15 under the control of a different climate and both stations have a homogenous record over the 19 years.

We did quality control for the data sets in terms of the homogeneity and measuring frequency (the ratio of available observations to the entire period). The resulting 40 homogeneous stations are unevenly distributed and most of the stations are located in Northern or Central China, mainly in Yellow River basin and Song-Liao River basin (Figure 2.1). There are only three stations in less populated Western China and two stations in Southern China.

We also calculated the measuring frequency for the period from May to October, which generally covers the growing season, and we classified it into three categories: more than 80% of the time, between 60% and 80%, and less than 60%. There are 9 stations with measuring frequencies of more than 80% (Figure 2.1). Generally fewer measurements are available for Northern China due to the comparatively long frozen seasons when soil moisture is hard to measure. As for the top 10 cm, 28 out of 40 stations have a measuring frequency over 85%, which highlights the potential for remote sensing evaluations.

2.3 Soil moisture and nudging in reanalysis

Bengtsson and Shukla [1988] and *Trenberth and Olson* [1988] were pioneers who proposed the idea of reanalysis. Since then, several reanalysis projects have been

conducted and three of the most well known global reanalyses are ERA40, R-1 and R-2. Recognizing the importance of soil moisture, these reanalyses archived model-calculated soil moisture at grid points. ERA40 produced soil moisture starting in 1957, and provided the values at a horizontal resolution of T159 (about 125 km) with global coverage. R-1 has soil moisture back to 1950 at a horizontal resolution of T62 (about 210 km) and recently R-2, an updated version of R-1, became available with the major advantages of reduced human errors and improved soil wetness [*Kanamitsu et al.*, 2002], but it only started in 1979.

The soil moisture calculated by reanalyses depends on the land surface scheme used, the forcing (particularly precipitation and solar insolation), and the nudging employed. In terms of land surface, ERA40 uses a scheme called TESSEL [Tiled ECMWF Scheme for Surface Exchanges over Land, *Van Der Hurk et al.*, 2000]. The scheme has 4 prognostic layers for temperature and soil moisture with layer thicknesses of 7 cm, 21 cm, 72 cm and 189 cm going down from the top. There are some basic differences from the old scheme [*Viterbo and Beljaars* 1995, VB95] employed in ERA15, especially the treatment of snow and vegetation, an added prognostic snow layer on top of the soil, and reduced infiltration over frozen soils. Offline validation showed cold season processes are more realistic in TESSEL than in VB95. The uniform vegetation over land in VB95 was replaced by a 20-type vegetation map, with land surface parameters, such as root distribution and leaf area index, varying according to vegetation type. *Van Der Hurk et al.* [2000] pointed out that "model performance becomes increasingly dependent on a proper choice of vegetation dependent model parameters."

R-1 and R-2 used the OSU LSM [*Pan and Mahrt*, 1987; *Pan* 1990] with two layer thicknesses of 10 cm and 190 cm separately. It was designed to model the essential characteristics of the land interactions with the atmosphere primarily for partitioning of net radiation into latent and sensible heat [*Mahrt and Pan* 1984]. Vegetation types were from Simple Biosphere model (SiB) climatology [*Dorman and Sellers* 1989], while many parameters like soil properties (type, wilting point, critical point and porosity) and vegetation canopy cover were fixed globally.

Because model-generated precipitation and insolation are not perfect in reanalyses, soil moisture tends to drift to a too dry or too wet state. To prevent this, the soil moisture is nudged based on different criteria. For ERA40, soil moisture increments were provided by a linear combination of the screen level relative humidity and temperature increments each 6 hr [*Douville et al.*, 2000; *Mahfouf et al.*, 2000]. This nudging technique is more reliable than the old nudging scheme in ERA15, which only assimilated specific humidity [*Douville et al.*, 2000].

In R-1, soil moisture was nudged to the *Mintz and Serafini* [1992] climatology with a 60-day time scale. This nudging term is quite large [*Maurer et al.*, 2001] so interannual variations are suppressed [*Srinivasan et al.*, 2000; *Kistler et al.*, 2001]. Another concurrent problem is the nonclosure of the water budget. In R-2, soil moisture is constrained more elegantly in that the difference between model precipitation and observed pentad (5-day) precipitation is used to correct soil moisture [*Kanamitsu et al.*, 2002]. This provides an opportunity for us to detect possible model deficiencies previously obscured by the strong nudging in R-1.

2.4 Comparison of soil moisture observations with reanalyses

Srinivasan et al. [2000] used soil moisture observations for Illinois [*Hollinger and Isard* 1994] and central China [*Robock et al.*, 2000] for 1981-1988 to evaluate R-1 and an earlier version of the ECMWF reanalysis [ERA-15, *Gibson et al.*, 1997]. They found that the reanalyses were able to capture some of the observed seasonal cycles, and the interannual variations in Illinois, but that the variations were damped out by the soil moisture nudging. *Kanamitsu et al.* [2002] compared R-2 to Illinois soil moisture, and found a better agreement than for R-1, in terms of mean, amplitude of seasonal cycle, and interannual variations. They cautioned about using R-2 for the first several years of the reanalysis due to spinup problems and because of problematic pentad precipitation (missing data were mistakenly reported as zero in the earlier period). We address the spinup issue later, showing that this anomalously long spinup period for R-2 is due to the too large moisture reservoir in the land surface model. This was also found by *Robock et al.* [1998] in some of the Atmospheric Modeling Intercomparison Project climate models based on the simplified simple biosphere model [*Xue et al.*, 1991]. *Xue et al.* [1996] and *Robock et al.* [1997] have shown that this long time scale is due to the slow exchange of soil moisture between the deep third layer and the upper 2 layers in these models.

To take full advantage of our long time records, we compared the reanalyses to 10 stations with relatively high measuring frequency (Figure 2.1), one station from Western China, four from Northern China and the other five from Central China. We used the values from the 28th of each month from each station and the corresponding daily value from the model grid point nearest the station. We used the original reduced Gaussian

grid output from ERA40 to correct for ocean influences in the lower-resolution gridded data publicly available.

Missing data in observations is one of the major concerns when performing data analysis. Interpolation techniques can be used to fill data gaps but may introduce errors, which would make the quality of the analysis questionable. Thus we have not adjusted the missing data in the observations to avoid introducing artificial relationships. When we compare to reanalyses, we only use model output from the reanalyses for times when observations exist, and treat the other reanalysis output as missing, unless otherwise explicitly specified.

Since the land surface scheme in R-1 and R-2 only has two soil layers (0-10 cm and 10-200 cm), we used the following equation to scale the soil moisture to the top 1 m for R-1 and R-2 to compare with observations and ERA40,

$$W = 100 \, (0.10 \times \theta_1 + 0.90 \times \theta_2) \tag{2.2}$$

where W represents the soil moisture (cm) in the top 1 m and θ_i is the fractional volumetric soil moisture for layer i. The fraction of each layer accounting for the contribution to the top 1 m was used as the weighing factor. Although other methods, such as extracting the unavailable soil moisture or simply summing up the soil moisture in the top 2 m and dividing by 2 would result in different amounts of soil moisture, they would tend to only shift the time series up or down along the vertical axes of the figures and the variations in time would not be very different. Estimating the top 1-m soil moisture via equation (2) does not consider the possible difference in temporal dynamics between 1-m and 2-m soil moisture profile. This is likely to exacerbate the discrepancies between modeled and observed 1-m soil moisture.

As first explained by *Vinnikov et al.* [1996], the scale of soil moisture variations includes a very small scale related to local soil, root, and topographic features and a much larger scale driven by the atmosphere. The atmospheric-driven spatial scale of soil moisture, which represents most of the variance, is about 500 km [*Entin et al.*, 2000; *Liu et al.*, 2001]. As the resolution of ERA40 is about 215 x 275 km^2 over China, and that of R-1 and R-2 is about 160 x 210 km^2, the mismatch of scale between point observations and reanalysis grid will not present a problem. However, for those stations that have strong local effects, the results might be biased toward local effects (i.e., more representative of local effects instead of atmospheric forcing control).

2.4.1 Time series and correlations

Figure 2.3 shows comparisons of observed soil moisture for three stations with the three reanalyses. Generally, R-1 has very large amplitude of seasonal variation but very small interannual variability, the only exception being for Station 15, which has nearly constant soil moisture and small amplitudes of variation for both R-1 and ERA40. At the same time the amplitude of variations in R-2 is also comparable to observations, but R-2 underestimates the soil moisture most of the time for 8 out of our 10 stations, and such systematic biases do not exist in ERA40 or R-1. Other soil moisture indices, such as plant-available soil moisture, may not necessarily give the same result. However our results are in agreement with the analysis of *Dirmeyer et al.* [2004], who used a soil wetness index for Illinois (see their Figure 14).

We have also calculated the correlation coefficients of monthly soil moisture (28th day of each month) between models and observations (Figure 2.4). Generally, R-2 had a higher correlation than R-1 (7 out of 10 stations). The correlation of ERA40 is

smaller, but still comparable to that of R-2. For station 23, both R-1 and R-2 had negative correlations. Removal of the seasonal cycle generally improved the correlations for ERA40 and R-1 but not for R-2, discussed next.

2.4.2 Seasonal Cycle

Figure 2.5 gives the seasonal cycles of soil moisture for our three representative stations. Station 15 has nearly constant soil moisture estimates for both R-1 and ERA40, which do not reproduce the observed seasonal cycle. For ERA40, the value is virtually constant at the wilting point, while for R-1 it is constant at the saturation value. In both cases, the seasonal cycle of precipitation and evapotranspiration are so much out of balance that soil moisture cannot change as observed. For most stations, R-2 has a good climatology and patterns of seasonal variation similar to observations, but underestimates the mean soil moisture amount. This is in contrast with R-1, which has quite a strong seasonal variation, because it is nudged to the *Mintz and Serafini* [1992] climatology, as also pointed out by *Kanamitsu et al.* [2002]. In terms of monthly average values, ERA40 is closest to observations. For the non-western stations, all models produce the soil moisture peak correctly around late summer due to the arrival of the summer monsoon precipitation.

Spring Snow Melt

Melting snow is an important source of moisture for northern and western agricultural regions since it can recharge the soil and produce runoff. Whether the melting snow will recharge the soil or run off as streamflow depends on the soil conditions. In the case of saturated soil, there is no extra space for water to infiltrate [*Robock et al.*, 1998, 2003], and thus it is very likely the melting snow produces spring

runoff. Generally, ERA40 has a small soil moisture peak in early spring due to snow melting recharging, while such a soil moisture peak is basically missing in R-1, especially for northern China where the soil is pretty wet in winter. Although the soil in R-2 is not as wet as in R-1, the spring soil moisture peak is still missing or too weak. Our speculation is that this may be attributed to the physical configuration of R-1 and R-2, since the deep layer in R-1 and R-2 is too thick (190 cm) and the water holding capacity is unrealistically too large. Although missing observations in the cold season inhibit a deeper investigation for spring snow melting events, limited observations from stations in central China in cold seasons confirm the existence of a soil moisture peak in early spring. This may be similar to the observations in Russia [*Robock et al.*, 1998] where the water table intrudes into the top 1 m, a phenomenon which is not included in the R-1 and R-2 reanalysis land surface schemes.

2.4.3 Monthly and Interannual Variability

Figure 2.6 shows the monthly and interannual variations of soil moisture for selected stations and the reanalyses, and Figure 2.7 shows the soil moisture anomalies. R-1 shows a rather small interannual variation, especially during winter. Since snow melting is mainly responsible for soil moisture changes in cold season, and a unit error for snow melt in R-1 wets the ground excessively [*Kanamitsu, personal communication*], this is especially evident for Northern stations. R-2 shows a larger interannual and seasonal variations than R-1 although the soil generally is too dry. Drier soil in R-2 may partly be attributed to warmer soil and 2-m air temperature as well as to a better albedo algorithm than R-1 [*Kanamitsu et al.*, 2002]. The variability of ERA40 is closest to the observations. Models generally did a pretty good job of reproducing the anomalous wet

and dry years, such as the wet years of 1984 at Station 33 and the dry year of 1982 at Station 23 (Figure 2.7). In a test of how closely the interannual variability of reanalyses matches the observations, we calculated the anomaly correlation between the models and observations for the summer months (JJA). Generally ERA40 has the best interannual variability with respect to observations (Figure 2.8).

In Figure 2.7 it is quite obvious that the soil moisture does not change in the winter for R-2. This means that the time scale of soil moisture anomaly in R-2 is comparatively large. *Delworth and Manabe* [1988] developed a theory that soil moisture variations can be approximated as a first-order Markov process,

$$r(t) = e^{-\frac{t}{T}} \qquad (2.3)$$

where r is the autocorrelation, t is the time lag, and T is the time scale. This theory has been extensively used to investigate the scales of soil moisture variations using observations [*Vinnikov et al.*, 1996, 1999a, 1999b]. Using this theory, *Entin et al.* [2000] calculated the temporal scale of Chinese soil moisture to be 1.6-2.4 months, which increases from south to north.

Here we adapt the same theory and assume that the soil moisture variation is stationary. We removed the seasonal cycle and calculated the temporal scale for all the 10 stations. Two groups of calculations are carried out. One considers the missing values in observations by taking out the corresponding data in reanalyses, thus making the results comparable. To investigate the possible influence of the cold season on temporal scale (because missing values in observations are generally in winter), we did another set of calculations for the full data sets for the reanalyses. Figure 2.9 shows the

temporal autocorrelation results and Table 2.2 gives the numeric values. The slopes of the lines in Figure 2.9 correspond to the temporal scales.

ERA40 shows the highest variability between stations. The soil moisture increments were set to be zero when the air temperature is below freezing or the snow covers the ground in ERA40 (ECMWF 2003), so this should increase the temporal scale (about 1 month in general, see Table 2.2) for the northern stations.

Station 15 exhibits a much lower autocorrelation than the other stations in R-1 and R-2, which must be related to the parameters for the land surface model at that point. The calculated temporal scale for R-1 shows the largest similarity between stations and between full data and only data that correspond to the observations. This must be the effect of relaxing the values to the *Mintz and Serafini* climatology. R-2 has a temporal scale longer than 6 months for all nonwestern stations. The mean temporal scale of R-1 and ERA40 is comparable to observations, which is consistent with the results of *Entin et al.* [2000], while R-2 has an unrealistically long mean time scale of about 8 months. Thus these calculations support that the deep layer in R-2 is too thick and dominates the overall variability of soil moisture [*Roads et al.*, 1999]. This could further impact the evaporation and precipitation.

Since R-1 uses the same land surface scheme as R-2, this brings up the question of why its temporal scale is so much smaller. This is to a large extent because R-1 nudges soil moisture to the *Mintz and Serafini* [1992] climatology with a 60-day time scale while nudging in R-2 is based on observed precipitation. However this advantage of R-2 is compromised by its use of a model with a very large soil moisture reservoir, which produces an unrealistically large time scale. To most clearly separate nudging

effects from other influences, since other improvements in R-2 also contribute to soil moisture simulations, would require additional experiments that keep all other physics exactly the same but with different nudging schemes.

2.5   Conclusions

An updated Chinese soil moisture data set has proven valuable to evaluate reanalysis simulations of soil moisture. This new data set is available without restriction at the Global Soil Moisture Data Bank (http://climate.envsci.rutgers.edu/soil_moisture).

Using 19 years soil moisture observations from a monsoon-dominated region; we evaluated three prominent soil moisture reanalysis data sets: ERA40, R-1 and its updated counterpart R-2. *Kanamitsu et al.* [2002] in their studies found improved soil moisture fields from R-2 when validating with Illinois soil moisture observations [*Hollinger and Isard*, 1994]. Our analysis supports their conclusions with soil moisture observations from a different climate, where R-2 also exhibits the highest correlation with observations among the three soil moisture reanalyses. But this is a result of R-2 having a good mean climate. A reanalysis product with good mean state but poor year-to-year variations may not be a good choice for use in climate modeling. ERA40 is also generally highly correlated with observations after removing seasonal cycle, and produces less bias and a time scale closer to observations. Although *Kanamitsu et al.* [2002] argued that direct comparison between observed soil moisture and model simulations could be misleading, negative R-2 biases exist when comparing the Illinois soil moisture observations with R-2 even after removing the unavailable soil moisture [see Figure 1 of *Kanamitsu et al.*, 2003]. Whether these results are universal would

require further investigation for different regions. In terms of interannual variability, ERA40 is the best among the three reanalyses products.

The temporal scale of soil moisture anomalies in ERA40 (disregarding stations 9 and 23) and R-1 are comparable to that of observations, but the scale of R-2 is extraordinarily long, about 2 times of that of observations in growing season, and cold season tends to prolong soil moisture memory around 1 month in ERA40 and 3 months for R-2. This prolonged memory may further propagate into evaporation and precipitation. Our suspicion is that R-2 has a too thick deep layer which has a dominant influence on the soil moisture variability of the whole soil column. Clearly it is responsible for the long spinup problems found by *Kanamitsu et al.* [2002]. An improved land surface scheme is capable of resulting in a much better precipitation prediction [e.g., *Betts et al.*, 1996; *Beljaars et al.*, 1996], which will be beneficial to weather forecasting. We expect that improved land surface models in future reanalyses combined with actual precipitation forcing will produce an excellent soil moisture product. The new regional reanalysis [*Mitchell et al.*, 2004], which uses a descendant of OSU LSM − the Noah model [*Chen et al.*, 1996; *Chen et al.*, 1997; *Ek et al.*, 2003], which performed well in North American Land Data Assimilation System experiments [*Robock et al.*, 2003] and which assimilates actual precipitation observations, has the potential to produce such excellent soil moisture simulations.

3 Evaluation of Intergovernmental Panel on Climate Change Fourth Assessment Soil Moisture Simulations for the Second Half of the Twentieth Century

3.1 Introduction

Global-warming-induced climate changes are experienced from regional to global scales. How components of the hydrological cycle changed in the past and will evolve in a warming climate will have strong impacts on human society. Higher temperature will accelerate the global hydrological cycle in general [e.g., *Milly et al.,* 2002; *Bosilovich et al.,* 2005]. However, model studies with increased amounts of absorbing aerosol tend to show a slow down of the hydrological cycle [e.g., *Liepert et al.,* 2004]. Unlike other terms in the water budget, however, soil moisture (the water residual) has been relatively less studied due to paucity of available observations, in spite of its importance.

Soil moisture is crucial to agriculture and is an important part of the agricultural drought outlook in many areas of the world. From the perspective of water balance, soil moisture directly influences the rate of evaporation, groundwater recharge and runoff generation. Soil moisture, along with other land surface conditions, also determines the partitioning of available energy at the surface between sensible heat and latent heat. Since there are no global *in situ* observations, model-simulated soil moisture (usually outputs from physically based land surface schemes driven by observed near surface atmospheric variables) has been used as a substitute for observations in climate change studies [e.g., *Zhu et al*., 2004]. A general drying in mid-latitude summer was reported in

several model simulations [e.g., *Manabe and Wetherald,* 1987; *Gregory et al.,* 1997; *Manabe et al.,* 2004], which, if correct, poses a great threat to future food security. The drying was attributable to earlier snow melting and higher evaporation in winter and spring and lower precipitation during summer [*IPCC*, 2001]. However, other models presented quite an opposite scenario [e.g., *Meehl and Washington*, 1988; *Seneviratne et al.,* 2002]. These model-dependent predictions cannot be a reliable reference point in explaining the direction of future changes yet [*IPCC*, 2001].

Vegetation plays an important role in the climate system. In response to increasing atmospheric CO_2 concentration, many plant species tend to reduce stomatal openings to reduce water loss through transpiration [*Field et al*., 1995]. Such a mechanism has profound implication for the hydrological cycle since it potentially leads to an increase for water storage and streamflow [*Gedney et al.*, 2006]. *Wigley and Jones* [1985] analytically illustrated the strong dependence of changes in streamflow on the direct CO_2 effect on plant evapotranspiration which is controlled by stomata. Modeling results suggested that the climatic impact of doubling stomatal resistance could be as large as the effect of doubling atmospheric CO_2 [*Henderson-Sellers et al*., 1995]. On the other hand, there also exists a compensating mechanism, namely the structural response, which may offset the physiological effects. Increased CO_2 uptake by plants with elevated CO_2 can stimulate plant growth (i.e., increase in root depth and foliage), thus boosting transpiration. This may further enhance the resultant surface cooling through a series of feedbacks in the planetary boundary layer [*Pitman*, 2003]. However, given that our knowledge of these physical processes is rather limited and the parameterizations of these features in climate models are still rather simple, uncertainties concerning the net effect

of these two mechanisms on the hydrological cycle remain high. In terms of root-growth feedbacks, *Milly* [1997] demonstrated a 14% decrease of plant accessible water in soil column would generate the same summer dryness comparable to a doubling of atmospheric CO_2.

The ability to calculate accurate soil moisture in a climate model depends on several factors: a good land surface model, and good precipitation and radiation forcing. Both off-line experiments [e.g., *Guo et al.,* 2005] and coupled simulations [e.g., *Kanamitsu et al.,* 2002] demonstrate that realistic lower atmospheric conditions are extremely important for accurate soil moisture simulations. By adopting a more realistic radiation scheme, *Wild et al.* [1996] demonstrated that the resultant improvements in radiation and precipitation could attenuate simulated summer desiccation in a climate model. Soil with low field capacity is more prone to reach field capacity in late winter or spring, which ensures that much of the extra precipitation in winter is lost as runoff. Without proper accounting for cold season soil dynamics, models in the Atmospheric Model Intercomparison Project [*Gates*, 1992] were unable to capture the observed month-to-month changes in winter [*Robock et al.*, 1998]. Including soil-water freezing in a model can also improve the simulation of the soil thermal state [*Luo et al.*, 2003a].

In July 2004, the Working Group on Coupled Models Climate Simulation Panel invited voluntary groups to analyze climate model outputs [*Meehl et al.*, 2004]. These analyses will lead to the Fourth Assessment Report of the Intergovernmental Panel on Climate Change (IPCC). These coupled models represent the latest model developments with improved parameterizations of physical processes of the climate system.

Recent updates at the Global Soil Moisture Data Bank, especially several long term observations from the Former Soviet Union (FSU), make it possible to use these benchmark observations to evaluate the soil-moisture-related climate change in these models. In this study, I focus on the second half of the 20th century when most observations are available. I will address the following scientific questions with an emphasis on the second one: 1) How realistic are the seasonal cycle and interannual variations of the model simulated soil moisture? and 2) Can IPCC models capture observed soil moisture trends in the summer? The data sets are described in subsection 2. Comparisons between observations and model outputs in terms of seasonal cycle and interannual variations are presented in subsection 3. Analysis of long-term soil moisture in summer is given in subsection 4, with a summary in subsection 5.

3.2 Data Sets

Soil moisture observations from FSU, China, Mongolia, and Illinois (Figure 3.1, Table 3.1) from the Global Soil Moisture Data Bank [*Robock et al.*, 2000] were used in this study. We used a subset of the FSU soil moisture (now called Russian and Ukrainian data), measured separately for winter cereal crops and spring cereal crops, composed of 66 district averages at 0-20 cm and 0-100 cm depth. There is a good agreement between these two independent observations taken in winter cereal and spring cereal crop fields [*Entin et al.*, 1999; *Robock et al.*, 2005]. Since the data for winter cereal crops contain fewer missing values, we only used soil moisture for winter cereal crops in our analysis. Measurements for top 1 m soil moisture began in 1958 and started in the 1970s for the top 0-20 cm. We recently updated the Ukrainian data through 2004. The Chinese soil moisture consists of 40 stations and spans the period of 1981-1999 [*Li et al.*, 2005].

There are 17 stations for Mongolia for the period of 1970-2002; a few of them started in the 1960s. The state of Illinois has been measuring soil moisture since 1981 at 19 stations [*Hollinger and Isard*, 1994]. The data for the first three years are inhomogeneous with the rest of the data so were excluded from our analysis. The data sets are describe in great detail by *Hollinger and Isard* [1994], *Vinnikov et al.* [1996, 1997], *Robock et al.* [2000, 2005], and *Li et al.* [2005]. These quality-controlled data sets have been widely used in various aspects of model evaluation [e.g., *Robock et al.*, 1998; *Entin et al.*, 1999; *Srinivasan et al.*, 2000; *Schlosser et al.*, 2000; *Luo et al.*, 2003a; *Dirmeyer et al.*, 2004]. Monthly mean observations were calculated to be compatible with model outputs. In addition to soil moisture, monthly mean precipitation and temperature from the Climate Research Unit at the University of East Anglia [*New et al.*, 1999, 2000] and monthly precipitation data from the University of Delaware [*Legates and Willmott*, 1990] were utilized to evaluate corresponding model fields.

Eighteen modeling groups sent their latest IPCC results to the Program for Climate Model Diagnosis and Intercomparison of Lawrence Livermore Laboratory. Each group was asked to report soil moisture in the top 10 cm and in the total soil column. Due to large inter-model differences, not all models produced top 10 cm values and the depth of the total soil column varied from model to model. To ensure consistence, we selected nine models that had multiple simulations and outputs for the top 10 cm and seven models for the top 1 m for this study (Table 3.2). For the 20th century runs, models were initialized from conditions derived from pre-industrial control runs. Each realization differed only in initial conditions. Thus, ensemble averages from multiple simulations can better detect signal from noise. The models differed not only in land

surface schemes but also in resolution. The only exception was the two Goddard Institute for Space Studies models that had identical atmosphere model and resolution but different oceans. We calculated regional averaged soil moisture to account for the scale of soil moisture variances and the differences in model resolutions (see Figure 3.1 for the domain and Table 3.1 for details).

Meanwhile, surface layer Russian soil moisture data was archived for the 0-20 cm top layer. Some conversion was needed to get top 0-10 cm soil moisture. By analyzing the data from other places where soil moisture at both levels is available, we found that top 10 cm soil moisture is highly correlated with that in 0-20 cm with a mean correlation coefficient of 0.98. This might be explained by strong vertical interaction in the near surface zone. Moreover, the magnitude of top 20 cm soil moisture was roughly twice that in the 0-10 cm layer. Thus, we divided the 0-20 cm soil moisture by 2 to approximate the value for the 0-10 cm layer. As our focus was on the seasonal pattern and interannual changes that are not dependent on absolute values, this procedure will not affect our analysis in general.

3.3   Seasonal cycle and interannual variability

Figure 3.2 gives the soil moisture seasonal cycles for the top 0-10 cm and top 0-1 m for the models and observations. As models tended to have their own climatology or effective range [*Koster and Milly*, 1997], we adjusted soil moisture simulations from each model according to the difference between the averages of monthly mean values of that model and observations. In terms of correlation coefficient, model-simulated seasonal patterns are in better agreement with those of observations for Ukraine, Russia, and Illinois where seasonal cycles are qualitatively reproduced by the models, particularly for

the 0-1 m depth where the signal-to-noise ratio is larger. For the other locations, there were relatively large inter-model differences and model-to-observation differences. Another conspicuous feature is that the warm season climatology shows less inter-model disparity than that for cold season, with large spread between the models, particularly for top layer soil moisture of Russia and Illinois. The variety of schemes for frozen soil treatment in land surface models, even driven by identical meteorological forcing in stand-alone mode, can bring about large disparities of simulated soil temperature and snow water equivalent [*Luo et al.*, 2003]. Spread of the duration and extent of global snow cover in climate models may further exacerbate differences in simulated soil moisture. Detailed analysis about the cold season soil moisture is of special interest but is beyond the scope of this paper.

To quantitatively understand how good model simulations were compared to observations, we utilized Taylor Diagrams [*Taylor,* 2001], which nicely summarize several important statistical quantities in just one plot. In Figure 3.3, the azimuthal angle (clockwise angle from north) represents the correlation coefficient between monthly mean values of models and observations, and the radial distance from the origin is the standard deviation normalized by that of observations. Correlation coefficients were generally higher for the Russian regions and Illinois where the models also showed a better and strong climatology. In terms of interannual variability, the two UK models had variability comparable to observations for all six regions. The Canadian model exhibited stronger interannual variability in all climates. To investigate whether precipitation has a similar pattern to soil moisture, we plotted the Taylor Diagram for monthly precipitation (Figure 3.4). The precipitation fields for China and Mongolia actually were better,

probably due to the strong seasonality of the Asian monsoon and that we did not have winter soil moisture observations for comparison to models. In Russia and Illinois, precipitation was not simulated well. Further analysis of the precipitation climatology indicates that models capture the seasonal changes better for Mongolia and China, where relatively strong (and simple) seasonal precipitation changes are primarily driven by Asian monsoon (Figure 3.5). Similar to soil moisture analysis, this suggests a better climatology to a large extent explains higher correlation coefficients between models and observations (for soil moisture and precipitation). Better precipitation forcing does not, however, always guarantee more realistic soil moisture in coupled models.

The spatial pattern of interannual variations, defined as the coefficient of variance (standard deviation divided by mean), was plotted in Figure 3.6. Observations show that dry regions usually had stronger interannual variations and moist regions tended to have weak variations. There were large model-to-observation differences and model-to-model differences. For example, MRI and HADGEM1 models showed very strong interannual variability for Northern Africa but GISS and FGOALS and CCSM3 had rather weak variability there. The greatest discrepancy areas were for tropical Africa and the Indian monsoon area. The interannual variability of soil moisture usually follows that of precipitation, which suggests possible large discrepancies for precipitation in those locations.

3.4 Trends

Because soil moisture simulations were more realistic for the two FSU regions and those two regions had relatively long measurements available (over 40 years), we chose Russia and the Ukraine for long-term trend analysis. We used the least squares

method for trend detection. An additional analysis by the nonparametric Mann-Kendall method [*Hirsch et al.*, 1982] showed similar results. We calculated the monthly trends for Ukraine and Russia (Figure 3.7). There was a general increase in April, June, July, August, and September for observations for both regions (10% significance level). The mean trends of models showed a slight increase for Ukraine but a small decrease for Russia. The number of realizations that show an increase is roughly equal to that exhibiting a decrease. The observed trends in April and May are relatively well captured by models. However, in the warm months of July and August, less than 8% of model realizations have trends comparable to the observed patterns.

To see whether similar patterns exist in precipitation and temperature, we analyzed the monthly trends for precipitation and temperature, too (Figs. 3.8-3.9). In general, there are small upward trends in the observed precipitation, which is characterized by large interannual variations. Mean trends from models indicate a weak increase, relatively larger in spring and late winter. The observed temperature increased slightly in the warm season. Models simulated an almost ubiquitous increase of temperature for all seasons, larger in winter and smaller in summer. There was a good agreement between models and observations for summer months. Observed temperature trends lay within model predictions fairly well from July to October (Figure 3.9), which validates the model-predicted warming. In terms of solar irradiance, there was an overall small decrease for the model ensemble. Models tended to agree with each other well in winter but there was a large spread in the warm seasons (not shown). We do not have observations for these regions, but the downward model trends of insolation are an order of magnitude lower than those observed for nearby regions in Europe [*Wild et al.*, 2005].

Robock et al. [2005] reported an increase in summer soil moisture for Ukraine from 1960s to 1990s but this pattern started to level off at the end of the period. Here we extend their study to both Ukraine and Russia, using these Russian data for the first time. Figure 3.10 gives the soil moisture anomaly time series (JJA average) for observations and each model, and the linear trend estimations. The amplitude of the upward trends in top 0-1 m observations is about 8.0 mm/decade for Ukraine and 8.6 mm/decade for the Russia. The IPCC models, however, simulated a very small upward trend for Ukraine and essentially no trend for Russia in terms of mean trends. In both cases, the observed trends were larger than most trends of the model simulations. Only two out of 25 model realizations have trends comparable to those of observations. These two realizations come from different climate models and other realizations from those two models do not show similar patterns. Thus the two trends are due to internal model variability as different realizations for the same model only differ in initial conditions. Similar to the model trends discussed earlier, there was a slight increase in both precipitation and temperature (Figures 3.11-3.12). Again, the observed temperature pattern is well constrained in model results, highlighting the reliability of the model-simulated warming.

An interesting question remains about what drives the observed pattern in soil moisture. Precipitation and solar radiation are the driving forces for the water cycle. A phenomenon called "from dimming to brightening" has been observed for solar radiation data from both ground stations [*Wild et al.,* 2005] and satellite measurements [*Pinker et al.*, 2005] for many places around the world. A widespread decrease for shortwave radiation for 1950s to 1990s was observed and followed by a gradual recovery since 1990s. Such a pattern (solar dimming) may well explain the observed soil moisture

change for FSU regions. *Peterson et al.* [1995] reported a decrease in pan evaporation in FSU around the same period. Showing evidence from the observed decreases in solar irradiance and associated changes in diurnal temperature range and vapor pressure deficit, *Roderick and Farquhar* [2002] suggested that the decrease in pan evaporation was in line with the change of evaporation. The upward trend in soil moisture is consistent with these results, as suggested by *Liepert et al.* [2004] and *Robock et al.* [2005].

Another line of supportive evidence can also be found in independently measured streamflow. I collected monthly river discharge data of several stations from the Global River Discharge that were compiled and prepared by scientists of University of New Hampshire, distributed by data center of Oak Ridge National Lab [see Figure 3.13a for station locations]. Although the river discharge data for the data center are only available to mid of 1980s, there is a good correspondence between river discharge and soil moisture for the overlapping period (Figure 3.13b). For Ukraine there was a general increase for river discharge. A decline to mid of 1970s and then a gradual recovery afterwards were found for Russia.

Using a sophisticated land surface model, *Robock and Li* [2006] demonstrated that changes in precipitation and temperature are not enough to explain the amplitude of the observed soil moisture increases. They further quantitatively showed that solar dimming from tropospheric pollutions is the main cause for the soil moisture trends. In other words, soil moisture increases for Ukraine and Russia are likely externally forced rather than due to model internal variability as suggested by the IPCC models we analyzed here. The lack of solar dimming in the IPCC models explains their inability to model the soil moisture trends.

The failure to capture the observed dimming effects for many models might be partly attributable to the lack of an adequate representation of aerosol. Scientists at the Max Planck Institute recently developed a special version of the ECHAM5 model that incorporates a sophisticated treatment of aerosol effects based on a flexible microphysical approach [ECHAM5-HAM, *Stier et al.*, 2005]. Sulfate aerosols, black carbon, particulate organic matter, sea salt, and mineral dust are included in the aerosol scheme. By comparing the special version to the standard ECHAM5 model [*Roeckner et al.*, 2003], which only prescribes direct and the first indirect effect of sulfate aerosols, the soil moisture sensitivity to changes in solar radiation caused by aerosol might be understood.

Figure 3.14 gives the JJA soil moisture from 1958-2002 for both models and the observations for Russia and Ukraine. Soil moisture decreased slightly for both models in contrast to the general increases found in observations. Measurements from a nearby station indicate that solar radiation decreased until 1980 and began to gradually recover afterwards [*Wild et al.*, 2005]. Accordingly, we split the data into two equal periods to investigate how soil moisture evolved. We found an increase in observations for both regions from 1958-1980. The standard ECHAM5 model also had an increase in soil moisture. However, the special version showed a drying pattern. For the second period from 1980 to 2002, observed soil moisture started to level off for Ukraine but continued to increase for Russia. There was a downward trend for the special version but an upward pattern for the standard model for Ukraine. An increase was found for the special version but a decline in the standard model for Russia.

We further analyzed the clear-sky shortwave radiation and precipitation fields for both models to explore probable causes of the differences between the models and

observations. Clear-sky shortwave radiation for both models exhibited the process from dimming to brightening but the special version showed a much stronger signal and more closely resembled the observations. At the same time, the clear-sky shortwave radiation for the special version is noticeably higher than that of the standard one (Figure 3.15a). However, in terms of precipitation, simulated precipitation decreased over the entire period of 1958-2002 for both models for Ukraine. Also, there was a conspicuous dry bias for the special version (Figure 3.15b). We conclude that these unfavorable conditions simulated by the special version may create a more water-limited rather than energy-limited climate in which precipitation plays a dominant role. Therefore, the simulated soil moisture patterns more closely follow those of precipitation. The same reasoning can be used to explain the pattern of simulated soil moisture by the special version for Russia, too. To conclude, neither the special version model nor the standard version model can simulate the precipitation well. This explains the disparity between simulated soil moisture patterns and the observed ones to large extent.

3.5 Summary

To investigate how realistic the soil moisture simulations in IPCC models are, we compared the seasonal cycle, interannual variability, and long-term pattern in summer for observations and model outputs. Generally, IPCC models have limited capacity to reproduce observed seasonal cycle and interannual variability, although better simulations are found for Russia, Ukraine and Illinois than for Mongolia and China with respect to seasonal cycle.

To capture the observed soil moisture trends, we need realistic forcings, particularly both precipitation and radiation, in addition to a good land surface scheme.

Regarding water balance, either precipitation increase or evaporation decrease may result in soil moisture increase, and the latter is closely related to available energy. The observed solar dimming can dampen the evaporative demand of atmosphere and lead to water storage increase, which may explain the observed soil moisture patterns for Ukraine and Russia. Our analysis of the ECHAM5 model simulations supports the argument that including a comprehensive representation of aerosol effects may exert considerable impacts on hydrological cycle [*Liepert et al.*, 2004]. Through incorporating a sophisticated aerosol scheme, the special ECHAM5 model showed promising results with respect to the simulated radiation fields. But the explicit treatment of aerosol-cloud interactions remains a challenge [*Stier et al.*, 2005].

Wang [2005] analyzed soil moisture in IPCC models in a future scenario. Interestingly, her results showed that FSU regions were the places where models disagreed most, highlighting the sophisticated nature of sensitivity of land hydrology to elevated CO_2 concentrations in models. In response to elevated CO_2 concentrations, many plant species reduce their stomatal openings [*Field et al.*, 1995], leading to a reduction in evaporation to the atmosphere. More water is likely to be stored in the soil or run off consequently. Figure 3.16 shows the relative change of summer soil moisture for a future scenario from our IPCC models. The relative change is defined as the difference between the mean of 2060-2099 (scenario SRESA1B) and that of 1960-1999 normalized by the average of 1960-1999. In spite of large spatial differences, many models did not produce summer desiccation. The response of plants to elevated CO_2 concentrations might explain why some models project wetter land surface for some

regions[1]. Recent modeling results also demonstrated the direct carbon dioxide effects on continental river runoff [*Gedney et al.*, 2006]. These results are encouraging and underlining the nature that global climate models should better integrate the biological, chemical, and physical components of the Earth system [*Karl and Trenberth*, 2003]. On the other hand, the effects of CO_2 fertilization on soil moisture vary substantially from model to model. In view of photosynthesis-stomatal coupling in climate models, such disparities arise from parameterizations of (1) stomatal function (e.g., using the Jarvis' formulation or the Leuning's physiological formulation or other types), (2) partitioning of transpiration in total evapotranspiration, (3) scaling (of photosynthesis and stomatal conductance) from leaves to canopy level (e.g., using leaf area index or the nitrogen contents).

To our knowledge, no soil moisture evaluation using observations has been done in the previous IPCC reports. We attempt to provide quantitative evidence for the forthcoming IPCC AR4 about the observed and model simulated soil moisture patterns. We hope our analysis will assist modelers to identify model deficiencies and further improve model performances. With better parameterization systems implemented in the next generation models, we expect to see more realistic soil moisture products.

---

[1] In Figure 3.16, seven out of nine models include carbon fertilization effects.

4 Relative contribution of solar dimming and CO$_2$ effects on soil moisture trends

4.1 Introduction

Understanding soil moisture variation is crucial to modeling and understanding climate changes due to its long meteorological memory [*Vinnikov et al.*, 1996], active role in land-atmosphere interactions [*Koster et al.*, 2004], and contribution to atmospheric predictability [*Dirmeyer*, 2000]. Potential soil moisture changes from global warming, especially desiccation in growing seasons, are a grave threat to food security on which human society relies. Numerical models have been utilized to explore how water storage will change with global warming. Many models predict a decline of soil moisture over the midlatitudes of the Northern Hemisphere [*Manabe and Wetherald*, 1987; *Gregory et al.*, 1997]. These analyses highlight possible climatic consequences, with an emphasis on the radiative effects of increased CO$_2$.

Many plant species tend to reduce stomatal openings with increasing atmospheric CO$_2$. The concurrent higher canopy resistance reduces water loss through plant transpiration and thus may have profound impacts on the hydrological cycle [e.g., *Henderson-Sellers et al.*, 1995; *Sellers et al.*, 1996]. A recent study suggests such CO$_2$ effects are to a large extent responsible for the continental runoff increases for the 20th century [*Gedney et al.*, 2006].

On the other hand, as the driving forces for land surface hydrology, precipitation and net radiation impose a first order control on evaporation and runoff at annual or longer timescales [*Koster et al.*, 2001]. In terms of soil moisture, more realistic

simulations can be obtained by assimilating observed precipitation into climate models [*Kanamitsu et al.*, 2002; *Li et al.*, 2005]. In short-term field experiments, an artificial increase in downward heat flux has been shown to cause a significant reduction in summer soil moisture [*Harte et al.*, 1995]. Both ground-based observations [*Abakumova et al.*, 1996; *Gilgen et al.*, 1998; *Stanhill and Cohen*, 2001; *Liepert*, 2002; *Wild et al.*, 2005] and satellite measurements [*Pinker et al.*, 2005] reveal a widespread reduction of solar irradiance from 1950s to 1990s and a gradual recovery [*Wild et al.*, 2005; *Pinker et al.*, 2005] afterwards, known as the "global dimming" phenomenon. Increasing atmospheric aerosol loading from rapid industrialization is believed to be the culprit. Aerosols can affect solar irradiance reaching the Earth's surface through scattering and absorbing radiation (direct aerosol effect), and modifying cloud properties (indirect aerosol effects). The net effect of the mechanisms is a reduction in downward surface solar radiation [*Ramanathan et al.*, 2001]. In the context of the hydrological cycle, the reported decline of shortwave radiation over such a long period may potentially increase water storage over land by damping evaporative demand from the atmosphere [*Liepert et al.*, 2004; *Wild et al.*, 2004]. Recent studies [*Robock et al.*, 2005; *Li et al.*, 2006] show no summer desiccation based on analysis of over 40 yr of gravimetrically-measured soil moisture observations for Ukraine and Russia during a period when surface air temperature rose. Rather, observations for Ukraine and Russia show an upward soil moisture trend. While *Robock et al.* [2005] suggested that solar dimming may have been responsible, this has not been tested before with a theoretical model. The reported upward summer soil moisture trends for many Former Soviet Union stations are consistent with the decrease of pan evaporation around the same period for the same

region [*Peterson et al.*, 1995] as pan evaporation can be thought as a direct measurement of the atmospheric evaporative demand.

4.2   Experiment Design

To understand the relative contribution of solar dimming and physiological effects of CO_2 on the observed soil moisture pattern for Ukraine and Russia (Figure 4.1), we conduct a series offline sensitivity experiments with the Community Land Model [CLM3, *Oleson et al.*, 2004]. A unique advantage of offline experiments is that the model can be forced with realistic precipitation and temperature, so the sensitivity of soil moisture can be better sorted out. We set the land cover type to "agricultural" for all grid points in the study regions, so we could compare the results to observations, which were made in agricultural fields. We evaluate the results with the longest available observational data sets of soil moisture, from the Ukraine [1958-2004, *Robock et al.*, 2005] and Russia [1958-1998, *Li et al.*, 2006].

4.2.1   Modified Community Land Model

The CLM approximates land surface heterogeneity through a nested sub-grid hierarchy in which grid cells are composed of multiple land units, snow/soil columns, and plant functional types (PFTs). Each grid cell can have a different number of land units (to capture the broadest spatial patterns of subgrid heterogeneity: glacier, lake, wetland, urban and vegetated), each land unit can have a different number of columns (to capture potential variability in the soil and snow state variables), and each column can have multiple PFTs (to capture the biogeophysical and biogeochemical differences between broad categories of plants). Figure 4.2 gives a schematic representation of the key land

biogeophysical and hydrologic processes simulated by CLM. Biogeophysical processes are simulated for each sub-grid land unit, column, and PFT independently and each sub-grid land unit maintains its own prognostic variables. The grid-averaged atmospheric forcing is used to force all sub-grid units within a grid cell. The surface variables and fluxes required by the atmosphere are obtained by taking the weighted averages of the subgrid quantities by their corresponding fractional areas.

4.2.1.1 Land surface hydrology module

A number of land model deficiencies have been found over various regions [*Bonan et al.*, 2002]. Two problems related to hydrology are that the model has too much interception and too much surface runoff so that the simulated soil moisture is usually too low (infiltration is calculated as the residual of surface water flux minus evaporation and surface runoff). Correspondingly, we made improvements to the land surface hydrology of CLM, following *Niu et al.* [2005] and *Niu and Yang* [2006]. In the CLM, the interception is expressed as:

$$q_{\mathrm{int}\,r} = f_p P$$
$$f_p = 1 - e^{-0.5(LAI+SAI)} \tag{4.1}$$

where P represents precipitation. f_p is the ratio of precipitation intercepted by canopy. *L/SAI* represents leaf/stem area index. Such expression was found to produce an excess of canopy interception loss and therefore was partially responsible for a too dry soil. *Niu et al.* [2005] scaled f_p by a factor f_{pi} based on the precipitation characteristics:

$$f_{pi} = \frac{P_C + P_L}{10 P_C + P_L} \tag{4.2}$$

where subscripts C and L represent convective and large-scale precipitation separately. If purely convective precipitation, the ratio will be 0.1 and if stratiform precipitation only, the ratio will be 1. Forcing data sets prepared for offline simulations usually only provides total amount (i.e., the sum of convective precipitation and large-scale precipitation), so the following formula is used to reduce interception:

$$f_p = \min(0.2, 1 - e^{-0.5(LAI+SAI)}) \tag{4.3}$$

(4.2) and (4.3) actually work very similarly since the CLM assumes an equal partitioning between convective and stratiform precipitation for the offline configuration.

To improve the runoff scheme, *Niu et al.* [2005] developed a scheme called a simplified TOPMODEL-based runoff scheme (SIMTOPR) in which the surface runoff is rewritten as:

$$\begin{aligned} R_s &= F_{sat}Q_{wat} \\ F_{sat} &= F_{max}e^{-C_s fZ_\nabla} \end{aligned} \tag{4.4}$$

where R_s is the surface runoff, Q_{wat} is the water input to the soil, F_{sat} is the saturated fraction of the soil. F_{max}, the maximum saturated fraction for a grid cell, is defined as the cumulative distribution function (CDF) of the topographic index when the grid cell mean water table depth is zero. z_∇ is the grid cell mean water table depth. C_s, used globally as 0.6, is a coefficient that can be derived by fitting the exponential function to the discrete CDF of the topographic index. f, a dimension index, is fixed as 2.0 m^{-1}. A major departure from the original CLM runoff scheme is the removal of infiltration excess runoff (Hortonian flow) which is negligible for TOPMODEL-based approaches [*Niu and Yang* 2003]. For the subsurface runoff,

$$R_{sb} = R_{sb,max}e^{-fZ_\nabla} \tag{4.5}$$

where $R_{sb,max}$ is the maximum subsurface runoff when the grid cell mean water table depth is zero. (See *Niu et al.*, 2005 for details about the calibrations and optimizations of these parameters). Sensitivity experiments and validation against observations suggest SIMTOPR lead to more realistic runoff and much better and wetter soil moisture. NCAR scientists currently are in the process of implementing these changes into the next version of CLM which is expected to be released soon.

4.2.1.2 Stomatal-photosynthesis module

The CLM uses the coupled stomata-photosynthesis model developed by *Collatz et al.* [1991, 1992] with further modifications (C_3 plants: *Farquhar et al.*, 1980 and *Collatz et al.*, 1991; C_4 plants: *Collatz et al.*, 1992 and *Dougherty et al.*, 1994). The response of g_s (leaf conductance) to the rate of CO_2 uptake and other environmental factors can be written as:

$$g_s = m \frac{A}{C_s} \frac{e_s}{e_i} P_{atm} + b \qquad (4.6)$$

where A is leaf photosynthesis, m is a plant type dependent parameter, C_s is the CO_2 concentration at the leaf surface, e_s and e_i are vapor pressure at the leaf surface and the saturation vapor pressure inside the leaf at the vegetation temperature T_v, P_{atm} is the atmospheric pressure, and b is the minimum stomatal conductance when there is no photosynthesis ($A = 0$). This formulation differs from the original proposal of *Ball* [1988] in that the CLM used gross photosynthesis instead of net photosynthesis (i.e., photosynthesis minus respiration). Leaf area index then is used to scale up the leaf conductance to get the canopy-level one.

The potential photosynthesis (defined as no soil moisture stress), according to the Liebig's Law of the Minimum, is calculated in terms of three limiting factors:

$$A_p = \min(J_E, J_C, J_S) \tag{4.7}$$

where J_E, J_C and J_S are separate expressions for photosynthetic CO_2 uptake in terms of a different rate-limiting step in the overall process of photosynthesis (J_E, light; J_C, Rubisco; J_S sucrose synthesis) [*Collatz et al.*, 1991, 1992] (refer to Chpt. 8 of *Oleson et al.* [2004] for details about these factors). Photosynthesis is related to atmospheric CO_2 concentration by:

$$A = \frac{C_a - C_i}{(1.37r_b + 1.65r_s)P_{atm}} = \frac{C_a - C_s}{1.37r_b P_{atm}} = \frac{C_s - C_i}{1.65r_s P_{atm}} \tag{4.8}$$

where subscripts a, i and s for term C represent atmospheric, internal and leaf surface CO_2 concentrations. r_b is leaf boundary layer resistance. r_s is the leaf resistance (the inverse of the leaf conductance).

We made changes to the model so that it can accept user specified CO_2 values instead of using the "hardwared" constant in the original model codes. We also rewrote the beta factor (soil moisture control on photosynthesis) with a formula similar to other studies [e.g., *Cox et al.*, 1999; *Daly et al.*, 2004] as:

$$A = \beta \times A_p \tag{4.9}$$

Where A is photosynthesis, A_p is the potential photosynthesis calculated by the leaf-photosynthesis module that is not constrained by water stress. β is the soil moisture availability weighted by root distribution:

$$W_i = \begin{cases} 0 & , \psi_i < \psi_w \\ \dfrac{\psi_i - \psi_w}{\psi_c - \psi_w}, & \psi_w \leq \psi_i < \psi_c \\ 1 & , \psi_i \geq \psi_c \end{cases}$$

$$\beta = \sum r_i \times W_i$$

(4.10)

Where r is the root percentage and ψ is matric potential and i represents soil layer, subscribe w and c represent wilting point and critical point (specified as 70% of field capacity here). Here we chose the matric potential instead of volumetric soil moisture since the former is independent of soil type and is easier to implement in the model. If soil moisture is below wilting level, corresponding W is set to zero. If some moisture is above critical point, W is always one. (4.6) – (4.10) gives the full stomata-photosynthesis model at leaf level which has been widely used.

4.3 Forcing data

Many efforts have been devoted to developing reliable atmospheric forcing data suitable for global land simulations. Such forcings were usually created by either adjusting reanalysis products [e.g., *Sheffield et al.*, 2004; *Ngo-Duc et al.*, 2005; *Qian et al.*, 2006] or deriving from available observations [e.g., *Nijssen et al.*, 2001; *Maurer et al.*, 2002]. We chose the forcing data sets recently created by *Qian et al.* [2006] (hereafter Qian) since the forcing is prepared in such a way that it can be easily used to force CLM. Other forcing data should produce similar results.

The Qian forcing data sets are based on National Center for Environmental Prediction/National Center for Atmospheric Research (NCEP/NCAR) reanalysis outputs [*Kalnay et al.*, 1996] but are adjusted by observations. The reanalysis values of surface air temperature and precipitation were adjusted so the monthly means matched

observations. Downward solar radiation was adjusted based on variations and trends from cloud observations, and then for the mean seasonal cycle of observed radiation, but not for observed trends in radiation (see table 4.1 for forcing adjustment procedures). Downward longwave radiation is calculated as a function of water vapor pressure and observed surface temperature. As such, the greenhouse effect is implicitly included. Specific humidity is corrected based on the adjusted temperature field as no direct specific humidity observations are available for such long term period. The adjustment implicitly incorporates changes in cloud lifetime but not the indirect aerosol effect that involves changes in radiative properties of clouds. Possible vegetation structural changes due to CO_2 increases (through land cover change) [e.g., *Levis et al.*, 2000; *Eastman et al.*, 2001] are not considered here since the study regions are primarily agricultural zones that remain quite consistent over the years.

The control experiment directly uses the Qian forcing data. To mimic the dimming, we conducted additional experiments that impose linear trends to the shortwave radiation field. For simplicity, we call the experiments with two different degrees of imposed trends as -0.5% EXP and -1% EXP respectively. For the -0.5% EXP, we use the following equation to mimic the dimming effect for 1961-1980:

$$SW_{-0.5\%}^{(s,t)} = (1 - \frac{year - 1960}{200})\% \times SW_{control}^{(s,t)} \qquad (4.11)$$

Where $SW^{(s,t)}$ is short wave radiation at every grid point and every time step. For each year from 1961-1980, a cumulative 0.5%/year is subtracted from the corresponding radiation field of the control forcings. After 1980, a constant 10% is subtracted from the control forcing to reflect possible transitions since then. The -1% EXP is similar to that of -0.5% EXP except that the denominator in eq. (4.11) is changed to 100 so that a

cumulative 1%/year rate is subtracted for 1961-1980 and a constant 20% is maintained afterwards, i.e., a much stronger dimming scenario.

Figure 4.3 shows that the imposed trends are quite similar for Ukraine and Russia, about -0.5wm^{-2}/year decline for the -0.5% EXP and about twice that for the 1% EXP for the annual means. Larger decreases are found for summer (JJA) which can be explained by higher radiation during summer (the same percent decrease means much larger magnitude). We use the surface radiation observations from Moscow as the reference, the closest long-term radiation station available, where observations are documented for the period of 1964 to the mid-1990s [*Gilgen and Ohmura*, 1999]. The imposed trends for -0.5% EXP are comparable to those of observations, although the latter exhibits stronger interannual variability. Both control and NCEP/NCAR reanalysis don not show significant trends. Interestingly, observations also exhibit much larger decrease in summer in comparison with annual mean. The magnitude of real solar dimming over these two regions might be larger or lower than that of Moscow, which, while the best available, is at one point and may have local urban influences.

In addition, to see how CO_2 increases may have impacted soil moisture, two parallel experiments, one with constant CO_2 and another with transient CO_2 increases, were conducted for each case described above. For the constant CO_2 experiments, CO_2 concentrations are fixed at the 1960 level of the observations from Mauna Loa Observatory (about 315 ppmv) [*Keeling et al., 2005*]. For the transient CO_2 experiments, prior to 1961, CO_2 concentration is fixed at the 1960 level. From 1961, the time-dependent CO_2 evolution follows the monthly mean values of Mauna Loa which increase to about 374 ppmv in 2002. The spin-up is done by repeatedly forcing the model with the

forcing data at 1955 until equilibrium (small year-to-year changes) and then the model is run over the 1955-2002 period with a 1°×1° resolution for the land surface.

One might have an immediate question about the spin-up issue, e.g., whether different model initialization approaches will change the results significantly. Thus, it is worthwhile to take some time to demonstrate that the results are insensitive to model initializations. In theory, the meteorological memory of soil moisture is about a few months for mid-latitude regions [*Vinnikov et al.*, 1996] and the autocorrelation between precipitation and soil moisture is probably on the same order. As such, the modeling results should not be tied to a particular spin-up method as long as the predefined equilibrium conditions are met. Because dry conditions tend to persist much longer than wet conditions for mid-latitudes [*Wu et al.*, 2004], the simulations will be representative if results from a dry initialization are similar to those from a wet initialization. I ran two additional experiments with fixed CO_2 concentrations for Ukraine, one experiment initialized with the forcing data of 1980 (the wettest year, called wet run) and the other initialized with the forcing data at 1961 (the driest year, called dry run). Same as the control one, both experiments are run for the entire 1955-2002 after reaching equilibrium.

The simulated top 0 - 1 m soil moisture is plotted in Figure 4.4, along with the results from the constant CO_2 control experiment described earlier. The results support the argument that the modeling results are independent on ways for model initialization as the three curves are almost identical. Interestingly, a wet initialization took less time for the model to reach equilibrium. This is related to the basic nature of the spin-up process as explained by *Cosgrove et al.* [2003]. For the wet initialization, this process progresses steadily as the soil column loses excess water through evaporation, drainage

and base-flow runoff. In the case of a dry initialization, this spin-up process proceeds as the soil column moistens, and thus can only occur during precipitation events. With this reliance on potentially scarce precipitation events, spin-up from a dry initialization can be expected to take longer than spin-up from a wet-initialization – especially in areas where precipitation amounts are small over spans of time.

4.4   Modeling results

We evaluate the model simulations with the longest available observational data sets of soil moisture, from the Ukraine [1958-2004, *Robock et al.*, 2005] and Russia [1958-1998, *Li et al.*, 2006], freely available from the Global Soil Moisture Data Bank [*Robock et al.*, 2000]. We focus on the summer soil moisture since it is closely related to plant growth. We analyze soil moisture from the top 0-1 m where most of plant roots reside (for the model, 96% of the crop roots are in the top 1 m, too).

Figure 4.5 shows the simulated and observed soil moisture in summer. To account for the differences between observations (plant-available soil moisture, i.e., with wilting levels subtracted) and model simulations (total soil moisture), we adjust each model simulation to the mean of observations for 1958-1960. The observed soil moisture for Ukraine exhibits an increase from 1958 to early 1980s and then starts to level off afterwards. So does the soil moisture in the control but with much smaller magnitude. Imposed dimming brings additional soil moisture increase compared to the control. The stronger the dimming, the higher the increase in soil moisture. Such response in soil moisture is a response to evapotranspiration, which serves as the crucial linkage between atmosphere and land surface for energy and water exchange. When energy availability becomes limited, evapotranspiration decreases to balance energy reduction. The

simulated evapotranspiration in summer for Ukraine on average decreases about 5% and 16% for -0.5% EXP and -1% EXP runs respectively for the period of 1961-2000 compared to the control. The numbers are 6% and 20% for Russia (Figure 4.6).

As can be seen in Fig. 4.5, the drier region of Ukraine has a slightly larger sensitivity to changes of insolation than Russia, even though the absolute changes in radiation are about the same (Fig. 4.3). This is because of subtle differences in the interconnected changes of all the terms in the water budget, including runoff and drainage, connected to different specifications of the seasonal cycle of the leaf area index in the two regions in CLM. In the control run for Russia, the combined runoff and drainage is almost twice as large as in Ukraine, and in the dimming experiments increases more than in the Ukraine, providing a larger compensation for the decreased evapotranspiration.

In terms of soil moisture, the -1% EXP essentially reproduces the observed pattern for both regions, showing an increase from 1961-1980 and then leveling off for Ukraine, and a general increase for soil moisture observations for Russia during the entire period. Although model simulations exhibit weaker interannual variations, the simulated soil moisture with dimming included follows that of observations better, especially for the -1% EXP. The correlation coefficients in Fig. 4.5, while not an ideal statistical measure, also support the finding that the -1% EXP produces the best simulations.

The simulated increases in photosynthesis (Figure 4.7) and decreases in canopy conductance (Figure 4.8) with rising CO_2 concentrations are in agreement with the established theory about CO_2 effects. Interestingly, dimming induced similar plant responses as CO_2 effects but with much smaller magnitude. Potential photosynthesis, on the other hand, declined with dimming and the extent is proportional to the dimming

imposed. This seeming paradox can be explained by the increase in soil moisture availability, i.e., larger beta, from reductions in solar radiation. The elevated CO_2 caused, however, very small soil moisture increases in contrast with the constant CO_2 scenario. This is no surprise since in the elevated CO_2 cases, evapotranspiration decreased by only about 0.1%. The lines for the transient CO_2 runs are essentially identical to those for the constant CO_2 runs in Figure 4.5. Over decadal scale, therefore, this model shows that carbon fertilization may have limited influence on regional soil moisture changes. Such effects, however, are not negligible for the past century [*Gedney et al.*, 2006]. Also, model-simulated plant transpiration accounts for only about 30% of the total evapotranspiration for these two regions. Over regions where evapotranspiration is composed of primarily transpiration (e.g., Amazon rainforest), CO_2 effects are likely to cause a much larger sensitivity.

4.5 Final remarks

Recent studies [*Robock et al.*, 2005; *Li et al.*, 2006] show that reanalysis systems and the latest IPCC AR4 models cannot capture the magnitude of the observed soil moisture increase for Ukraine and Russia. In addition to precipitation and temperature, our analysis suggests that solar dimming played a significant role on the regional soil moisture variations. Over aerosol emission source regions, the aerosol effects are expected to continue to play a major role unless effective pollution controls are in effect. In agreement with our results, *Lipert et al.* [2004] argued that reduced surface solar radiation from increasing anthropogenic aerosols are able to reduce evaporation to the extent that it can slow down the water cycling (locally) despite global warming. Thus, the observed intensification of the hydrological cycle over extratropical land is more

likely attributable to increased moisture advection from the oceans rather than to increased local moisture release through evaporation [*Wild et al.*, 2004]. To capture the hydrological cycle and its components more realistically, we need better parameterization systems to characterize aerosol effects in climate models. In spite of the relative small CO_2 effects as indicated from our study on decadal scale, increasing CO_2 may be one of the most important modifiers to water cycle for the past century and the effects may become more conspicuous if CO_2 and other greenhouse gases concentrations keep going up. To that end, these human induced external forcings have to be better understood to reduce uncertainties in future predictions and for better water availability assessments.

The results presented here use a current state-of-the-art land surface model, but should be repeated with other models to test for model dependency on the specifications of evapotranspiration, hydrology, and CO_2 effects. As a complementary, estimates based on a water-mass balance approach [e.g., *Milly and Dunne*, 2001] can also be used to infer the hydroclimatic changes over these regions. Our best agreement between model results and solar dimming are with a dimming slightly larger than that observed at the one available station. A better agreement awaits testing this hypothesis with better data sets and better models.

5 SUMMARY AND CONCLUDING REMARKS

With the objective of improving our understanding of soil moisture climatology and its long term changes, I collected and analyzed ground-based soil moisture observations, and used the observations to evaluate climate model simulations. To answer the scientific questions posed at the beginning, three studies were conducted. Based on the analysis, I summarize the main findings as follows.

How does soil moisture vary on seasonal to interannual scales?

I analyzed the reanalysis soil moisture for East Asian Monsoon climate at the point scale (i.e., point to point comparison) by using 19 yr of Chinese soil moisture observations. Over this region, soil moisture seasonality is not very strong and seasonal fluctuations lie within a small range for the representative stations. A similar pattern is also found for Mongolian soil moisture [*Robock et al.*, 2000, *Li et al.*, 2006]. Soil gets wet during winter and the following spring while it dries out during warm seasons for Central China stations, out of phase with precipitation that mainly pours down in warm seasons [*Srinivasan et al.*, 2000]. The soil is very wet in autumn and winter from 1981-1985. There are anomalous dry periods for 1994-1995 and 1992-1993. Interestingly, drought seems prone to persist long. Similar conclusion is suggested by modeling studies [*Wu and Dickinson*, 2004]. Soil moisture observations are limited to growing seasons only for Northern China stations, with small peaks in late May, likely due to snowmelt recharge. The seasonal variations for Western China stations are small. And drought is a frequent visitor, i.e., more dry years than wet years in terms of soil moisture anomaly for the study period.

With an additional eight years of observations, the results presented here is in agreement with early findings of *Robock et al.* [2000] and *Srinivasan et al.* [2000], indicating the robustness of these analyses. Meanwhile, the soil moisture observations from Western China, though limited to only three stations, give a clue of the soil moisture evolutions in a dry climate for the first time. These observations collectively depict a vivid picture of the climate diversity.

As discussed in chapter 1, soil moisture has crucial role in the climate system and modeling due to its long meteorological memory, contribution to atmospheric predictability, and its active role in land-atmosphere interaction. But the fact is that physical processes of the climate system are too complex and can only be treated with rough approximations by climate models. Consequently, the simulated soil moisture always exhibits disparities from observations, sometimes quite large, in various ways. The reanalysis systems, which assimilate many observed quantities, presumably should produce good soil moisture. *Srinivasan et al.* [2000] evaluated soil moisture simulations in ERA15 and R-1. They concluded reanalyses do capture some of the observed soil moisture variations (better than AMIP models), but the nudging damps out the amplitude of the variations. The weak variability of surface water in R-1 was also found by *Roads et al.* [1999] and they attributed this problem to the nudging term too. Later developments in reanalysis systems, e.g., employing a new land surface scheme in ERA40 and using observed precipitation to adjust soil moisture in R-2 (see chapter 2 for details), are expected to provide better soil moisture simulations than their ancestors. *Maurer et al.* [2001] evaluated the surface water characteristics in R-1 and R-2 with model simulated surface fluxes, and they reported that evapotranspiration in R-2 shows

less biases than R-1. Soil moisture related validations, however, are still too limited to explicitly show how much improvements have been achieved and what aspects should be further improved. I hope that my evaluation work can help end users of reanalysis soil moisture aware limitations of such outputs and also provide useful feedbacks to reanalysis groups for future reanalysis system improvements.

Compared to the Chinese soil moisture observations, R-2 generally shows better interannual variability and better seasonal patterns of soil moisture than R-1 as the result of incorporation of observed precipitation and the removal of nudging term. R-1 has rather small year-to-year changes primarily due to the nudging to a fixed climatology that dominates the interannual variations. *Kanamitsu et al*. [2002] found improved soil moisture simulations in R-2 compared to R-1 for Illinois. My results support their conclusions showing evidence from a different region.

ERA40 produces a better mean value of soil moisture for most Chinese stations and good interannual variability. ERA40 is also generally highly correlated with observations after removing seasonal cycle, and produces less bias to observations. This might be attributable to the new land surface scheme employed and using screen-level information to constrain soil moisture errors.

Dirmeyer et al. [2004] compared ERA40, R-1 and R-2 with observed soil moisture. They concluded that the mean annual cycle is generally better simulated than interannual variations, particularly where there are pronounced wet and dry seasons. My recent evaluation of IPCC models also suggest models generally capture the observed seasonal cycles better if the observed soil moisture exhibits strong seasonal changes. The exact reasons are unknown yet but this issue definitely deserves further studies.

Limited observations in the spring indicate a spring soil moisture peak for most of the stations. ERA40 generally reproduced this event, while R-1 or R-2 generally did not capture this feature, either because the soil was already saturated or the deep soil layer is too thick and damps such a response. This feature should be further investigated preferably in a cold climate where snowmelt has significant contribution to spring runoff and soil moisture recharge. Because higher temperature with global warming can lead to a shift in peak river runoff to winter and early spring and result in a shortage of water in summer and autumn when the demand is highest [*Barnett et al.*, 2005], particularly for mid to high latitudes and over mountainous areas where snow is an important water source.

The persistence of soil moisture anomalies, or the temporal scale, has significant impact on land-atmosphere interaction and atmospheric predictability. We estimated the temporal scale of soil moisture in reanalyses. We found the soil moisture memory in R-2 is far too large compared to observations and to R-1 and ERA40. Our calculations are complementary to the findings of *Roads et al.* [1999] suggesting that the deep layer in R-2 is too thick and dominates the overall variability of soil moisture. This also highlights the importance of vertical resolution of soil column in the land surface scheme which can be improved by using, e.g., a simple geometric progression approach that is used in many modern land surface models as recognition of stronger gradient and activities near the surface.

As many other aspects of reanalysis systems are being continuously improved, I suggest a complete update/replacement of the current land surface model used in R-1 and R-2 with a more physically realistic model, e.g., its descendant, the Noah model that has

been extensively assessed and has been implemented in Eta data assimilation system and in NCEP's 25-year North American Regional Reanalysis [*Mitchell et al.*, 2005].

For future reanalysis projects or improvements, it is desirable to directly assimilate precipitation forcing and drop the soil moisture adjustment, or even directly assimilate satellite soil moisture [*Lu et al.*, 2005] which is currently in an experimental stage [e.g., *Reichle and Koster*, 2005]. This can close the water budget and is expected to provide more physically realistic soil moisture simulations. Moreover, to provide realistic past climate analysis, the reanalysis systems should also allow the greenhouse gases to change, which means the vegetation dynamics should be incorporated into the current land surface schemes.

Lu et al. [2005] recently evaluated R-2 and R-1 with extensive soil moisture observations from GSMDB. They argued "because of the lack of large-scale, long-term, and continuous observations of soil moisture, it remains very challenging to evaluate model generated soil moisture fields." This is true, but some high quality data sets are emerging, e.g., soil moisture observations from Oklahoma Mesonet and data sets from Gravity Recovery and Climate Experiment. The former is extremely useful to understand hydrometeorology on sub-daily to daily scales as demonstrated in NLDAS projects [e.g., *Robock et al.*, 2003; *Luo et al.*, 2003b; *Schaake et al.*, 2004] and the latter can be used to investigate the water storage changes at continental scale. Also, outputs from the NCEP's 25-year North American Regional Reanalysis might be utilized to understand hydroclimate and to improve the hydroclimatic simulations in reanalyses. The prerequisite, of course, is that such regional reanalysis products, presumably better than the global reanalysis, are validated with available observations. These data sets together

should be able to provide more insights and improve our understanding of the hydrological aspects of climate system.

How has soil moisture changed for the past several decades?

Robock et al. [2005] showed summer soil moisture for Ukraine increased for the past 45 years. Such changes are not captured by ERA40 and R-1. I further extended their analysis by including 42 yr observations for Russia and found the patterns are similar. This seems contradictory to the classic summer drying issue. However, we should be aware that Russia and Ukraine are the only places on the planet that we have such long soil moisture observations, so my results may not necessarily apply elsewhere, in different climate regimes.

To see whether the IPCC models can capture the observed features, I analyzed soil moisture simulations from a few state-of-the-art models. Soil moisture observations from Russia and Ukraine show significant increases in summer for the period from 1958-1999, which were much larger than most (92%) trends in the model realizations. Those two model realizations that have comparable trends to those of observations are due to internal model variability other than external forced response that is suggested by the sensitivity experiments detailed in Chapter 4. Given model's fidelity to reproduce temperature changes even for small regions with an area of about 1.0×10^6 km^2 (the Ukrainian box), my analysis highlights the fact that models are capable of reproducing climate changes but not in every aspect. There is still a long way for climate modelers to realistically represent the hydrological cycle in climate modeling systems.

Sun et al. [2005] recently evaluated daily precipitation in IPCC models. They found IPCC models are able to simulate the land precipitation amount well but most of

them are unable to capture precipitation frequency and intensity correctly. Most models overestimate the frequency for light precipitation (1–10 mm/day) but produce patterns of the intensity similar to observations. On the contrary, most models considerably underestimate the intensity but simulate the frequency relatively well for heavy precipitation (>10 mm/day). Similar findings are suggested by *Dai* [2005] who also discovered the newest generation of coupled models rains too frequently, mostly within the 1-10 mm/day category. Future studies should try to investigate how such distorted precipitation features may affect soil moisture on daily to monthly scales.

What are the likely reasons for such changes?

Changes in precipitation and temperature alone are not enough to explain the magnitudes of the observed increases, which implies that other factors might have a significant contribution. We propose that changes in solar irradiance (the dimming effect) and resultant evaporative demand explain most of the observed soil moisture trends. To test this hypothesis, we analyzed soil moisture outputs in a special version of the ECHAM5 model that was capable of capturing the observed radiation pattern as a result of incorporating a sophisticated aerosol scheme. While the radiation pattern was fairly well simulated, precipitation was still quite different from observations, so the model was not able to reproduce the observed soil moisture trends. Results suggest that both radiation and precipitation patterns are required to be adequately simulated to reproduce the observed soil moisture trends realistically.

To further validate the hypothesis of solar dimming effects on regional soil moisture, I conducted a series offline sensitivity experiments with a sophisticated land surface model, forced by realistic precipitation and temperature. This avoids problematic

precipitation in coupled models that may cause difficulties in explaining the results. I also examined possible contribution from CO_2 effects, mainly the physiological responses of plants. I demonstrate, by imposing a downward trend to shortwave radiation forcing to mimic the dimming, the observed soil moisture pattern can be essentially reproduced. On the other hand, the effects of elevated CO_2 are relatively small for the past 40 yrs. The results suggest solar dimming plays an important role in land water storage at regional scale and thus support our hypothesis.

The answer is not fully satisfactory yet due to lack of observations to validate the exact magnitude of solar dimming. Observations from a single ground station are not enough to derive regional solar radiation changes. Satellite data sets are available but are too short to tell us what happened before 1980s. Models then probably are the best tools we have (until we are confident they are good enough). I am also aware that important aspects of structural changes (more LAI and more roots) from plant growth under rising CO_2 are not considered in this study. So the idea should be further validated with other models including these features. To fully account for land and atmosphere interactions, it is desirable to use coupled models. In this case, observed precipitation probably should be assimilated so that the sensitivity of soil moisture and/or water storage to other changes can be better sort out.

In spite of a high likelihood of cause and effect relationship between solar dimming and soil moisture increases for Ukraine and Russia, this study by no means tried to rule out other possibilities that might also contribute to the observed soil moisture increase. For example, changes in soil physical properties (e.g., field capacity, wilting point), resulting from natural environmental changes or human management, might also

have played a role. Unfortunately, these properties are usually treated to be time invariant constants, and thus are not available for attribution study. But a simple scenario calculation might provide some insights. The area averaged wilting level for Ukraine is about 20 % (volumetric percent) 40 years ago. Let's assume half of the observed soil moisture increases are attributable to changes in wilting level. Wilting level for top 0-1 m soil will be around 22% now, roughly 2 cm increase – a rather noticeably increase. Greater share of historical/existing observational records and freer exchange of data among scientists across political boundaries in future should help a better and comprehensive understanding of climatic changes.

Final remark

Just taking a glimpse of the statistics in the subject of soil moisture and climate, I am glad to find the science community is increasingly aware of the importance of soil moisture to climate. A total of 2,132 papers have been published in science citation index journals since 1993 (source: www.isiknowledge.com). And the trend is that more papers are published every year. In 1993, there are only nine papers appeared in this field. This number increased to 256 in 2005, and 151 papers were published already this year (as of July 21, 2006) (Figure 5.1).

The soil moisture observations archived at GSMDB are far more useful than I showed in my graduate work. Since the GSMDB website update on June 9, 2004 (see Figure 5.2 for a snapshot of the website), there are 7,265 visits to the data bank as of July 22, 2006 (same day repeated visits from the identical IP not accounted). These visits themselves already suggest the importance of *in situ* soil moisture observations. I am sure the users are not just climate scientists. These ground-based observations, together

with other emerging products from satellites and other instruments, eventually can help us for a better understanding of hydroclimate.

References

Abakumova, G. M., E. M. Feigelson, V. Bussak, and V. V. Stadnik (1996), Evaluation of long term changes in radiation, cloudiness and surface temperature on the territory of the former Soviet Union, *J. Climate*, *9*, 1319-1327.

Adler R. F., et al. (2003), The Version-2 Global Precipitation Climatology Project (GPCP) monthly precipitation analysis (1979–present). *J. Hydrometeor., 4*, 1147–1167.

Avissar, R., and R.A. Pielke (1989), A parameterization of heterogeneous land-surface for atmospheric numerical models and its impact on regional meteorology, *Mon. Wea. Rev., 117,* 2113-2136.

Avissar, R. (1995), Recent advances in the representation of land-atmosphere interactions in global climate models. *Rev. Geophys.*, *33*, 1005-1010.

Ball J. T. (1988), An analysis of stomatal conductance. Ph. D. Thesis, Stanford University, CA, 89 pp.

Barnett, T. P., J. C. Adam and D. P. Lettenmaier (2005), Potential impacts of a warming climate on water availability in snow-dominated regions. *Nature*, *438*, 303-309.

Beljaars, A. C. M., P. Viterbo, M. J. Miller, and A. K. Betts (1996), The anomalous rainfall over the US during July 1993: Sensitivity to land surface parameterization. *Mon. Weather Rev., 124*, 362-383.

Bengtsson, L., and J. Shukla (1988), Integration of space and in situ observations to study global climate change. *Bull. Amer. Meteor. Soc.*, *69*, 1130-1143.

Betts, A. K., J. H. Ball, and A. C. M. Beljaars (1993), Comparison between the land surface response of the ECMWF model and the FIFE-1987 data, *Quart. J. Roy. Meteorol. Soc., 119,* 975-1001.

Betts, A. K., J. H. Ball, A. C. M. Beljaars, M. J. Miller, and P. Viterbo, Coupling between land-surface, boundary-layer parameterizations and rainfall on local and regional scales: Lessons from the wet summer of 1993, (1994), *Fifth Conference on Global Change Studies,* Nashville, TN, January 23-28, Amer. Meteorol. Soc., Boston, MA.

Betts, A. K., J. H. Ball, A. C. M. Beljaars, M. J. Miller, and P. Viterbo (1996), The land surface-atmosphere interaction: A review based on observations and global modeling perspectives. *J. Geophys. Res.*, *101*, 7209-7225.

Bonan, G. B. (1995), Land-atmosphere CO_2 exchange simulated by a land surface process model coupled to an atmospheric general circulation model. *J. Geophys. Res.*, *100D*, 2817-2831.

Bonan, G. B., et al. (2002), The land surface climatology of the Community Land Model coupled to the NCAR Community Climate Model, *J. Clim.*, *15*, 3123–3149.

Bosilovich, M. G., S. D. Schubert, and G. K. Walke (2005), Global change of the water cycle intensity, *J. Clim.*, *18*, 1591-1608.

Chen, F., et al. (1996), Modeling of land-surface evaporation by four schemes and comparison with FIFE observations. *J. Geophys. Res.*, *101*, 7251-7268.

Chen, F., Z. Janjic and K. E. Mitchell (1997), Impact of atmospheric-surface layer parameterizations in the new land-surface scheme of the NCEP mesoscale Eta numerical model. *Boundary Layer Meteorol., 85*, 391-421.

Chen, M., P. Xie, J. E. Janowiak, and P. A. Arkin (2002), Global land precipitation: A 50-yr monthly analysis based on gauge observations. *J. Hydrometeor.*, *3***,** 249-266.

Chen, T. H., et al. (1997), Cabauw experimental results from the Project for Intercomparison of Land-surface Parameterization Schemes (PILPS). *J. Clim.*, 10, 1194-1215.

Collatz, G. J., J. T. Ball, C. Grivet, and J. A. Berry (1991), Physiological and environmental regulation of stomatal conductance, photosynthesis, and transpiration: A model that includes a laminar boundary layer. *Agric. For. Meteorol. 54*, 107-136.

Collatz, G. J., M. Ribas-Carbo, and J. A. Berry (1992), Coupled photosynthesis-stomatal conductance model for leaves of C plants. *Aust. J. Plant Physiol. 19*, 519-538.

Cosgrove, B. A., et al. (2003), Land surface model spinup behavior in the North American Land Data Assimilation System (NLDAS). *J. Geophys. Res.*, *108 (D22)*, 8845, doi:10.1029/2002JD003119.

Cox, P. M., et al. (1999), The impact of new land surface physics on the GCM simulation of climate and climate sensitivity. *Climate Dyn.*, *15*, 183-203.

Dai, A. (2006), Precipitation characteristics in eighteen coupled climate models. *J. Clim.*, in press.

Dai, A., T. R. Karl, B. Sun, and K. E. Trenberth (2005), Recent trends in cloudiness over the United States: A tale of monitoring inadequacies. *Bull. Am. Met. Soc.*, in press

Daly, E. A. Porporato, I. Rodriguez-Iturbe (2004), Coupled dynamics of photosynthesis, transpiration, and soil water balance. Part I: upscaling from hourly to daily level, *J. Hydrometeor.*, *5*, 546-558

Delworth, T., and S. Manabe (1988), The influence of potential evaporation on the variabilities of simulated soil wetness and climate. *J. Clim.*, *1*, 523-547.

Delworth, T., and S. Manabe (1993), Climate variability and land surface processes. *Adv. Water Resources*, *16*, 3-20.

Dickinson, R. E. (1995), Land atmosphere interaction, *Rev. Geophys*, *33*, 917-922.

Dickinson, R. E., A. Henderson-Sellers, P. J. Kennedy, and M. F. Wilson (1986), *Biosphere-Atmosphere Transfer Scheme (BATS) for the NCAR Community Climate Model,* NCAR Technical Note: NCAR/TN-275+STR, p. 69.

Dirmeyer, P. A. (2000), Using a global soil wetness data set to improve seasonal climate simulation. *J. Clim.*, *13*, 2900-2922.

Dirmeyer, P. A., Z. Guo, and X. Gao (2004), Validation and forecast applicability of multi-year global soil wetness products, *J. Hydrometeor.*, *5,* 1011-1033.

Dorman, J. L., and P. J. Sellers (1989), A global climatology of albedo, roughness length and stomatal resistance for atmospheric general circulation models as represented by the Simple Biosphere model (SiB). *J. Appl. Meteor.*, *28*, 833-855.

Dougherty, R. L., J. A. Bradford, P. I. Coyne, and P. L. Sims (1994), Applying an empirical model of stomatal conductance to three C-4 grasses. *Agric. For. Meteor.*, *67*, 269-290.

Douville, H., P. Viterbo, J.-F. Mahfouf, and A. C. M. Beljaars (2000), Evaluation of the optimal interpolation and nudging techniques for soil moisture analysis using FIFE data. *Mon. Wea. Rev.*, *128*, 1733-1756.

Ducharne A., R. D. Koster, M. J. Suarez, M. Stieglitz, and P. Kumar (2000), A catchment-based approach to modeling land surface processes in a general circulation model. 2. Parameter estimation and model demonstration. *J. Geophys. Res.*, *105*, 24823-24838.

Durre, I., J. M. Wallace, and D. P. Lettenmaier (2000), Dependence of extreme daily maximum temperatures on antecedent soil moisture in the contiguous United States during summer. *J. Clim.*, *13*, 2641-2651.

Eastman, J. L., M. B. Coughenour, and R. A. Pielke (2001), The effects of CO_2 and landscape change using a coupled plant and meteorological model, *Glob. Change Biol.*, *7*, 797-815.

Ek, M. B., et al. (2003), Implementation of Noah land surface model advances in the National Centers for Environmental Prediction operational mesoscale Eta model, *J. Geophys. Res.*, *108 (D22)*, 8851, doi:10.1029/2002JD003296.

Eltahir, E. A. B. (1998), A soil moisture-rainfall feedback mechanism 1. theory and observations. *Water Resour. Res.*, *34*, 765-776

Entin, J., et al. (1999), Evaluation of Global Soil Wetness Project soil moisture simulations, *J. Meteorol. Soc. Japan*, *77*, 183-198.

Entin, J., et al. (2000), Temporal and spatial scales of observed soil moisture variations in the extratropics. *J. Geophys. Res.*, *105*, 11,865-11,877.

Essery, R., M. Best, and P. Cox (2001), MOSES2.2 Technical Documentation, *Hadley Centre Technical Note No. 30* (http://www.metoffice.com/research/hadleycentre/ pubs/HCTN), Met. Office, UK.

Eur. Cen. For Medium-Range Weather Forecast (2003), IFS Documentation (CY23r4), http://www.ecmwf.int/research/ifsdocs/CY23r4.

Farquhar, G. D., S. Caemmerer, and J. A. Berry (1980), A biochemical model of photosynthetic CO_2 assimilation in leaves of C species. *Planta*, *149*, 78-90.

Field, C., R. Jackson, and H. Mooney (1995), Stomatal responses to increased CO_2: Implications from the plant to the global-scale, *Plant Cell Environ.*, *18*, 1214-1255.

Food and Agriculture Organization (FAO) of the United Nations, 1970-78: *Soil map of the world*, scale 1:5,000,000, volumes I-X: United Nations Educational, Scientific, and Cultural Organization, Paris.

Friend, A. D., and N. Y. Kiang (2005), Land surface model development for the GISS GCM: Effects of improved canopy physiology on simulated climate, *J. Clim.*, *18*, 2883-2902.

Gates, W. L. (1992), AMIP: the Atmospheric Model Intercomparison Project, *Bull. Amer. Meteorol. Soc.*, *73*, 1962-1970.

Gedney, N., et al. (2006), Detection of a direct carbon dioxide effect in continental river runoff records, *Nature*, *439*, 835-838, doi:10.1038/nature04504.

Gibson, J. K., et al. (1997), *ERA Description*. ECMWF Reanal. Proj. Rep. Ser. 1. Eur. Cen. For Medium-Range Weather Forecast, Reading, UK, 77 pp

Gilgen, H., M. Wild, and A. Ohmura (1998), Means and trends of shortwave irradiance at the surface estimated from Global Energy Balance Archive data, *J. Climate*, *11*, 2042-2061.

Gilgen, H., and A. Ohmura (1999), The Global Energy Balance Archive, *Bull. Am. Meteorol. Soc.*, *80(5)*, 831–850.

Gregory, J. M., J. F. B. Mitchell, and A. J. Brady (1997), Summer drought in northern midlatitudes in a time-dependent CO2 climate experiment, *J. Clim.*, *10*, 662– 686.

Guo, Z., P. A. Dirmeyer, X. Gao, and M. Zhao (2005), Improving the quality of simulated soil moisture with a multi-model ensemble approach, *COLA Technical Report*, 187.

Harte J., et al., (1995), Global warming and soil microclimate: Results from a meadow-warming experiment. *Ecological Applications.*, *5*,132–150.

Hartmann, D. L. 1994, *Global Physical Climatology.* Academic Press, 411 pp.

Henderson-Sellers, A., A. J. Pitman, P. K. Love, P. Irannejad, and T. H. Chen (1995a), The project for intercomparison of land surface parameterisaton schemes (PILPS) Phases 2 and 3, *Bull. Amer. Meteorol. Soc.*, *76*, 489-503.

Henderson-Sellers, A., K. Mcguffie, and C. Gross (1995b), Sensitivity of global climate model simulations to increased stomatal resistance and CO$_2$ increases, *J. Clim.*, *8*, 1738-1759.

Henderson-Sellers, A., K. McGuffie, A. J. Pitman (1996), The Project for Intercomparison of Land-surface Parameterization Schemes (PILPS): 1992 to 1995, *Climate Dyn.*, *12*, 849-859.

Henderson-Sellers, A., P. Irannejad, K. McGuffie, A. Pitman (2003), Predicting land-surface climates-better skill or moving targets? *Geophys. Res. Lett.*, *30*, 1777.

Hirsch, R. M., J. R. Slack, and R. A. Smith (1982), Techniques of trend analysis for monthly water quality data, *Water Resour. Res.*, *18*, 107-121.

Hollinger, S. E., and S. A. Isard (1994), A soil moisture climatology of Illinois, *J. Clim.*, *7*, 822-833.

Intergovernmental Panel on Climate Change (IPCC, 2001), *Climate Change 2001: The Science of Climate Change*, edited by J. T. Houghton et al., 944 pp., Cambridge Univ. Press, New York.

Irannejad, P., A. Henderson-Sellers, Y. Shao, and P. K. Love (1995), Comparison of AMIP and PILPS off-line land surface simulation, 1st Int. AMIP Scientific Conf., Monterey, California, USA, WRCP-92, WMO/TD-No. 732, 465– 470.

Jones, P. D. and A. Moberg (2003), Hemispheric and large-scale surface air temperature variations: An extensive revision and an update to 2001. *J. Clim.*, *16*, 206-223.

Kagan, R. L. (1997), *Averaging of Meteorological Fields.* 279 pp., Kluwer Acad., Norwell, Mass.

Kalnay, E., et al. (1996), The NCEP/NCAR 40-year reanalysis project. *Bull. Amer. Meteor. Soc.*, *77*, 437-471.

Kanamitsu, M., et al. (2002), NCEP-DOE AMIP –II reanalysis (R-2), *Bull. Amer. Meteor. Soc.*, *83*, 1631-1643.

Kanamitsu, M., C. Lu, J. Schemm and W. Ebisuzaki (2003), The predictability of soil moisture and near-surface temperature in hindcasts of the NCEP seasonal forecast model. *J. Clim., 16*, 510-521.

Karl, T. R., and K. Trenberth (2003), Modern global climate change, *Science*, *302*, 1719-1723.

Keeling, C. D., et al. (2005), Scripps Institute of Oceanography (available at http://cdiac.ornl.gov/ftp/trends/co2/maunaloa.co2)

Kistler, R., et al. (2001), The NCEP-NCAR 50-year reanalysis: Monthly means CD-ROM and documentation, *Bull. Amer. Meteorol. Soc.*, *82*, 247-267.

Koster, R. D. and M. J. Suarez (1992), Modeling the land surface boundary in climate models as a composite of independent vegetation stands. *J. Geophys. Res., 97*, 2697-2715,

Koster, R. D. and M. J. Suarez (2001), Soil moisture memory in climate models, *J. Hydrometeor., 2*, 558-570.

Koster, R. D., M. J. Suarez, and M. Heiser (2000a), Variance and predictability of precipitation at seasonal-to-interannual timescales, *J. Hydrometeor., 1,* 26–46,

Koster, R. D., M. J. Suarez, A. Ducharne, M. Stieglitz, and P. Kumar (2000b), A catchment-based approach to modeling land surface processes in a general circulation model. 1. Model structure. *J. Geophys. Res.*, *105(D20)*, 24809-24822.

Koster, R. D., P. A. Dirmeyer, P. C. D. Milly, and G. L. Russell (2001), Comparing GCM-generated land surface water budgets using a simple common framework. In, *Land Surface Hydrology, Meteorology, and Climate: Observations and Modeling*, Water Science and Application, Vol. 3, Washington, DC: American Geophysical Union, 95-105.

Koster, R. D., and P. C. D. Milly (1997), The interplay between transpiration and runoff formulations in land surface schemes used with atmospheric models, *J. Clim.*, *10*, 1578-1591.

Koster, R. D., et al. (2004), Regions of strong coupling between soil moisture and precipitation. *Science*, *305*, 1138-1140.

Lau, N.-C., and M. J. Nath (1990), A general circulation model study of the atmospheric response to extratropical SST anomalies observed in 1950-1979. *J. Clim.*, *2*, 965-989.

Legates, D. R. and C. J. Willmott (1990), Mean seasonal and spatial variability in gauge-corrected, global precipitation, *Int. J. Climatol.*, *10*, 111-127.

Levis S, J. A. Foley, D. Pollard (2000), Large scale vegetation feedbacks on a doubled CO_2 climate. *J. Clim., 13*, 1313–1325.

Li, B., and R. Avissar (1994), The impact of spatial variability of land-surface characteristics on land-surface heat fluxes, *J. Clim., 7*, 527-537.

Li, H., A. Robock and M. Wild (2006), Evaluation of Intergovernmental Panel on Climate Change Fourth Assessment Soil Moisture Simulations for the Second Half of the Twentieth Century, submitted to *J. Geophys. Res.*

Li, H., A. Robock, S. Liu, X. Mo, and P. Viterbo (2005), Evaluation of reanalysis soil moisture simulations using updated Chinese soil moisture observations, *J. Hydrometeor.*, *6*, 180-193.

Liepert B. G. (2002), Observed reductions of surface solar radiation at sites in the United States and worldwide from 1961 to 1990, *Geophys. Res. Lett.*, *29(10)*, doi:10.1029/2002GL014910.

Liepert, B. G., J. Feichter, U. Lohmann, and E. Roeckner (2004), Can aerosols spin down the water cycle in a warmer and moister world?, *Geophys. Res. Lett.*, *31*, L06207, doi:10.1029/2003GL019060.

Liu, S., X. Mo, H. Li, G. Peng, and A. Robock (2001), Spatial variation of soil moisture in China: Geostatistical characterization. *J. Meteorol. Soc. Japan*, *79*, 555-574.

Lorenz, E. N. (1963), Deterministic nonperiodic flow. *J .Atmos. Sci.*, *20*,130-141.

Lorenz, E. N. (1993), *The Essence of Chaos.*, University of Washington Press, Seattle, 227 pp.

Love, P. K., A. Henderson-Sellers, and P. Irannejad (1995), AMIP diagnostic subproject 12 (PILPS Phase-3): Land surface processes. 1st Int. AMIP Scientific Conference Proc., Monterey, California, USA, WRCP-92, WMO/TD-No. 732, 465– 470.

Lu, C.-H., et al. (2005), Evaluation of Soil Moisture in the NCEP–NCAR and NCEP–DOE Global Reanalyses, *J. Hydrometeor.*, *6*, 391-408.

Luo, L., et al. (2003a), Effects of frozen soil on soil temperature, spring infiltration, and runoff: Results from the PILPS 2(d) experiment at Valdai, Russia, *J. Hydrometeor.*, *4*, 334-351.

Luo, L., et al. (2003b), Validation of the North American Land Data Assimilation System (NLDAS) retrospective forcing over the Southern Great Plains. *J. Geophys. Res.*, *108 (D22)*, 8843, doi:10.1029/2002JD003246.

Luo, L. (2003), Evaluation of land surface models using ground-based point-scale measurements. Ph.D. thesis, Rutgers University, 143pp.

Lynn, B. H., D. Rind, and R. Avissar (1995), The importance of mesoscale circulations generated by subgrid-sale landscape heterogeneities in general circulation models. *J. Clim.*, *8*, 191-205.

Mahfouf, J.-F., P. Viterbo, H. Douville, A. C. M. Beljaars and S. Saarinen (2000), A revised land-surface analysis scheme in the integrated forecasting system. *ECMWF Newsletter*, *88*, 8-13.

Mahrt, L. and H.-L. Pan (1984), A two layer model of soil hydrology. *Bound. Layer Meteorol.*, *29*, 1-20.

Manabe, S., and R. T. Wetherald (1987), Large-scale changes of soil wetness induced by an increase in atmospheric carbon dioxide, *J. Atmos. Sci.*, *44*, 1211-1235.

Manabe, S. (1969), Climate and the ocean circulation 1. the atmospheric circulation and the hydrology of the earth's surface. *Mon. Weather. Rev.*, *97*, 739-774.

Manabe, S., P. C. D. Milly, and R. Wetherald (2004), Simulated long-term changes in river discharge and soil moisture due to global warming, *Hydrol. Sci. J.*, *49*, 625-643.

Maurer, E. P., A. W. Wood, J. C. Adam, D. P. Lettenmaier, B. Nijssen (2002), A Long-Term Hydrologically Based Dataset of Land Surface Fluxes and States for the Conterminous United States. *J. Clim.*, *15*, 3237-3251

Maurer, E. P., G. M. O'Donnell, D. P. Lettenmaier, and J. O. Roads (2001), Evaluation of the land surface water budget in NCEP/NCAR and NCEP/DOE reanalyses using an off-line hydrologic model, *J. Geophys. Res.*, *106(D16)*, 17,841-17,862.

McCumber, M. C., and R. A. Pielke (1981), Simulation of the effects of surface fluxes of heat and moisture in a mesoscale numerical model, 1. soil layer, *J. Geophys. Res.*, *86*, 9929-9938.

Meehl, G. A., and W. M. Washington (1988), A comparison of soil-moisture sensitivity in two global climate models, *J. Atmos. Sci.*, *45*, 1476-1492.

Meehl, G. A., C. Covey, and M. Latif (2004), Soliciting participation in climate model analyses leading to IPCC Fourth Assessment Report, *EOS*, *85*, 274.

Milly, P. C. D. (1997), Sensitivity of greenhouse summer dryness to changes in plant rooting characteristics. *Geophys. Res. Lett., 24*, 269-271.

Milly, P. C. D., and K. A. Dunne (1994), Sensitivity of the global water cycle to the water-holding capacity of land. *J. Clim., 7*, 506-526.

Milly, P. C. D., and K. A. Dunne (2001), Trends in evaporation and surface cooling in the Mississippi River basin. *Geophys. Res. Lett.*, *28(7)*, 1219-1222.

Milly, P. C. D., R. T. Wetherald, K. A. Dunne, and T. L. Delworth (2002), Increasing risk of great floods in a changing climate, *Nature*, *415*, 514-517.

Mintz, Y., and Y. V. Serafini (1992), A global monthly climatology of soil moisture and water balance. *Climate Dyn.*, *8*, 13-27.

Mitchell, K., et al. (2004), The Eta regional reanalysis, *GEWEX News*, in press.

Mitchell, K., H. L. Wei, S. Lu, G. Gayno and J. Meng (2005), NCEP Implements Major Upgrade to Its Medium-Range Global Forecast System, Including Land-Surface Component, *GEWEX News*, *15(4)*, 8.

Mitchell, T. D., T. R. Carter, P. Jones, M. Hulme, M. New (2004), A comprehensive set of highresolution grids of monthly climate for Europe and the globe: the observed record (1901- 2000) and 16 scenarios (2001-2100). *J. Clim.*, submitted.

New, M., D. Lister, M. Hulme and I. Makin (2002), A high-resolution data set of surface climate for terrestrial land areas. *Climate Res., 21*, 1-25.

New, M., M. Hulme, and P. Jones (1999), Representing twentieth-century space-time climate variability, Part I: Development of a 1961 – 90 mean monthly terrestrial climatology, *J. Clim.*, *12*, 829-856.

New, M., M. Hulme, and P. Jones (2000), Representing twentieth-century space-time climate variability, Part II: Development of a 1901 – 90 mean monthly grids of terrestrial surface climate*, J. Clim.*, *13*, 2217-2238.

Ngo-Duc, T., J. Polcher and K. Laval (2005), A 53-year forcing data set for land surface models. *J. Geophys. Res.*, *110*, D06116, doi:10.1029/2004JD005434.

Nijssen, B., R. Schnur, and D. P. Lettenmaier (2001), Global retrospective estimation of soil moisture using the Variable Infiltration Capacity land surface model, 1980-1993. *J. Clim.*, *14*, 1790-1808.

Niu, G.-Y., and Z.-L. Yang (2003), The Versatile Integrator of Surface and Atmosphere processes (VISA) Part II: Evaluation of three topography based runoff schemes, *Global Planet. Change*, *38*, 191– 208.

Niu, G.-Y., and Z.-L. Yang (2006), Effects of frozen soil on snowmelt runoff and soil water storage at a continental scale, *J. Hydrometeor.*, in press.

Niu, G.-Y., Z.-L. Yang, R. E. Dickinson, and L. E. Gulden (2005), A simple TOPMODEL-based runoff parameterization (SIMTOP) for use in GCMs, *J. Geophys. Res.*, *110*, D21106, doi:10.1029/2005JD006111.

Oleson, K. W., et al. (2004), *Technical Description of the Community Land Model (CLM)*, NCAR Technical Note NCAR/TN-461+STR, National Center for Atmospheric Research, Boulder, Colorado, 173 pp.

Pan, H.-L. (1990), A simple parameterization scheme of evapotranspiration over land for the NMC medium-range forecast model. *Mon. Weather Rev.*, *118*, 2500-2512.

Peterson, T. C., V. S. Golubev, and P. Y. Groisman (1995), Evaporation losing its strength, *Nature*, *377*, 687-688.

Pielke, R. A. (2001), Influence of the spatial distribution of vegetation and soils on the prediction of cumulus convective rainfall, *Rev. Geophys.*, *39*, 151-177.

Pielke, R. A., G. A. Dalu, J. S. Snook, T. J. Lee, and T. G. F. Kittel (1991), Nonlinear influence of mesoscale land use on weather and climate, *J. Clim., 4,* 1053-1069.

Pinker, R. T., B. Zhang, E. G. Dutton (2005), Do satellites detect trends in surface solar radiation? *Science*, *308*, 850-854.

Pitman, A. J. (2003), The evolution of, and revolution in, land surface schemes designed for climate models, *Int. J. Climatol.*, *23*, 479-510.

Pitman, A. J. et al. (1993), Results from off-line control simulations (Phase 1a), PILPS, *GEWEX Report*, IGPO Pub. Ser. 7, 47 pp.

Pitman, A. J., and A. Henderson-Sellers (1998), Recent progress and results from the project for the intercomparison of land surface parameterization schemes, *J. Hydrol. (Amsterdam)*, 128-135.

Qian, T., A. Dai, K. E. Trenberth, and K. W. Oleson (2006), Simulation of global land surface conditions from 1948-2004. Part I: Forcing data and evaluation. *J. Hydrometeor.*, in press.

Qu, W. Q., and A. Henderson-Sellers (1998), Comparing the scatter in PILPS offline experiments with those in AMIP I coupled experiments, *Global Planet. Change*, *19*, 209– 224.

Qu, W. Q., et al. (1998), Sensitivity of latent heat flux from PILPS land-surface schemes to perturbations of surface air temperature, *J. Atmos. Sci.*, *55*, 1909-1926.

Quinn, P., Beven K., and Culf A. (1995), The introduction of macroscale hydrological complexity into the land surface atmosphere models and the effect on planetary boundary layer development. *J. Hydrol.*, *166*, 421-444.

Ramanathan, V., P. J. Crutzen, J. T. Kiehl, and D. Rosenfeld (2001), Aerosols, climate and the hydrological cycle, *Science*, *294*, 2119–2124.

Reichle, R. H., and R. D. Koster (2005), Global assimilation of satellite surface soil moisture retrievals into the NASA Catchment land surface model, *Geophys. Res. Lett.*, *32*, L02404, doi:10.1029/2004GL021700.

Roads, J. O., S. -C. Chen, M. Kanamitsu, and H. Juang (1999), Surface water characteristics in NCEP Reanalysis and Global Spectral Model. *J. Geophys. Res.*, *104(D16)*, 19,307-19,327.

Robock, A., C. A. Schlosser, K. Y. Vinnikov, N. A. Speranskaya, and J. K. Entin (1998), Evaluation of AMIP soil moisture simulations, *Glob. Planetary Change*, *19,* 181-208.

Robock, A., K. Y. Vinnikov, and C. A. Schlosser (1997), Evaluation of land-surface parameterization schemes using observations. *J. Clim.*, *10*, 377-379.

Robock, A., K. Y. Vinnikov, C. A. Schlosser, N. A. Speranskaya, and Y. Xue (1995), Use of midlatitude soil moisture and meteorological observations to validate soil moisture simulations with biosphere and bucket models. *J. Clim.*, *8*, 15-35.

Robock, A., and H. Li (2006), Solar dimming and CO_2 effects on soil moisture trends, submitted to *Geophys. Res. Lett*.

Robock, A., M. Mu, K. Y. Vinnikov, and D. Robinson (2003), Land surface conditions over Eurasia and Indian summer monsoon rainfall, *J. Geophys. Res.*, *108(D4),* 4131, doi:10.1029/2002JD002286

Robock, A., M. Mu, K. Y. Vinnikov, I. V. Trofimova, and T. I. Adamenko (2005), Forty five years of observed soil moisture in the Ukraine: No summer desiccation (yet), *Geophys. Res. Lett.*, *32*, L03401, doi:10.1029/2004GL021914.

Robock, A., et al. (2000), The Global Soil Moisture Data Bank, *Bull. Amer. Meteorol. Soc.*, *81*, 1281-1299.

Robock, A., et al. (2003), Evaluation of the North American Land Data Assimilation System over the Southern Great Plains during the warm season. *J. Geophys. Res.*, *108(D22)*, 8846, doi:10.1029/2002JD003245.

Roderick, M. L., and G. D. Farquhar (2002), The cause of decreased pan evaporation over the past 50 years, *Science*, *298*, 1410-1411.

Roeckner, E., et al. (2003), The atmospheric general circulation model ECHAM5, Part I: Model description, Max Planck Institute for Meteorology. Rep. 349, 127 pp.

Rosenzweig, C. and F. Abramopoulos (1997), Land-surface model development for the GISS GCM, *J. Clim.*, *10*, 2040-2056.

Sato, N., et al. (1989), Effects of implementing the Simple Biosphere Model in a general circulation model, *J. Atmos. Sci.*, *46*, 2757-2782.

Schaake, J. C., et al. (2004), An inter-comparison of soil moisture fields in the North American Land Data Assimilation System (NLDAS). *J. Geophys. Res.*, *109*, D01S90, doi:10.1029/2002JD003309.

Schlosser, C. A., et al. (2000), Simulations of a boreal grassland hydrology at Valdai, Russia: PILPS Phase 2(d), *Mon. Weather Rev*, *128*, 301-321.

Sellers, P. J., Y. Mintz, Y. C. Sud, and A. Dalcher (1986), A simple biosphere model (SiB) for use within general circulation models, *J. Atmos. Sci.*, *43,* 505-531.

Sellers, P. J., et al. (1996a), A Revised Land Surface Parameterization (SiB2) for Atmospheric GCMS. Part I: Model Formulation, *J. Clim.*, *9*, 676–705.

Sellers, P. J., et al. (1996b), Comparison of radiative and physiological effects of doubled atmospheric CO_2 on climate. *Science*, *271 (5254)*, 1402–1406.

Sellers P. J., et al. (1997), Modeling the exchanges of energy, water, and carbon between continents and the atmosphere, *Science*, *275*, 502-509.

Seneviratne, S. I., J. S. Pal, E. A. B. Eltahir, and C. Schar (2002), Summer dryness in a warmer climate: a process study with a regional climate model, *Climate Dyn.*, *20,* 69-85.

Sheffield, J., A. D. Ziegler, E. F. Wood, and Y. Chen (2004), Correction of the high-latitude rain day anomaly in the NCEP/NCAR reanalysis for land surface hydrological modeling, *J. Clim.*, *17*, 3814-3828.

Shukla, J. (1998), Predictability in the midst of chaos: A scientific basis for climate forecasting. *Science*, *282*, 728-731.

Shukla, J., and Y. Mintz (1982), Influence of Land-surface evapotranspiration on the Earth's climate. *Science*, *215*, 1498-1501.

Simmons, A. J., and J. K. Gibson (2000), The ERA-40 Project Plan, ERA-40 Project Report Series No. 1, ECMWF, Shinfield Park, Reading, UK, 63pp.

Srinivasan, G., et al. (2000), Soil moisture simulations in revised AMIP models. *J. Geophys. Res.*, *105*, 26,635-26,644.

Stanhill, G., and S. Cohen (2001), Global dimming: A review of the evidence for a widespread and significant reduction in global radiation with discussion of its probable causes and possible agricultural consequences, *Agric. For. Meteorol.*, *107*, 255-278.

Stern, W., and K. Miyakoda (1995), Feasibility of seasonal forecasts inferred from multiple GCM simulations. *J. Clim.*, *8*, 1071-1085.

Stier, P., et al. (2005), The aerosol-climate model ECHAM5-HAM, *Atmos. Chem. Phys.*, *5*, 1125-1156.

Sun, Y., S. Solomon, A. Dai, and R. Portmann (2006), How often does it rain? *J. Clim.*, *19*, 916-934.

Takata, K., S. Emori, and T. Watanabe (2003), Development of the minimal advanced treatments of surface interaction and runoff, *Glob. Plan. Change*, *38*, 209-222.

Taylor, K. E. (2001), Summarizing multiple aspects of model performance in single diagram, *J. Geophys. Res.*, *106(D7)*, 7183-7192.

Trenberth, K. E., and J. G. Olson (1988), An evaluation and intercomparison of global analyses from NMC and ECMWF. *Bull. Amer. Meteor. Soc.*, *69*, 1047-1057.

United States Geological Survey (USGS), (2004), GTOPO30 Documentation, http://edcdaac.usgs.gov/gtopo30/README.asp.

Van den Hurk., B. J. J. M., P. Viterbo, A. C. M. Beljaars, and A. K. Betts (2000), Offline validation of the ERA40 surface scheme. *ECMWF Tech Memo 295*, 42 pp.

Verseghy, D., N. McFarlane, and M. Lazare (1991), CLASS-A Canadian-land surface scheme for GCMs, Part I: Soil model, *Int. J. Climatol.*, *11*, 111-133.

Vinnikov, K. Y., A. Robock, N. A. Speranskaya, and C. A. Schlosser (1996), Scales of temporal and spatial variability of midlatitude soil moisture, *J. Geophys. Res.*, *101*, 7163-7174.

Vinnikov, K. Y., A. Robock, N. A. Speranskaya, and V. Zabelin (1997), Soil moisture data sets, *GEWEX News*, *7(2)*, May, 8-11.

Vinnikov, K. Y., et al. (1999a), Satellite remote sensing of soil moisture in Illinois, United States. *J. Geophys. Res*., *104*, 4145-4168.

Vinnikov, K. Y., A. Robock, S. Qiu, and J. K. Entin (1999b), Optimal design of surface networks for observation of soil moisture. *J. Geophys. Res*., *104*, 19,743-19,749.

Viterbo, P., and A. C. M. Beljaars (1995), An improved land-surface parameterization in the ECMWF model and its validation. *J. Clim.*, *8*, 2716-2748.

Wang, G. (2005), Agricultural drought in a future climate: Results from fifteen global climate models participating in the Intergovernmental Panel for Climate Change's 4th Assessment. *Climate Dyn.*, *25*, DOI: 10.1007/s00382-005-0057-9.

Wigley, T. M. L., and P. D. Jones (1985), Influences of precipitation changes and direct CO2 effects on streamflow. *Nature*, *314*, 149-152.

Wild, M., A. Ohmura, H. Gilgen, and D. Rosenfeld (2004), On the consistency of trends in radiation and temperature records and implications for the global hydrological cycle, *Geophys. Res. Lett.*, *31*, L11201, doi:10.1029/2003GL019188.

Wild, M., et al. (2005), From dimming to brightening: Decadal changes in solar radiation at Earth's surface, *Science*, *308*, 847-850.

Wild, M., L. Dümenil, and J.-P. Schulz, (1996), Regional climate simulation with a high resolution GCM: surface hydrology. *Climate Dyn., 12,* 755-774.

Wu, W., R. E. Dickinson (2004), Time Scales of Layered Soil Moisture Memory in the Context of Land–Atmosphere Interaction. *J. Clim.*, *17*, 2752-2764.

Xue, Y., F. J. Zeng, and C. A. Schlosser (1996), SSiB and its sensitivity to soil properties-a case study using HAPEX-Mobilhy data. *Glob. Plan. Change*, *13*, 183-194.

Xue, Y., P. J. Sellers, J. L. Kinter, and J. Shukla (1991), A simplified biosphere model for global climate studies. *J. Clim.*, *4*, 345-364.

Zhang, Y-C., W. B. Rossow, A. A. Lacis, V. Oinas, and M.I. Mishchenko (2004), Calculation of radiative fluxes from the surface to top of atmosphere based on ISCCP and other global data sets: Refinements of the radiative transfer model and the input data. *J. Geophys. Res*., *109*, D19105, doi:10.1029/2003JD004457.

Zhu,C., D.W. Pierce, T.P. Barnett, A.W. Wood, and D.P. Lettenmaier (2004), Evaluation of Hydrologically Relevant PCM Climate Variables and Large-scale Variability over the Continental U.S., *Climatic Change*, *62*, 45-74.

Table 2.1. List of soil moisture stations. Stations with "§"were selected in this study. "-" means that different types of vegetation were planted together and "/" means the vegetation changes from year to year. The elevation data with "*" were extracted from a 1 km x 1 km digital elevation map of China (USGS, 2004). Soil types are based on a 1°×1° soil type map of China (FAO, 1970-78), thus providing only the dominant soil type for that particular grid box, which may not be representative of the actual station soil type.

Station ID	Name	Elevation (m)	Soil type	Vegetation	Record Period
1	Huma	177	Silt clay	wheat/bean	1981-1999
2	Jiayin	90	Loam	wheat/bean	1981-1999
3	Fuyu	167	Loam	Not Available	1981-1999
4	Hailun	239	Loam	Not Available	1981-1999
5	Qinggang	205	Loam	wheat	1981-1999
6	Bayan	135	Loam	maize/bean	1981-1999
7	Jiamusi	81	Loam	cabbage-maize-bean	1981-1999
8	Baoqing	83	Loam	bean/wheat	1981-1999
§9	Fuyu2	*134	Loam	maize	1981-1999
10	Haerbin	*154	Silt clay	bean/maize	1981-1999
11	Boli	217	Clay loam	cabbage/beet	1981-1999
12	Hulin	100	Silt clay	wheat-bean	1981-1999
13	Wulanwusu	468	Sand	wheat	1981-1999
14	Tulufan	-49	Clay loam	cotton	1981-1999
§15	Shache	1231	Silt clay	wheat	1981-1999
16	Xilinguole	*1231	Clay loam	grass	1981-1999
17	Yongning	1117	Silt clay	wheat	1981-1999
18	Guyuan	1753	Silt clay	Not Available	1981-1999
19	Huanxian	*1302	Silt clay	wheat	1981-1999
§20	Tongwei	1768	Silt clay	Not Available	1981-1999
§21	Xifengzhen	1421	Silt clay	wheat	1981-1999
22	Xinxiang	79	Clay loam	wheat-maize	1981-1999
§23	Changling	189	Loam	Not Available	1981-1999
§24	Dunhua	524	Silt clay	maize/maize-bean	1981-1999
25	Hainong	*336	Silt clay	maize/millet	1981-1999
26	Chaoyang	169	Loam	Not Available	1981-1999
27	Jianping	*454	Loam	rice-maize-bean-potato	1981-1999
28	Xinmin	31	Loam	vegetables/bean/maize	1981-1999
§29	Jinzhou	*22	Silt clay	Not Available	1981-1999
30	Jinxian	27	Silt clay	maize/potato/bean/vegetables	1981-1999
§31	Tianshui	1083	Silt clay	wheat	1981-1999
32	Lushi	569	Silt clay	wheat-maize	1981-1999
§33	Nanyang	129	Sand	wheat-maize	1981-1999
34	Zhumadian	83	Loam	maize-wheat	1981-1999
35	Nanchong	309	Sand	Not Available	1981-1999
§36	Xuzhou	*46	Clay loam	wheat-potato-bean	1981-1999
37	Suxian	*30	Loam	wheat-bean/sesame	1981-1999
38	Zhenjiang	*15	Clay loam	vegetables-bean-wheat	1981-1999
39	Jinjiang	54	Loam	peanut-sweet potato	1981-1992
40	Baise	174	Clay loam	maize	1981-1999

Table 2.2. Temporal scale of soil moisture variation (months) for observations and each reanalysis for each station, and the mean values. Calculations for reanalyses were done only for the times when data existed for the observations, and for the complete time series (rows with * and in italics). Also shown in parenthesis is 1 standard deviation from the mean.

Station	West 15	North 9	23	24	29	Center 20	21	31	33	36	Mean
OBS	2.9	3.6	0.7	0.8	5.2	3.5	2.8	2.3	3.6	3.0	2.8 (± 1.4)
ERA40	6.1	11.5	4.2	2.7	2.7	1.2	1.2	2.8	5.5	8.0	4.6 (± 3.3)
ERA40*	*6.3*	*10.5*	*6.9*	*12.9*	*4.0*	*2.1*	*2.0*	*2.8*	*3.7*	*3.4*	*5.4 (± 3.7)*
R-1	4.4	2.2	2.1	2.0	1.8	2.9	1.6	2.0	2.8	2.1	2.4 (± 0.8)
R-1*	*6.1*	*1.8*	*1.9*	*1.8*	*1.8*	*1.8*	*1.8*	*1.8*	*2.6*	*2.0*	*2.3 (± 1.3)*
R-2	2.0	4.0	3.2	4.0	6.5	2.9	4.6	6.0	8.4	6.7	4.8 (± 2.0)
R-2*	*2.8*	*8.9*	*7.2*	*6.2*	*13.6*	*7.1*	*8.0*	*8.0*	*8.4*	*7.9*	*7.8 (± 2.7)*

Table 3.1. Soil moisture data sets.

Region	Domain	Record length		No. of stations
		(0-1 m)	(0-10 cm)	
Ukraine	46.0-52.0ºN, 22.0-40.0ºE	1958-1999	1976-1999	26*
Russia	51.0-59.0ºN, 32.0-57.0ºE	1958-1999	1970-1999	29*
Mongolia	46.5-50.5ºN, 101.0-107.0ºE	1970-1999	1970-1999	5
Northern China	43.0-48.0ºN, 123.5-128.5ºE	1981-1999	1981-1999	8
Central China	34.0-37.0ºN, 104.5-108.5ºE	1981-1999	1981-1999	5
Illinois	37.5-42.0ºN, 88.0-91.0ºW	1984-1999	1984-1999	18

*District data are derived from 3-6 stations each.

Table 3.2. IPCC AR4 climate models analyzed. IPCC AR4 climate models analyzed.

Model Name	Organization	Land surface model, resolution	Number of ensemble members	Reference
MIROC3.2 (medres)[a,b]	CCSR (Univ. of Tokyo), NIES, and FRCGC (JAMSTEC), Japan	MATSIRO (no tiling), ~2.8º	3	*Takata et al.* [2003]
MIROC3.2 (hires)[b]		MATSIRO (2x2 tiling), ~0.56º	1	
GISS – EH[a,d]	NASA / GISS, USA	Land Surface Model, 4ºx5º	5	*Rosenzweig and Abramopoulos* [1997], *Friend and Kiang* [2005]
GISS – ER[a,d]			9	
MRI-CGCM2.3.2[a,b,d]	MRI, Japan	SiB L3, ~2.8º	5	*Sellers et al.* [1986], *Sato et al.* [1989]
FGLOALS-g1.0[a,d]	LASG/IAP, China	CLM2.0, ~2.8º	3	*Bonan et al.* [2002]
CGCM3.1 (T47)[a]	CCCMA, Canada	CLASS, ~3.75 º	5	*Verseghy et al.* [1991]
CCSM3, USA[a,b,d]	NCAR, USA	CLM3.0, ~1.4º	6	*Oleson et al.* [2004]
PCM1, USA[b,d]	NCAR, USA	LSM1.0, ~2.8º	4	*Bonan* [1996]
GFDL_CM2_0[b,c]	GFDL, USA	LM2, 2.0ºx2.5º	3	*Milly and Shmakin* [2002]
GFDL_CM2_1[b,c]	GFDL, USA			
UKMO-HADCM3[a,d]	Hadley Centre, Met Office, UK	MOSES-I, 2.5ºx 3.75º	2	*Cox et al.* [1999]
UKMO-HADGEM1[a,d]		MOSES-II, 1.25ºx1.875º	2	*Essey et al.* [2001]

[a] Model has top 0-10 cm soil moisture output.
[b] Model has top 0-1 m soil moisture output.
[c] Model reported root-zone level (about 1 m) plant-available soil moisture.
[d] Model includes carbon fertilization effects.

Table 4.1. Summary of forcing adjustment procedures

Forcing Fields	Adjustment Method
Precipitation[a]	
Shortwave Radiation[b]	
Temperature[c]	$V_{r,adj} = (\frac{\overline{V_{obs}}}{\overline{V_r}}) \times V_r$
Specific Humidity	Adjusted according to adjusted temperature and pressure
Wind	—
Pressure	—

Vr is reanalysis Variable, Values with an overhead bar represent monthly mean. The ratios between monthly mean observations and monthly mean reanalysis values were used to adjust reanalysis fields.

[a]used a combination of *Chen et al*. [2002] for 1948-1996 and Global Precipitation Climatology Project (GPCP) V2 data [*Adler et al*. 2003] for 1997-2002 for precipitation observations.

[b]used Climate Research Unit (CRU) cloud cover data [*New et al*. 2002; *Mitchell et al*. 2004] for 1948 to 1974 and combination of CRU and *Dai et al*. cloud observations [2005] for 1975-2000 and *Dai et al*. data [2005] for 2001-2004 to correct anomalies and International Satellite Cloud Climatology Project (ISCCP) [*Zhang et al*. 2004] observations to correct mean radiation biases.

[c]used CRU temperature observations [*Jones and Moberg* 2003 and updates].
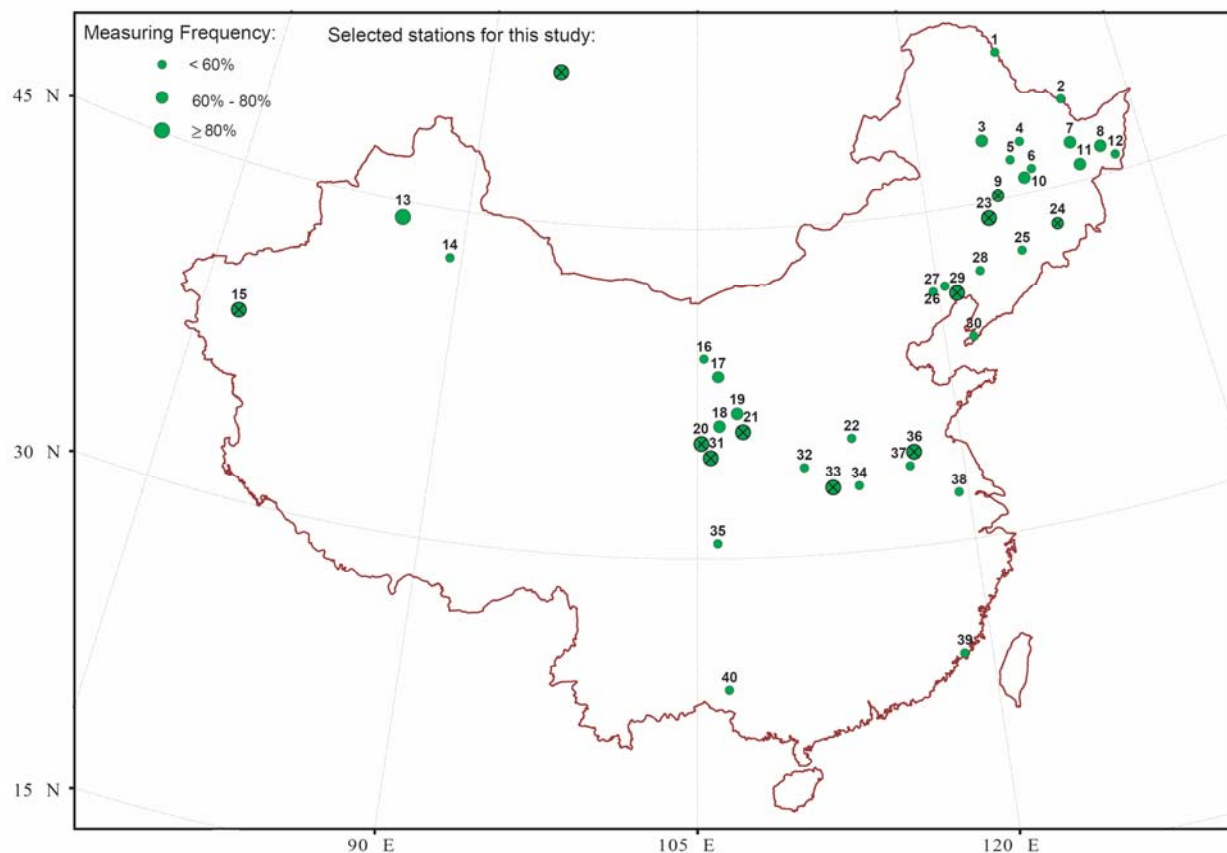
Figure 2.1. Chinese soil moisture station map. The number is the station ID (see Table 2.1). The size of the circles indicates the data quality (frequency of available observations during the period April-October) and circles with an "X" are the stations chosen for comparison with the models.
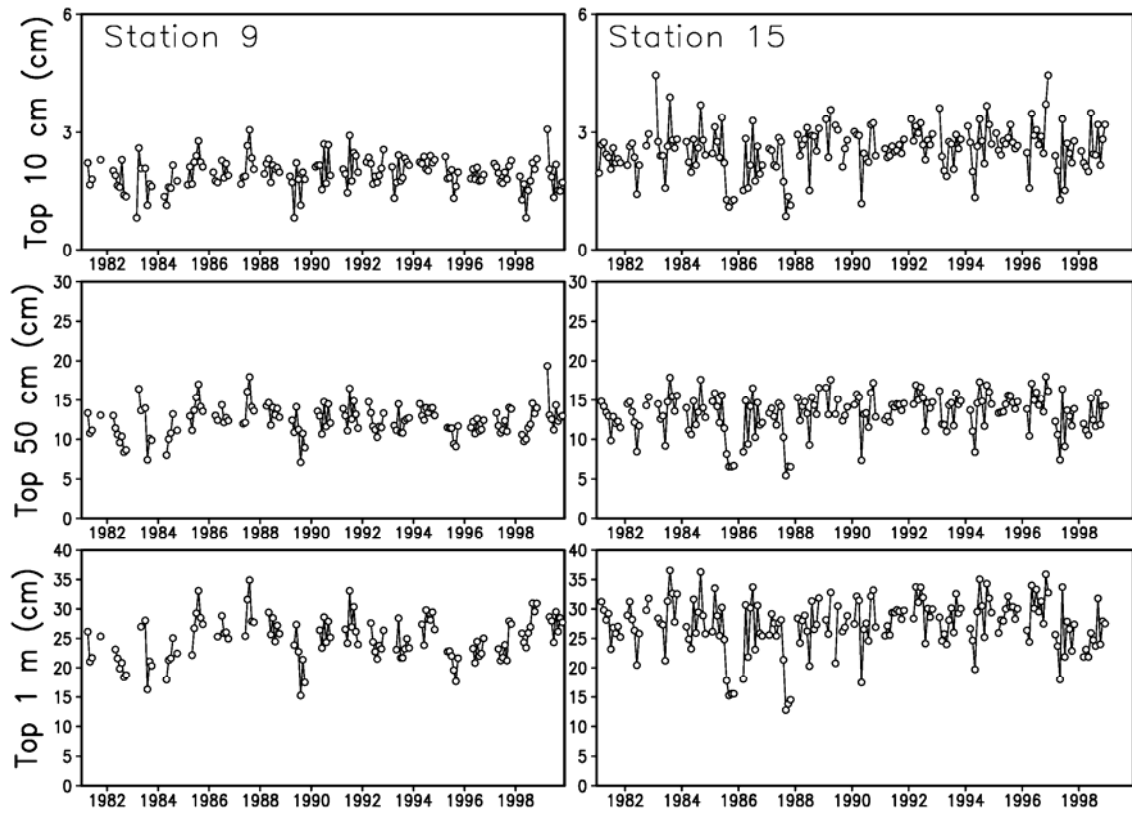
Figure 2.2. Total soil moisture (cm) at three levels: top 10 cm, top 50 cm and top 1 m for two representative stations, Station 9 from Northern China in the left column and Station 15 from Western China in the right column.
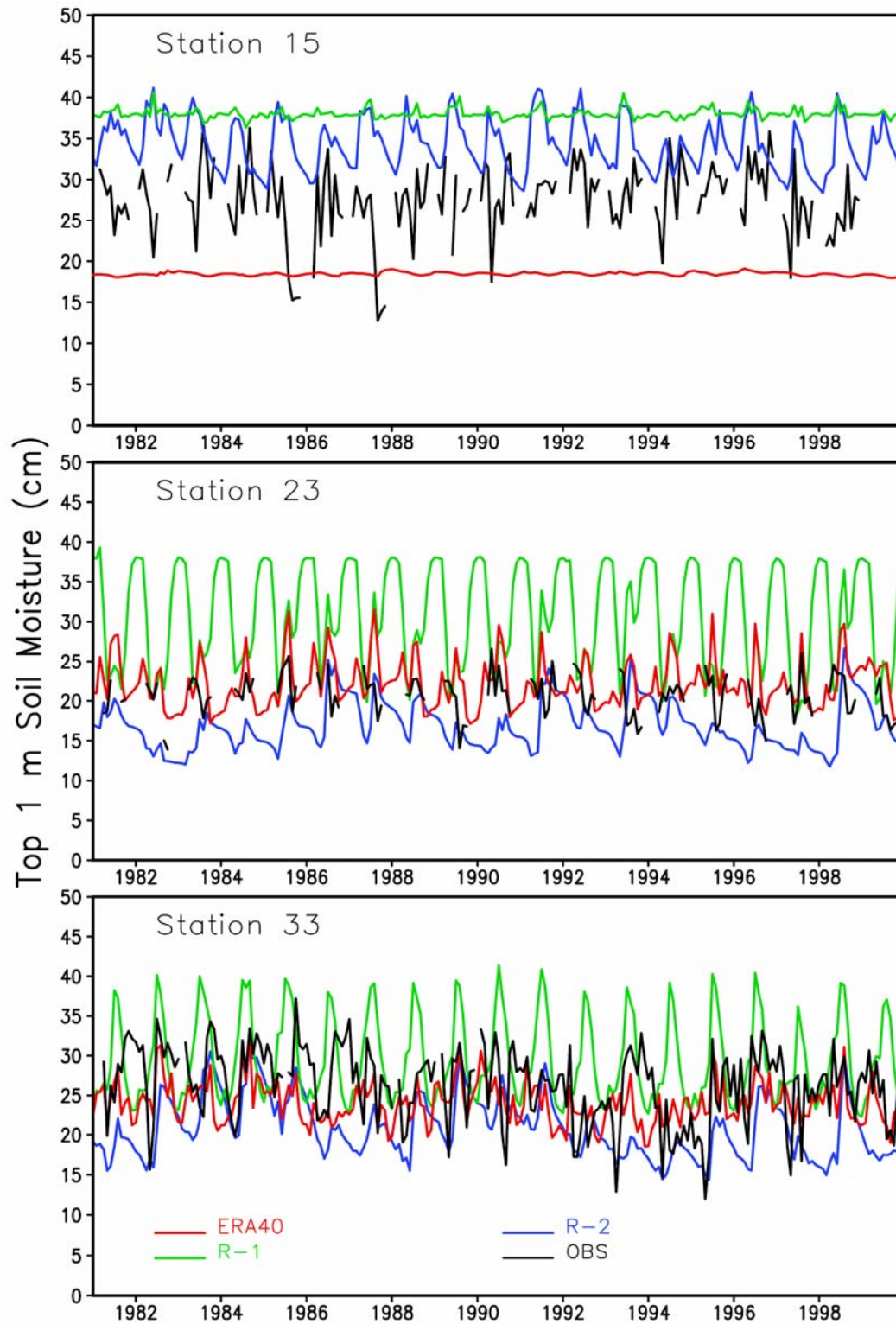
Figure 2.3. Total top 1 m soil moisture for Station 15 (Western China), Station 23 (Northern China) and Station 33 (Central China). R-1 has very little interannual variability. For Station 15, the amplitude of the interannual variability is too small for R-1 and ERA40.
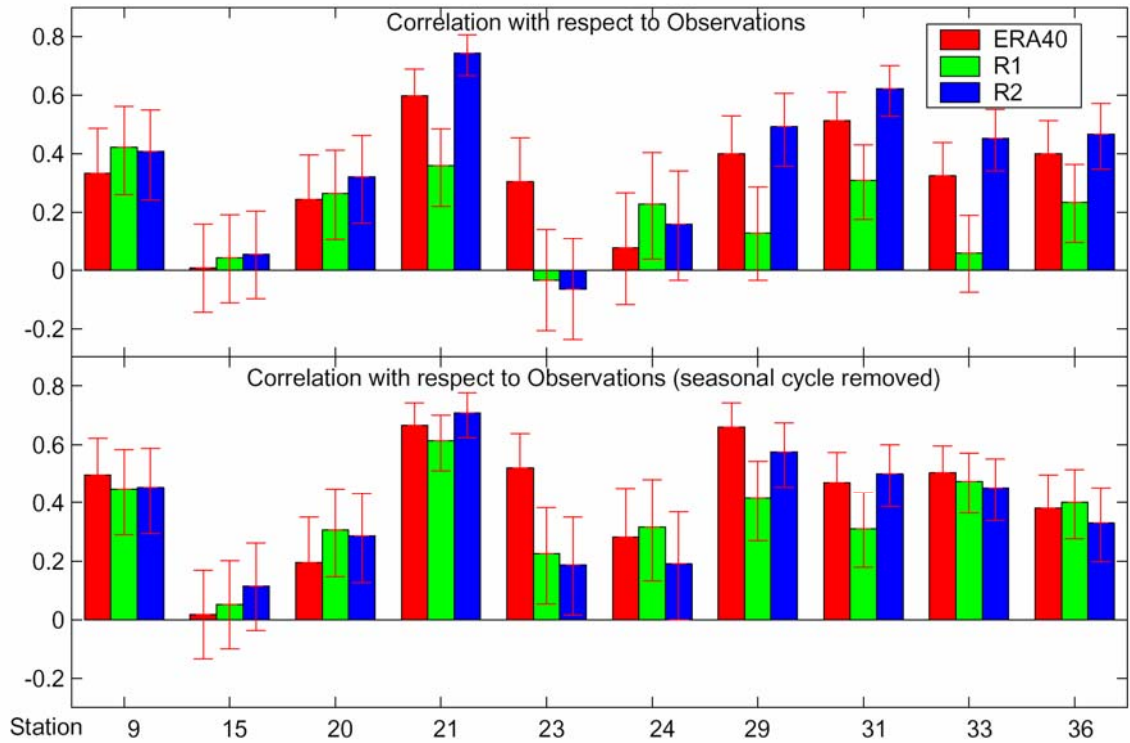
Figure 2.4. Correlation of monthly (day 28 of each month) soil moisture observations for 10 stations indicated in Figure 2.1 with reanalyses. Top panel includes the seasonal cycle and bottom panel has the mean seasonal cycle removed. The black error bars indicate the 95% significance level for the correlation coefficients. Remarkably, in general the correlations are higher with the seasonal cycle removed, except for R-2.
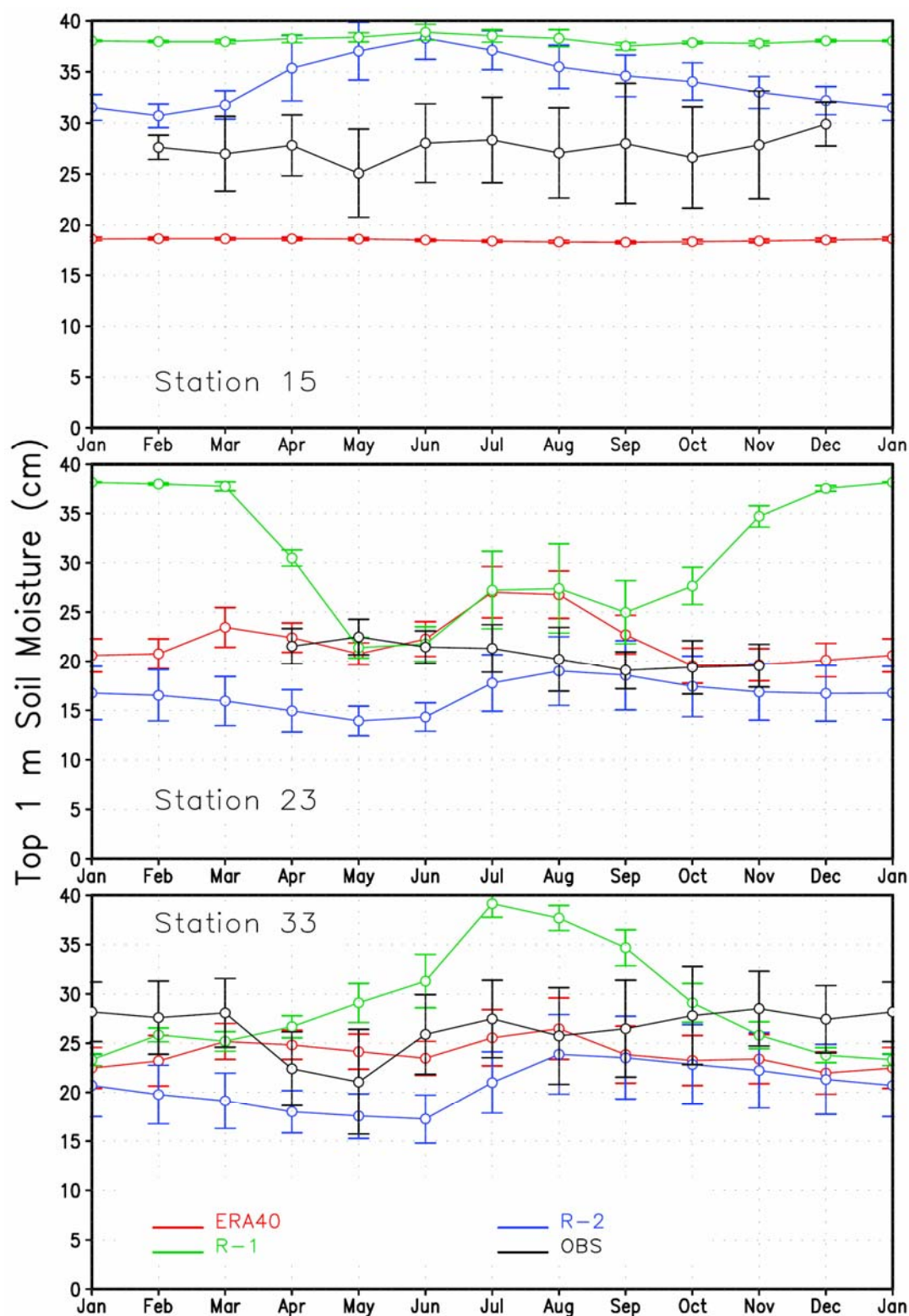
Figure 2.5. Seasonal cycle of top 1 m total soil moisture for three stations (see Figure 2.1) and reanalyses. The error bars are ±1 standard deviations from the means.
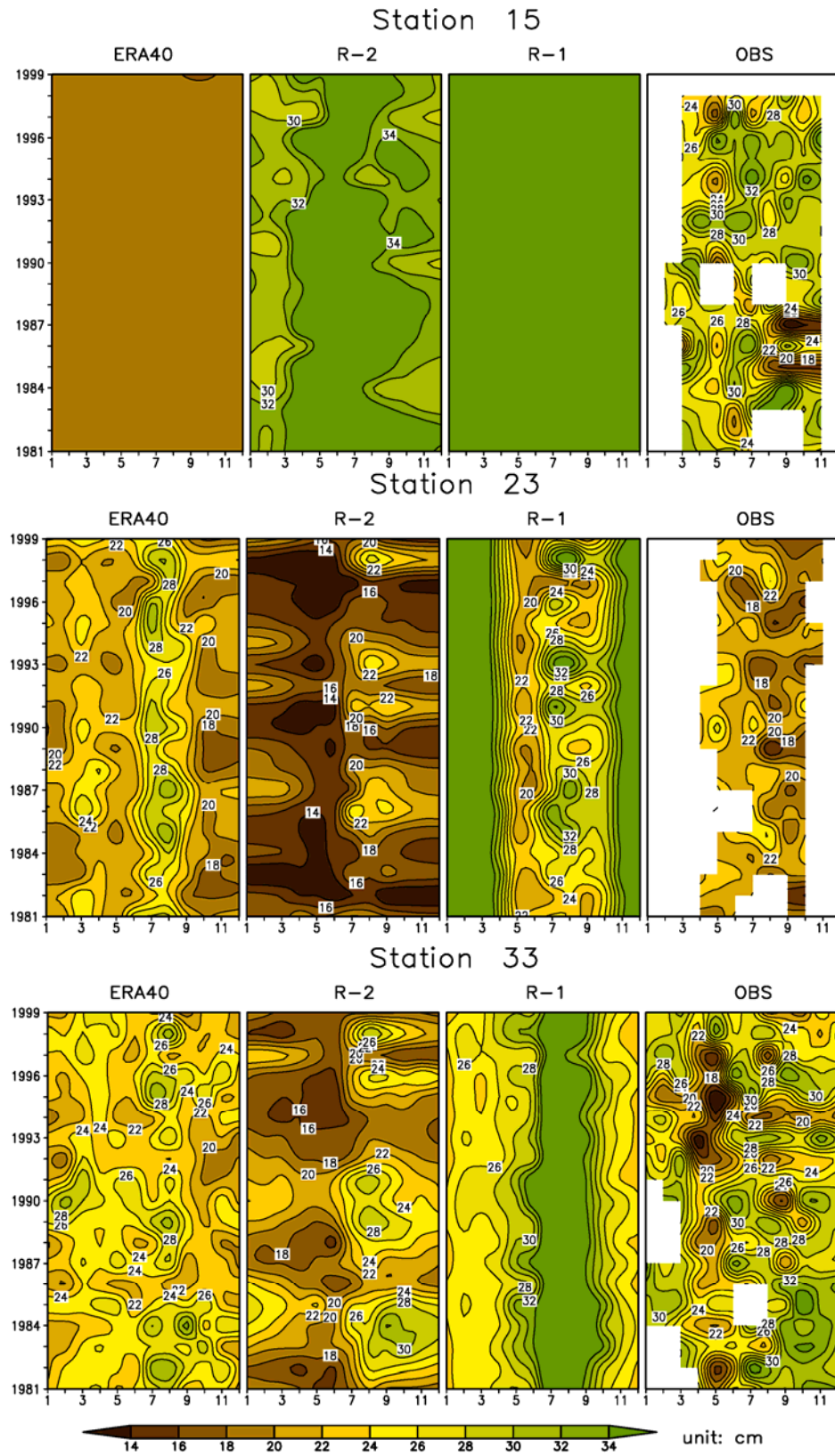
Figure 2.6. Month-year plots of top 1 m total available soil moisture evolution for three stations and reanalyses.
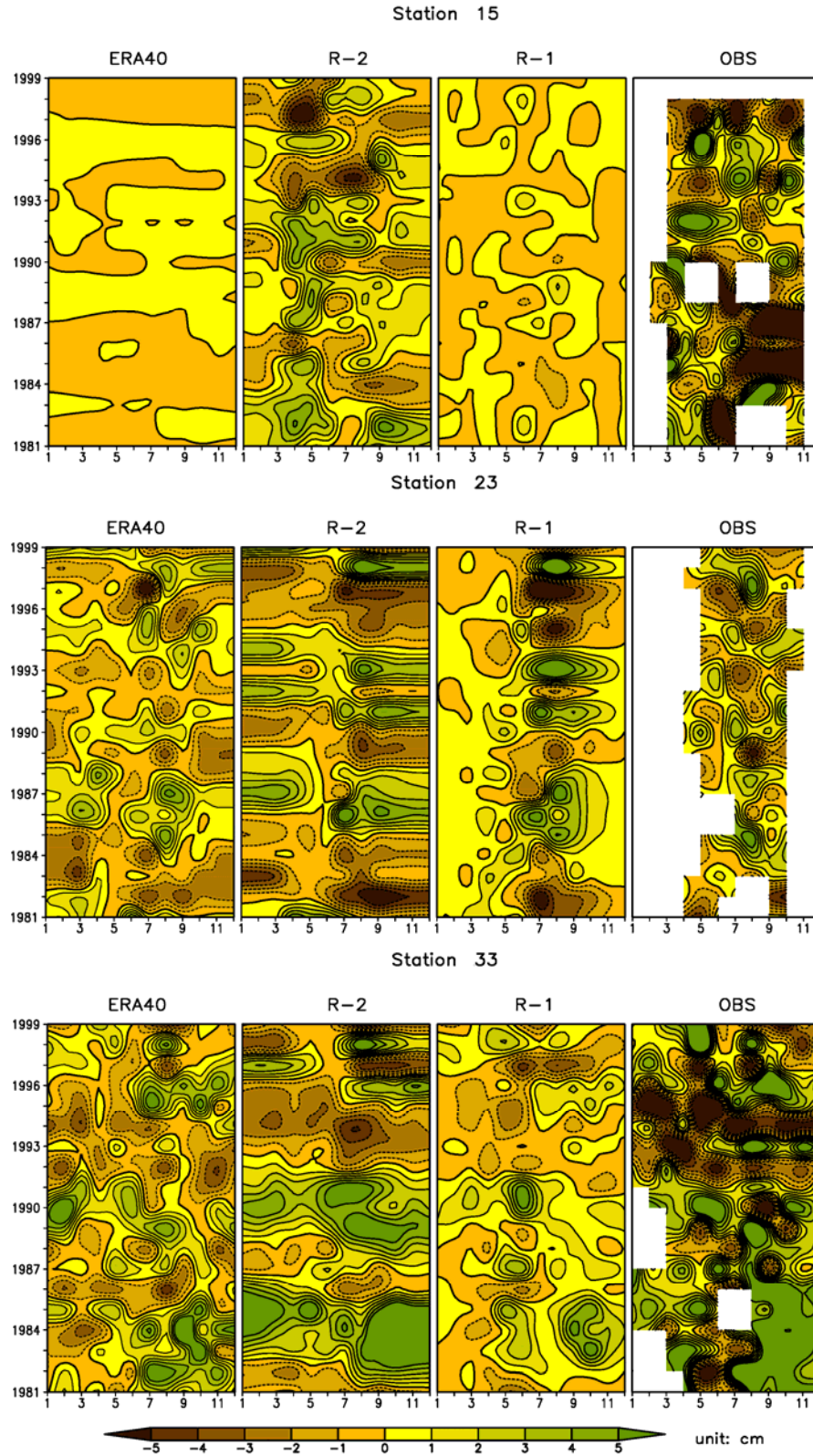
Figure 2.7. Same as Figure 2.6, but for anomalies with respect to the mean for 1990-1998. Thick line is 0, and contour interval is 1 cm.
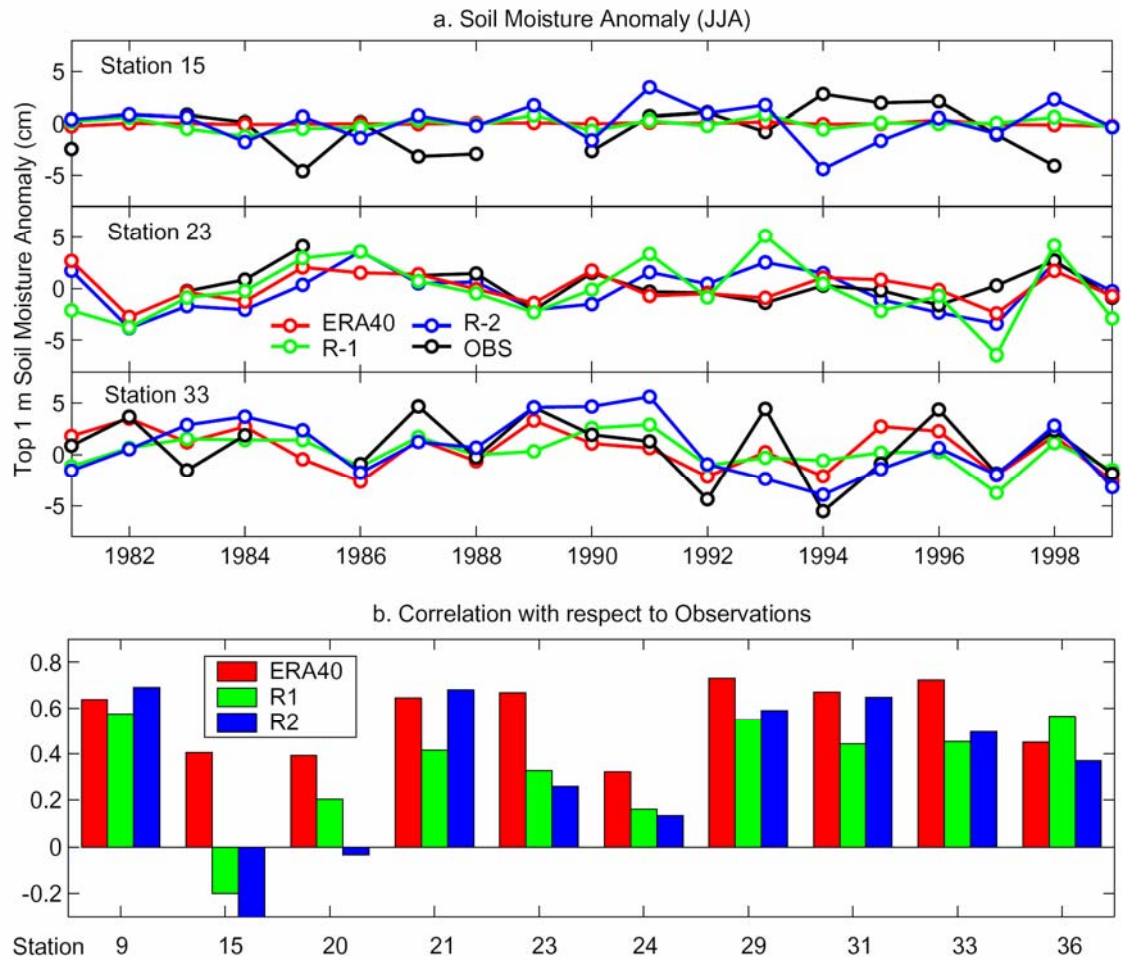
Figure 2.8. Soil moisture summer interannual variability. (a) Top 1 m soil moisture anomaly for Station 15 (Western China), Station 23 (Northern China) and Station 33 (Central China). Anomaly was calculated as the mean value for summer months (JJA) in every year based on climatology of 1990-1998. (b) Soil moisture anomaly correlation between models and observations for JJA. ERA40 generally exhibits the best interannual variability as compared to observations among three models.
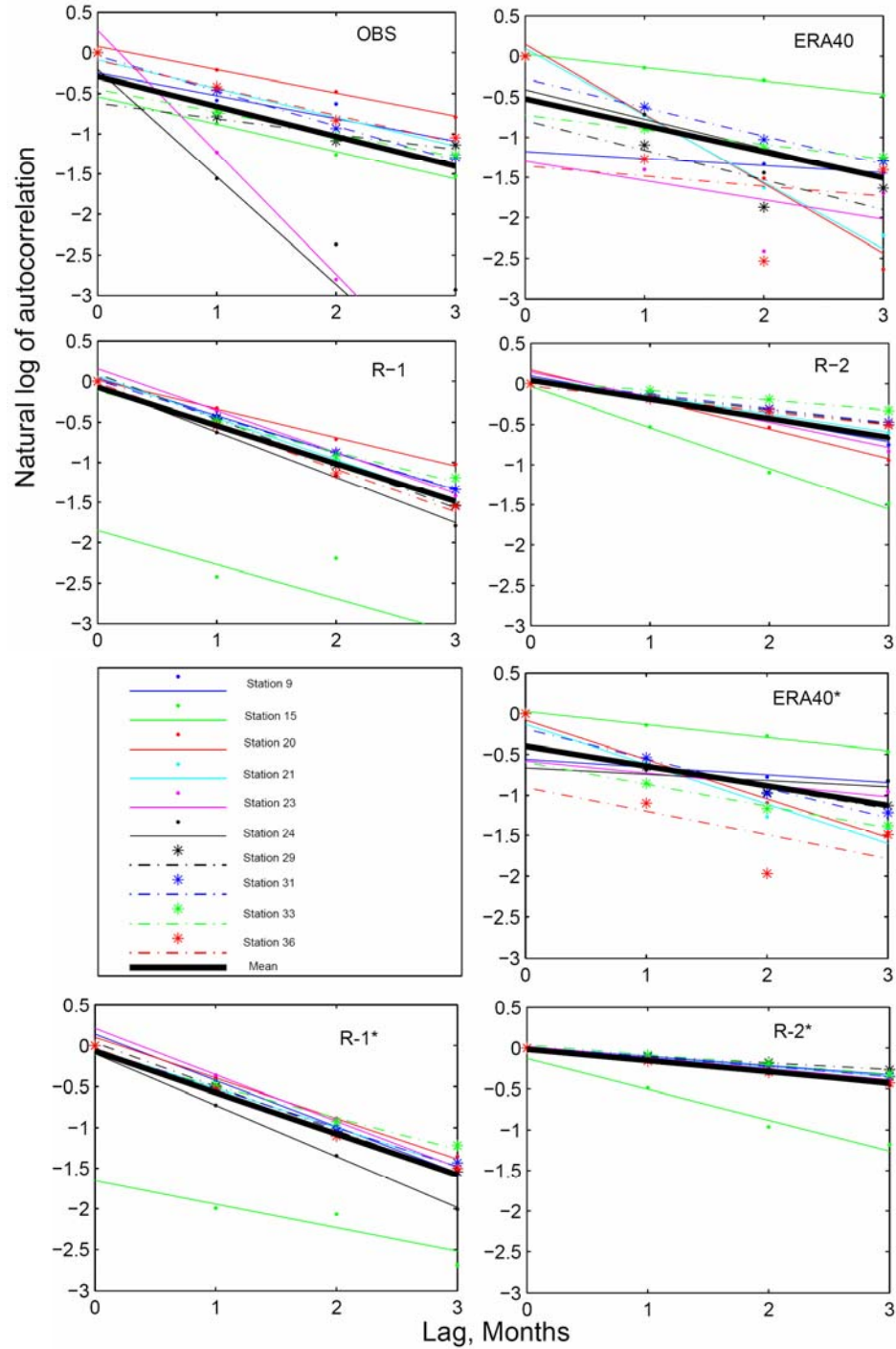
Figure 2.9. Temporal autocorrelations of observations and reanalyses for all 10 stations indicated in Figure 2.1, plotted as natural logarithm of the correlation coefficients. The slope of the best fit line gives the temporal scale. Top 4 panels are results when taking out the corresponding data from reanalyses if there have missing values in observations. Bottom 3 panels are calculations based on full data sets in reanalyses. The thick lines in black show the arithmetic average for all 10 stations.
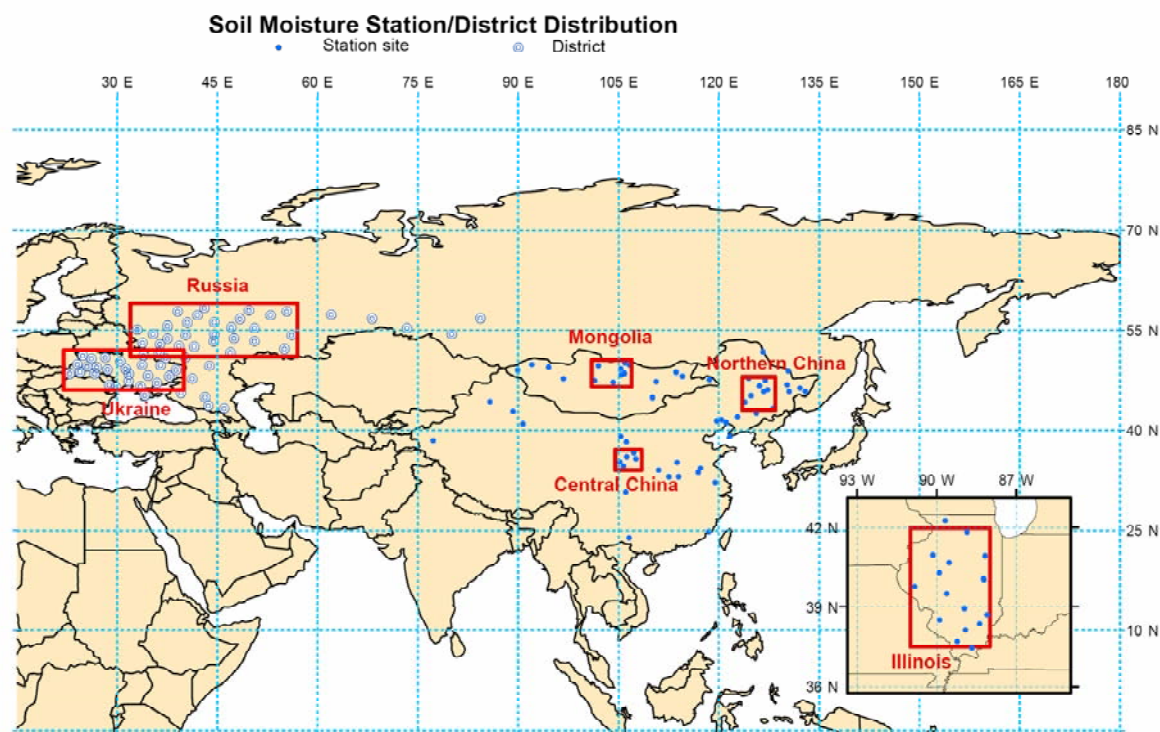
Figure 3.1. Distribution of soil moisture stations/district centers used in this study. District centers are plotted as double circles and stations as solid dots. Rectangles are domains used to derive regional averages (Table 3.1).
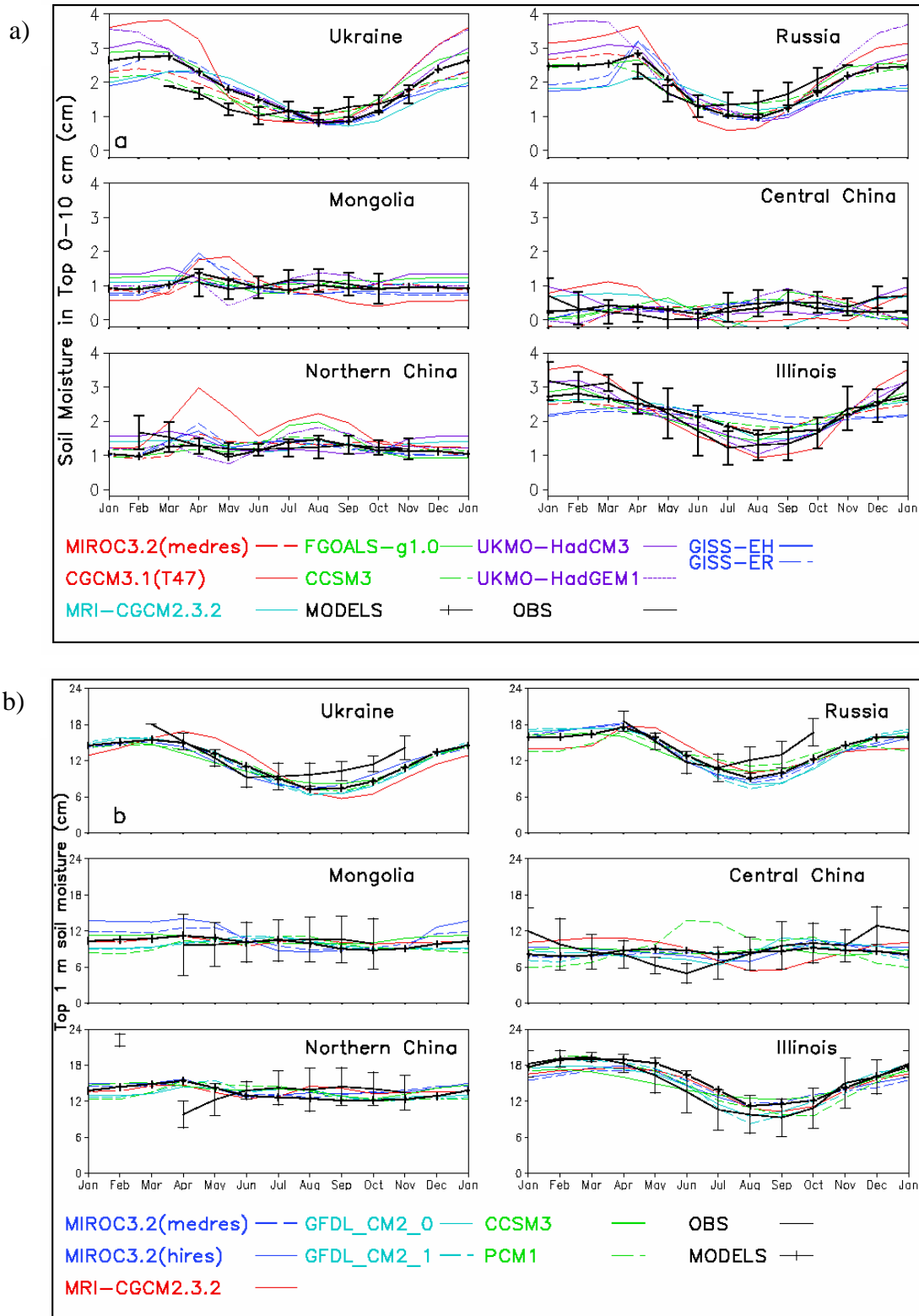
Figure 3.2. Mean soil moisture seasonal cycle: (a) top 10 cm (units: cm), (b) Mean soil moisture seasonal cycle for top 1 m (units: cm).
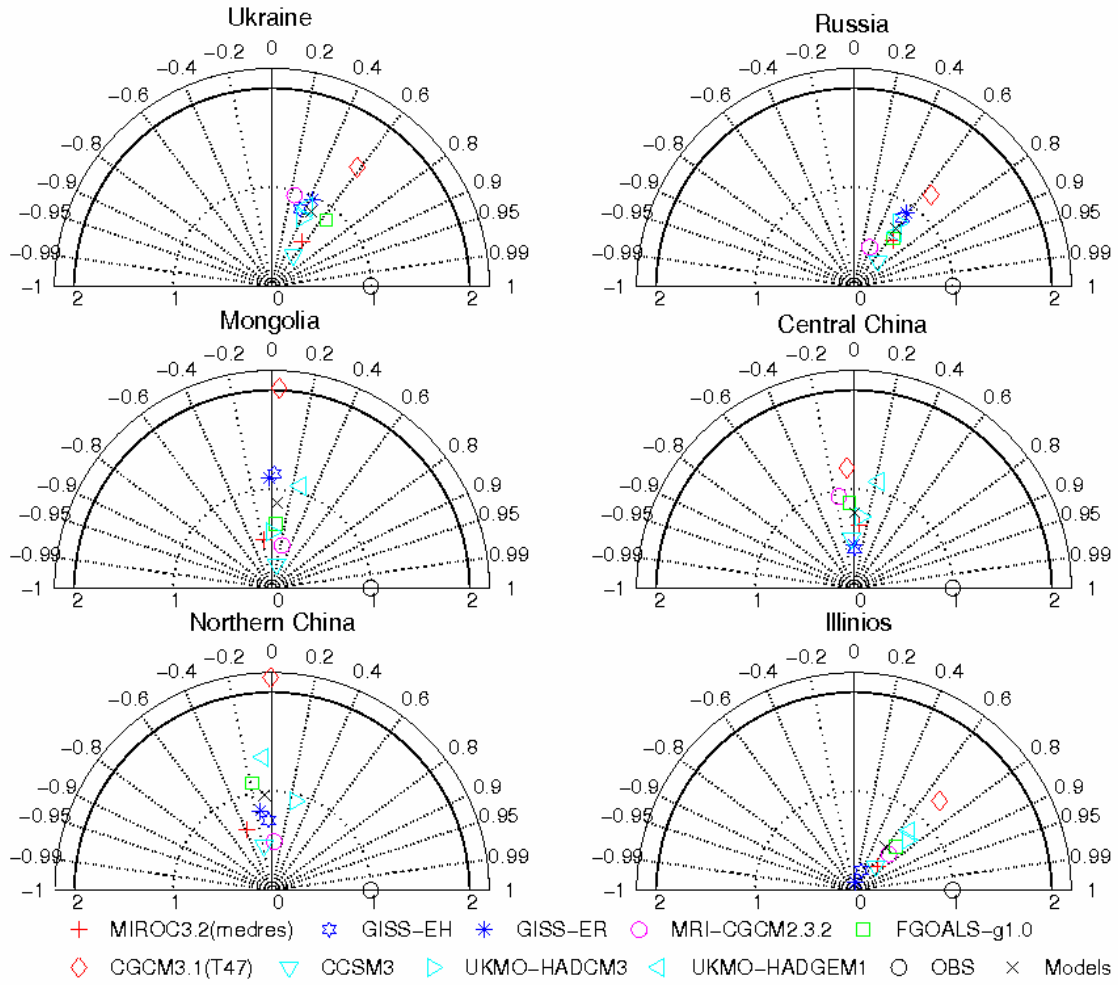
Figure 3.3. Taylor diagrams for top 10 cm soil moisture. Azimuthal angle represents correlation coefficient and radial distance is the standard deviation normalized to observations.
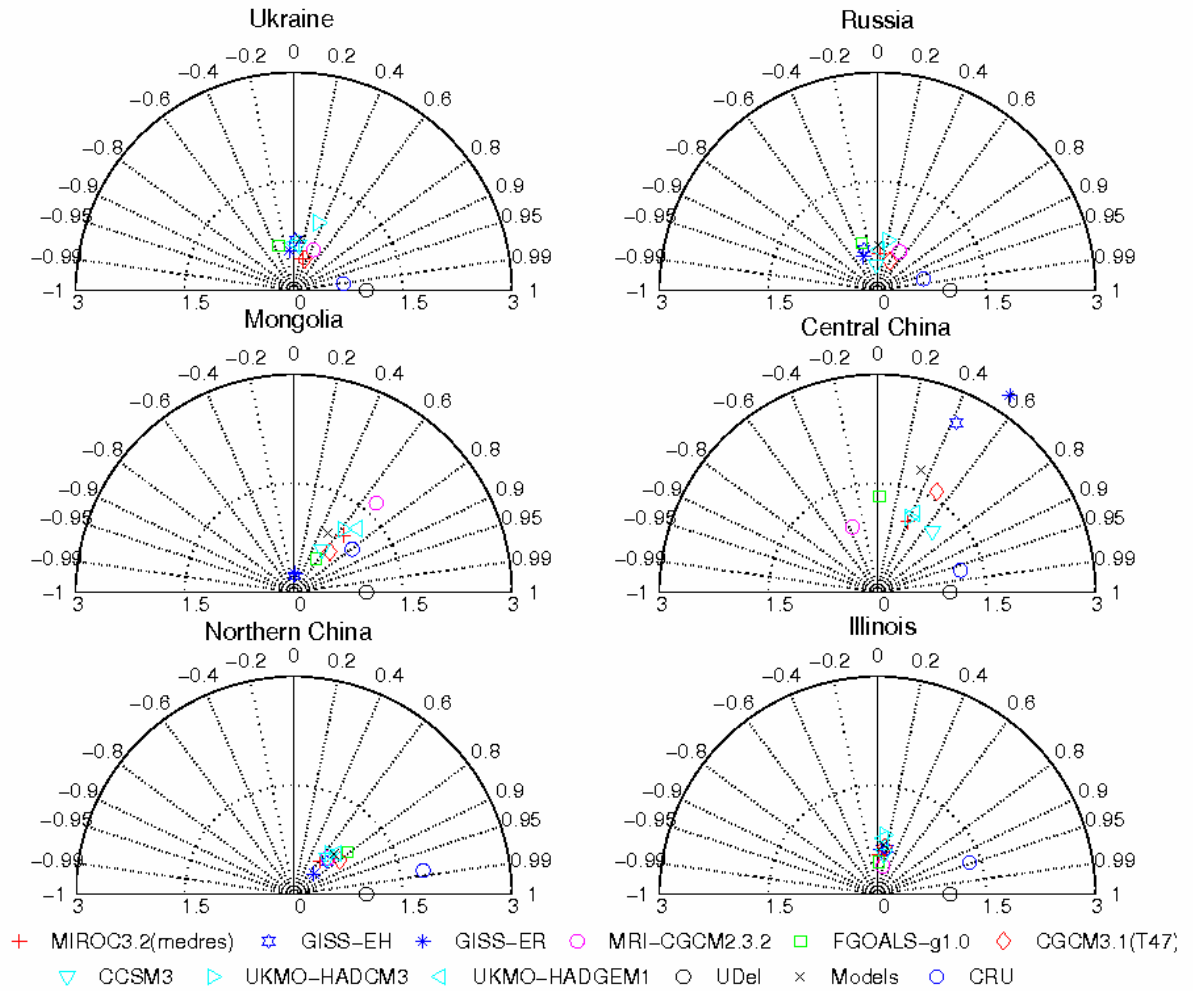
Figure 3.4. Taylor diagram for precipitation.
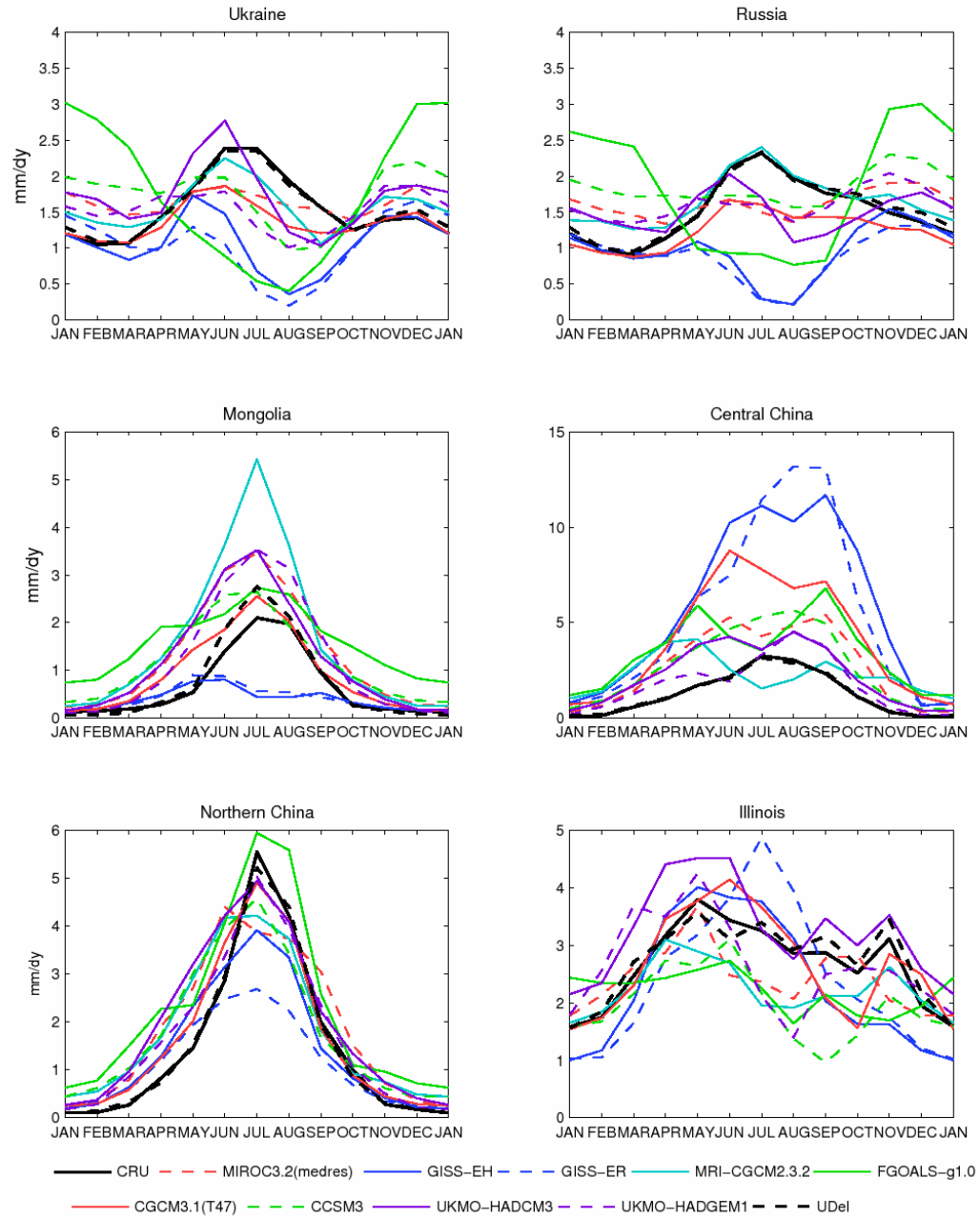
Fig 3.5. Same as Figure 3.2 except for precipitation.
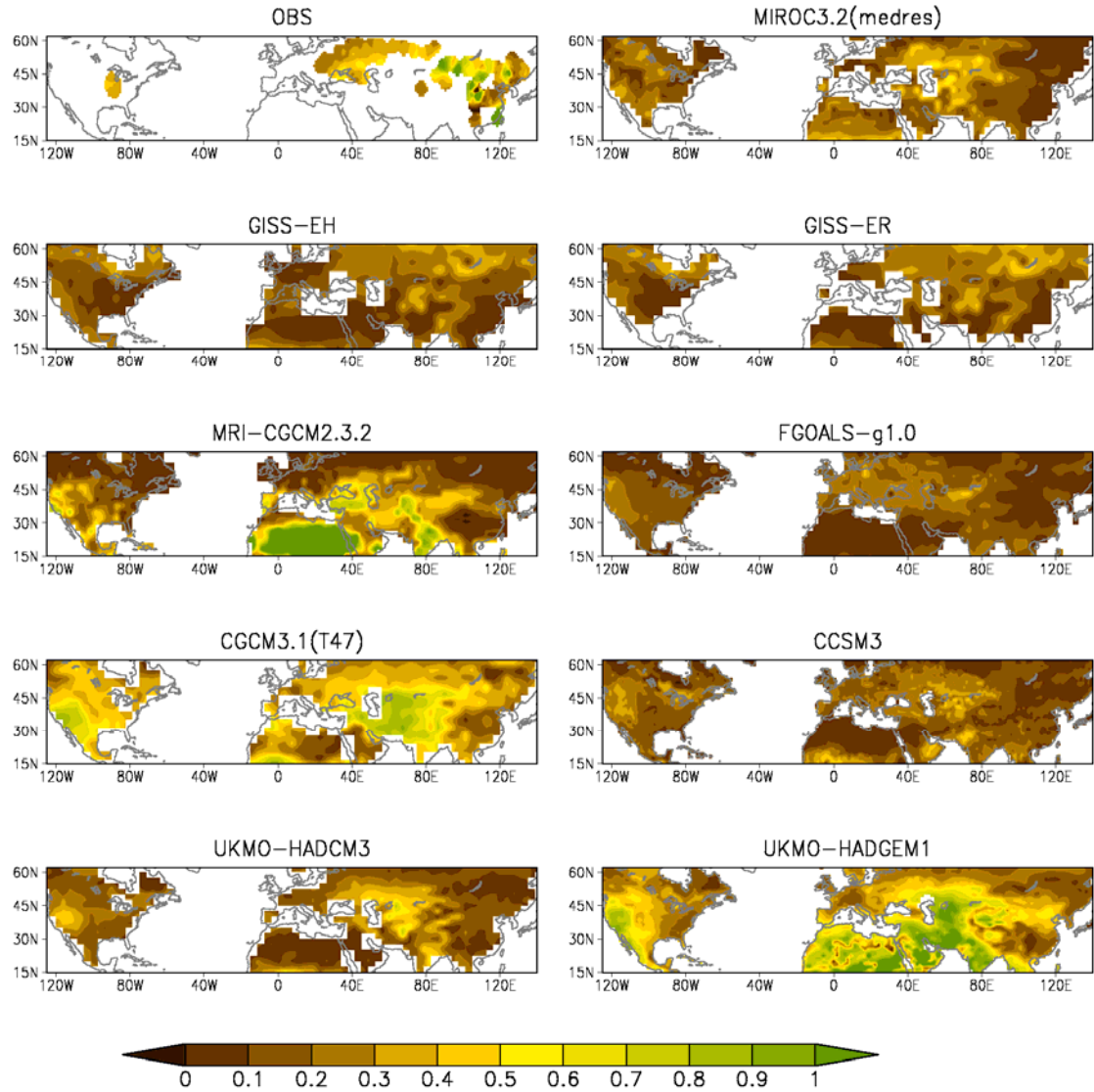
Figure 3.6. Interannual variations (coefficient of variance, defined as standard deviation divided by mean) of top 0-10 cm soil moisture for observations (Table 3.1) and IPCC models (Table 3.2).
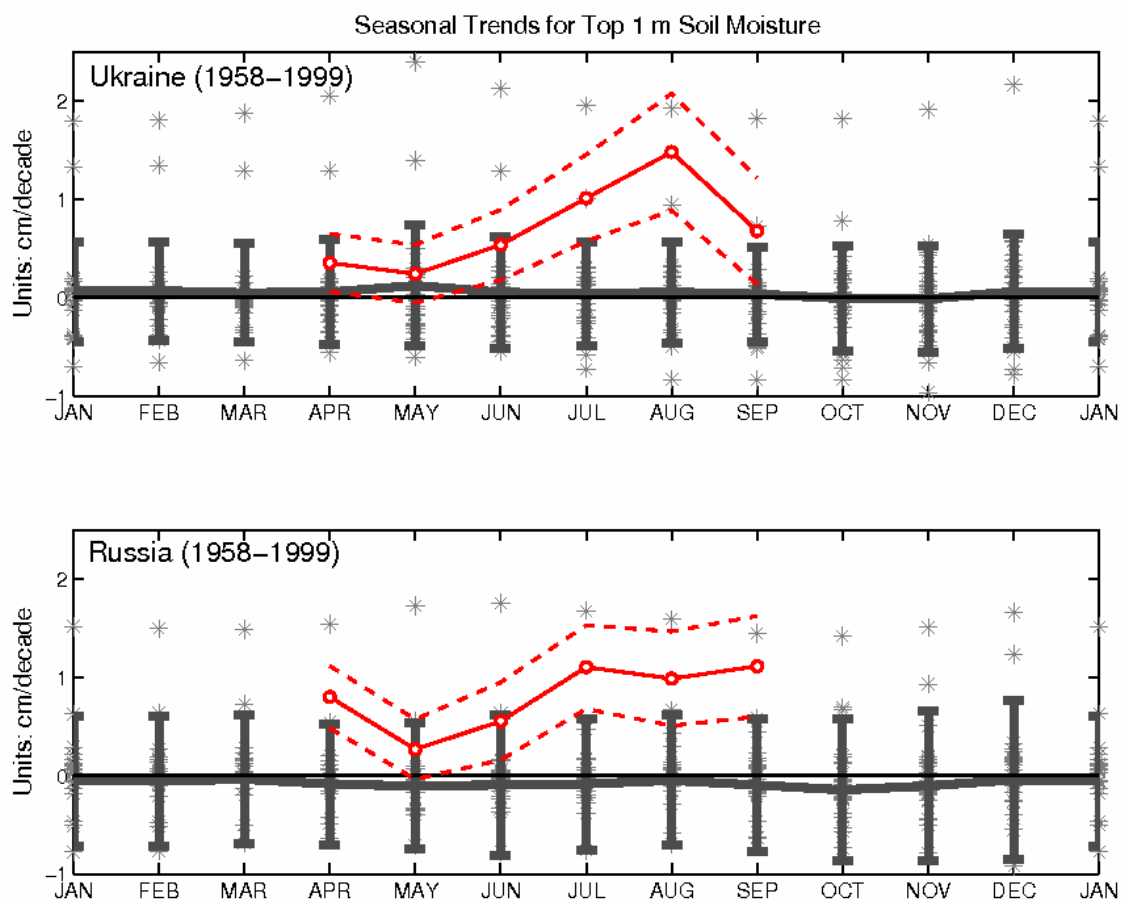
Figure 3.7. Seasonal cycle of top 1 m soil moisture trends for 1958-1999. Observations are circles, 90% confidence intervals are dashed lines, dark gray lines represent mean trends for individual model realizations (see Table 3.2 for list of models), and error bars show standard deviation for trends. Light gray symbols are estimated trends for individual realizations. For location of Ukraine and Russia boxes, see Table 3.1 and Figure 3.1.
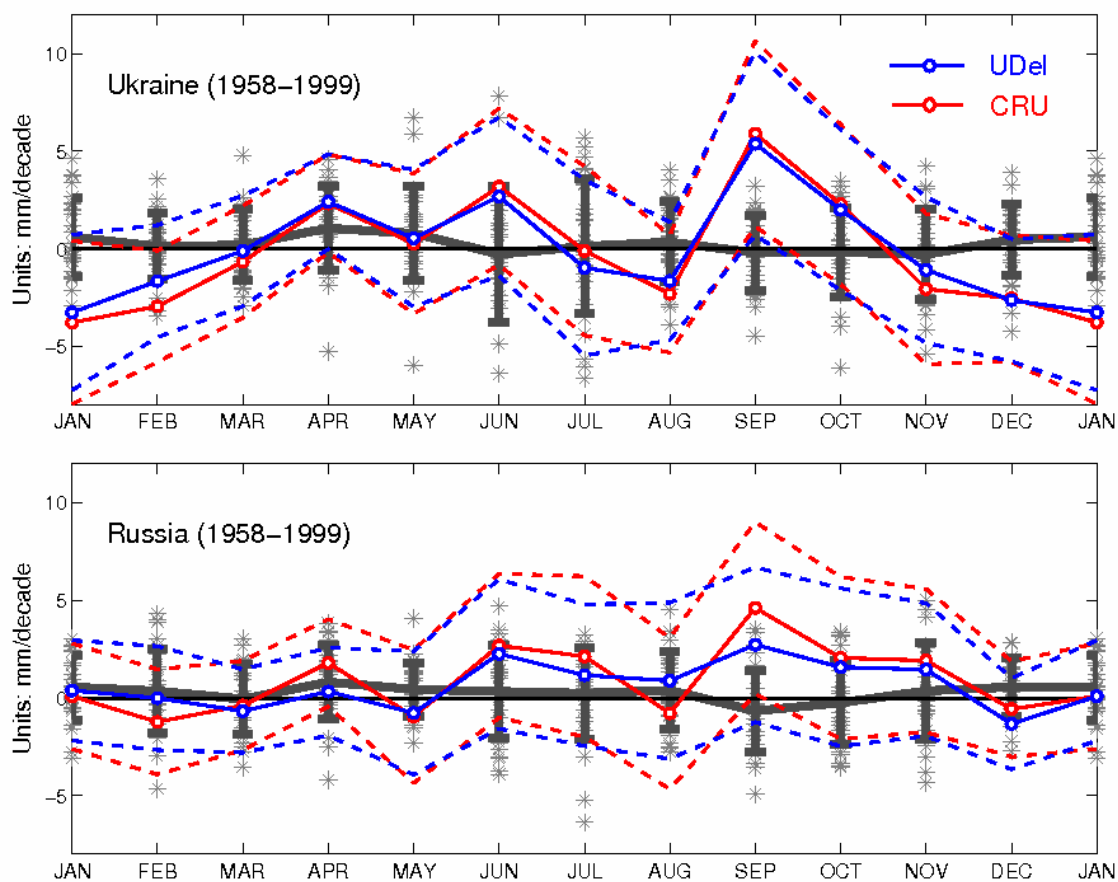
Figure 3.8. Same as Figure 3.7, but for precipitation. See text for references to CRU and UDel data.
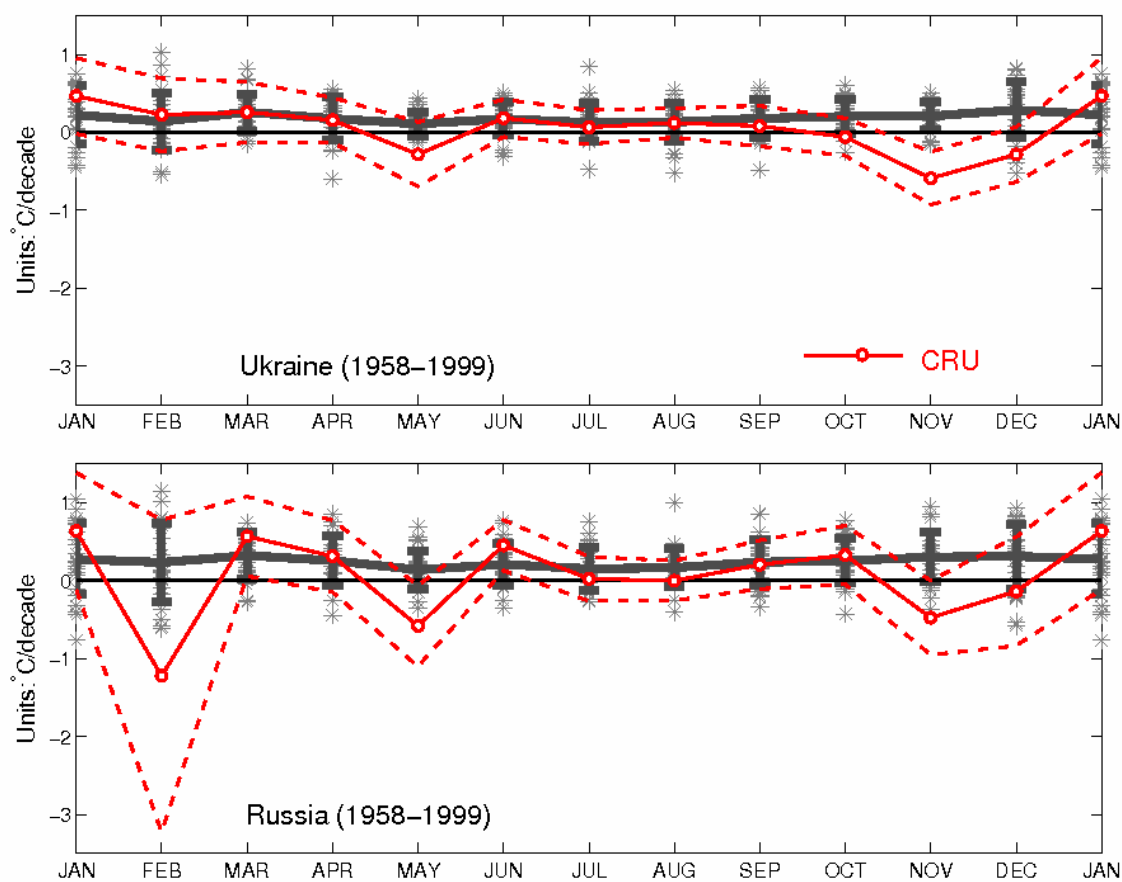
Figure 3.9. Same as Figure 3.7, but for temperature. See text for references to CRU data.
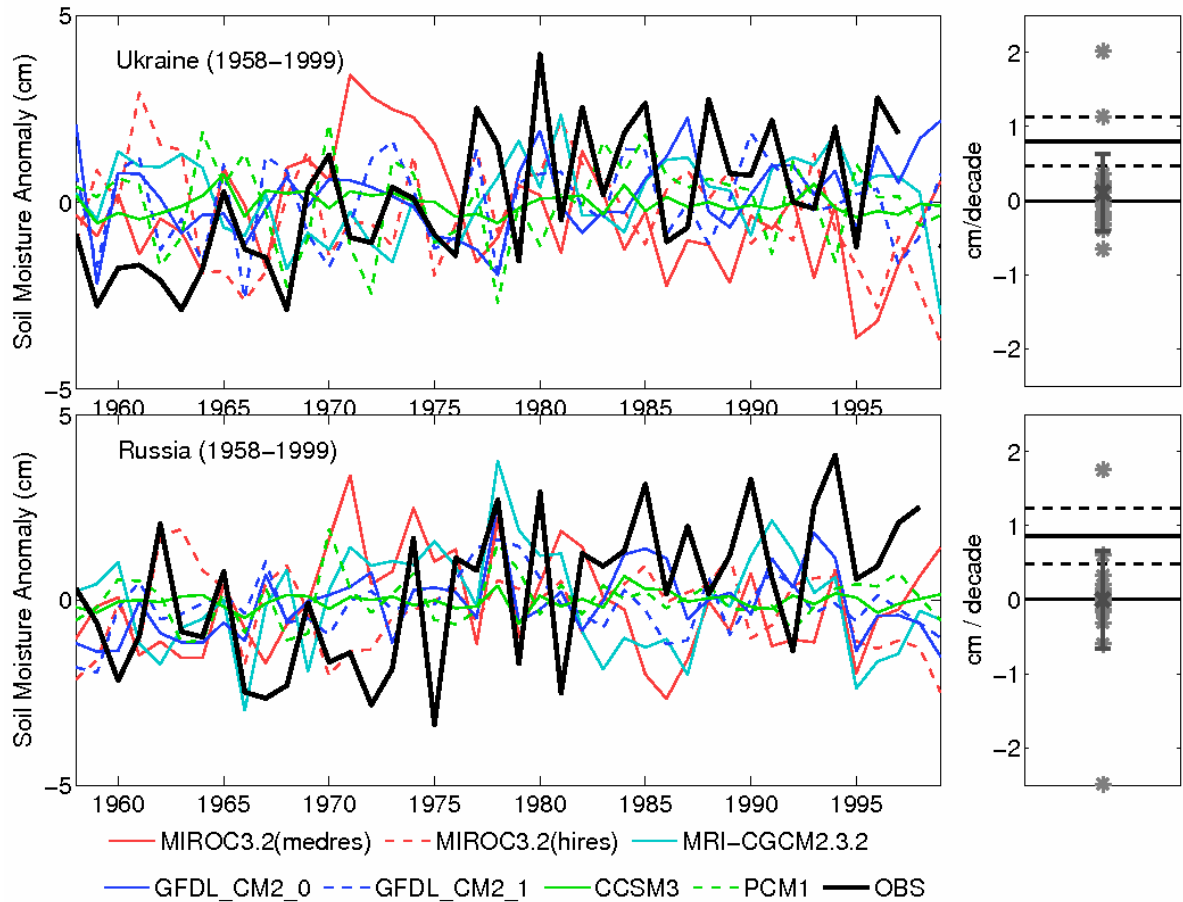
Figure 3.10. Summer (JJA) soil moisture changes for Ukraine and Russia for the period of 1958-1999 from observations and model ensembles, expressed as anomalies relative to the 1961-1999 means. Right panel shows linear trends. Thick solid lines are estimated trends for observations and 90% confidence intervals are dashed lines. Trends from individual model realizations (Table 3.2) are plotted as "*" in light gray. Error bar represents the standard deviation of the trends from 25 realizations.
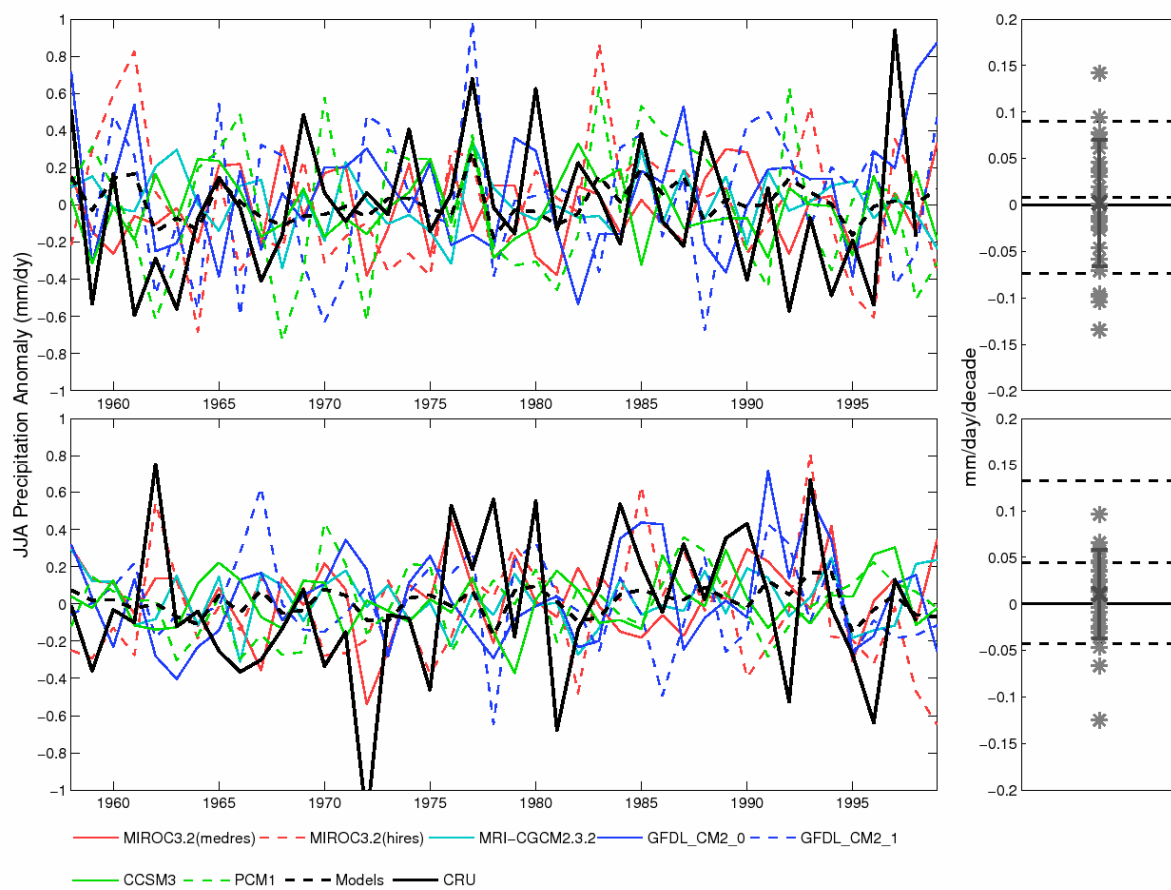
Figure 3.11. Same as Figure 3.10 except for precipitation.
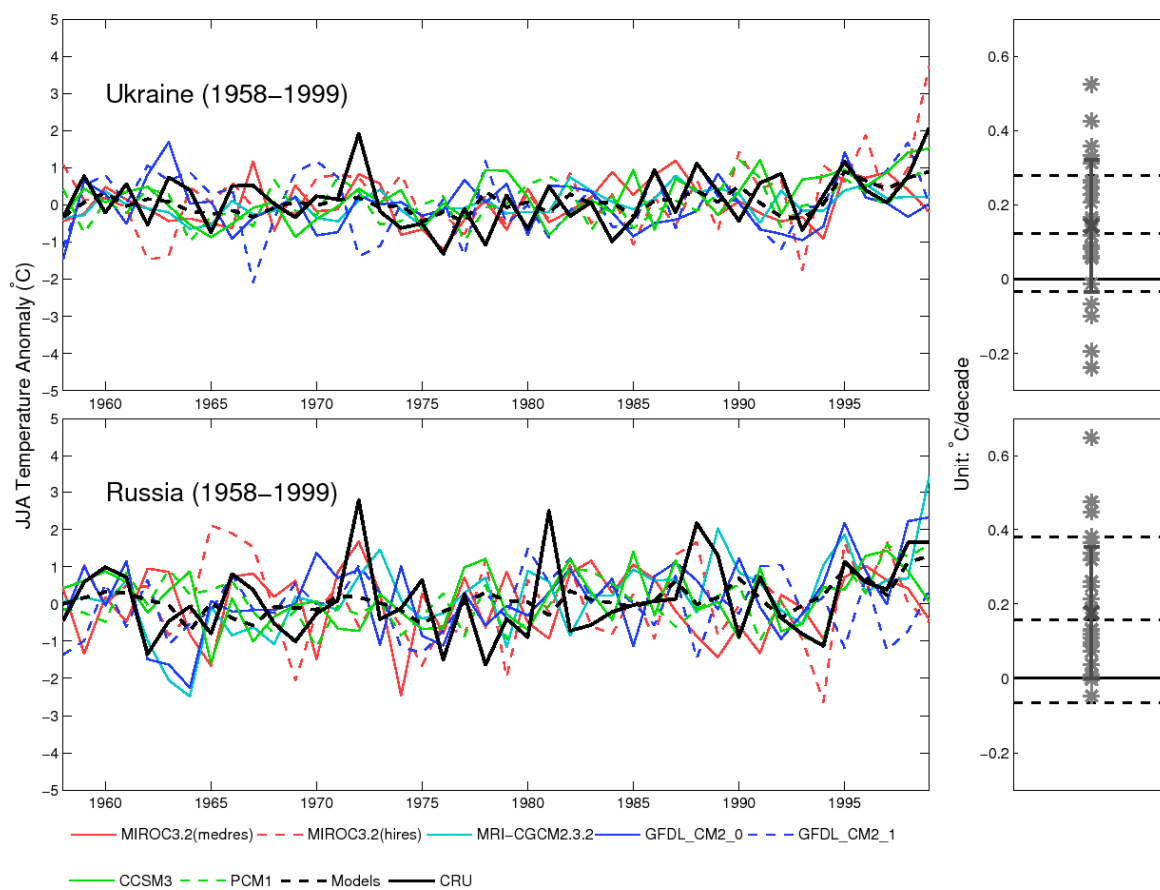
Figure 3.12. Same as Figure 3.10 except for temperature.

(a)

(b)
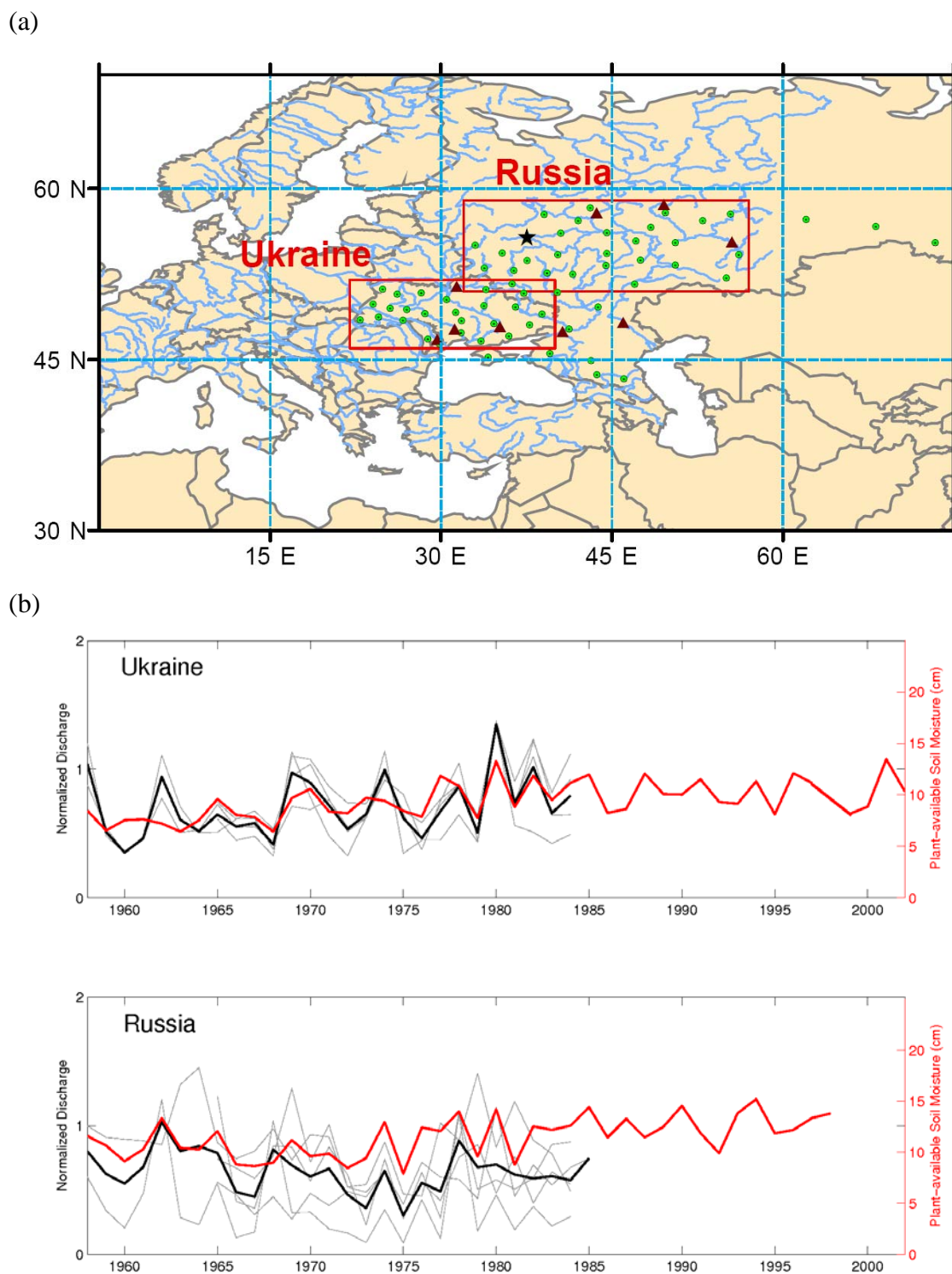
Figure 3.13. (a) Streamflow stations (triangle) from Global River Discharge data sets. (b). Normalized river discharge time series (light grey lines). Thick black line represents the normalized mean discharge of stations for each district. Soil moisture is plotted as thick red lines. There is a good correspondence between soil moisture and independent river discharge observations.
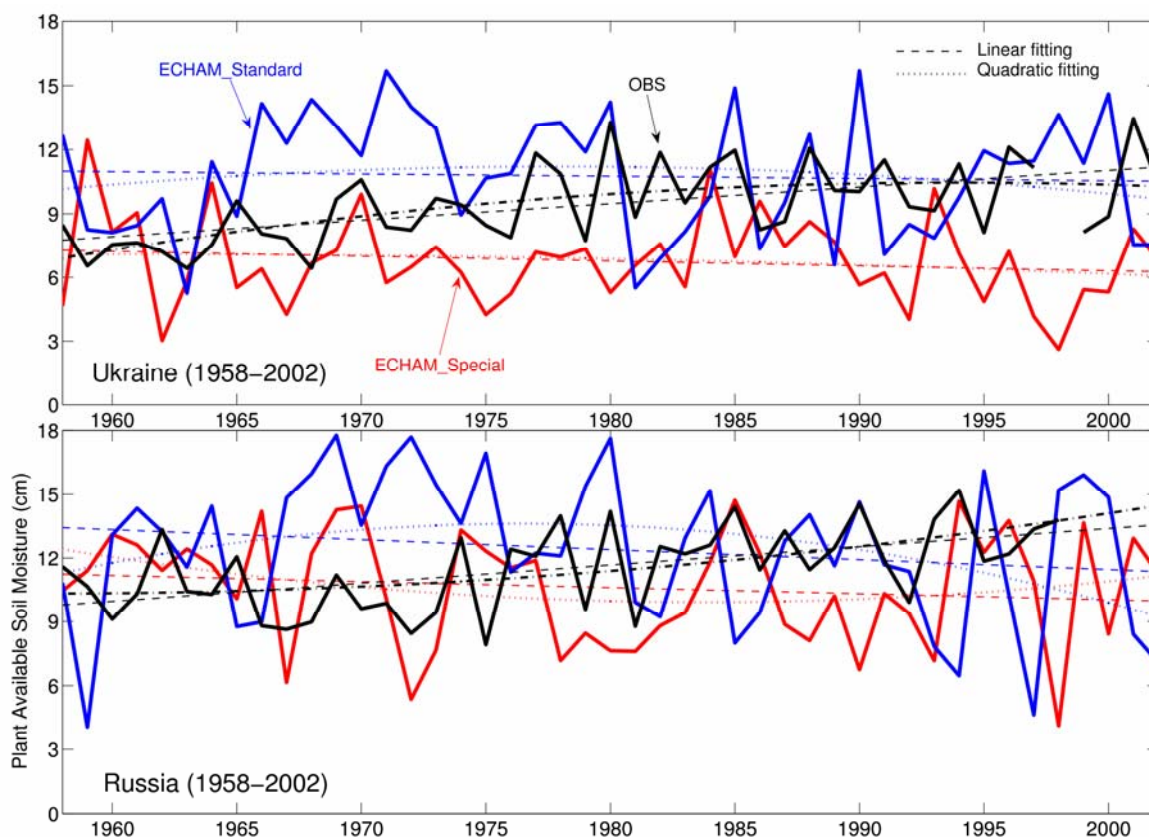
Figure 3.14. Summer (JJA) plant-available soil moisture for the top 1 m for special version of ECHAM5-HAM model (red), standard ECHAM5 model (blue), and observations (black). Also shown are linear and quadratic fitted trend lines.
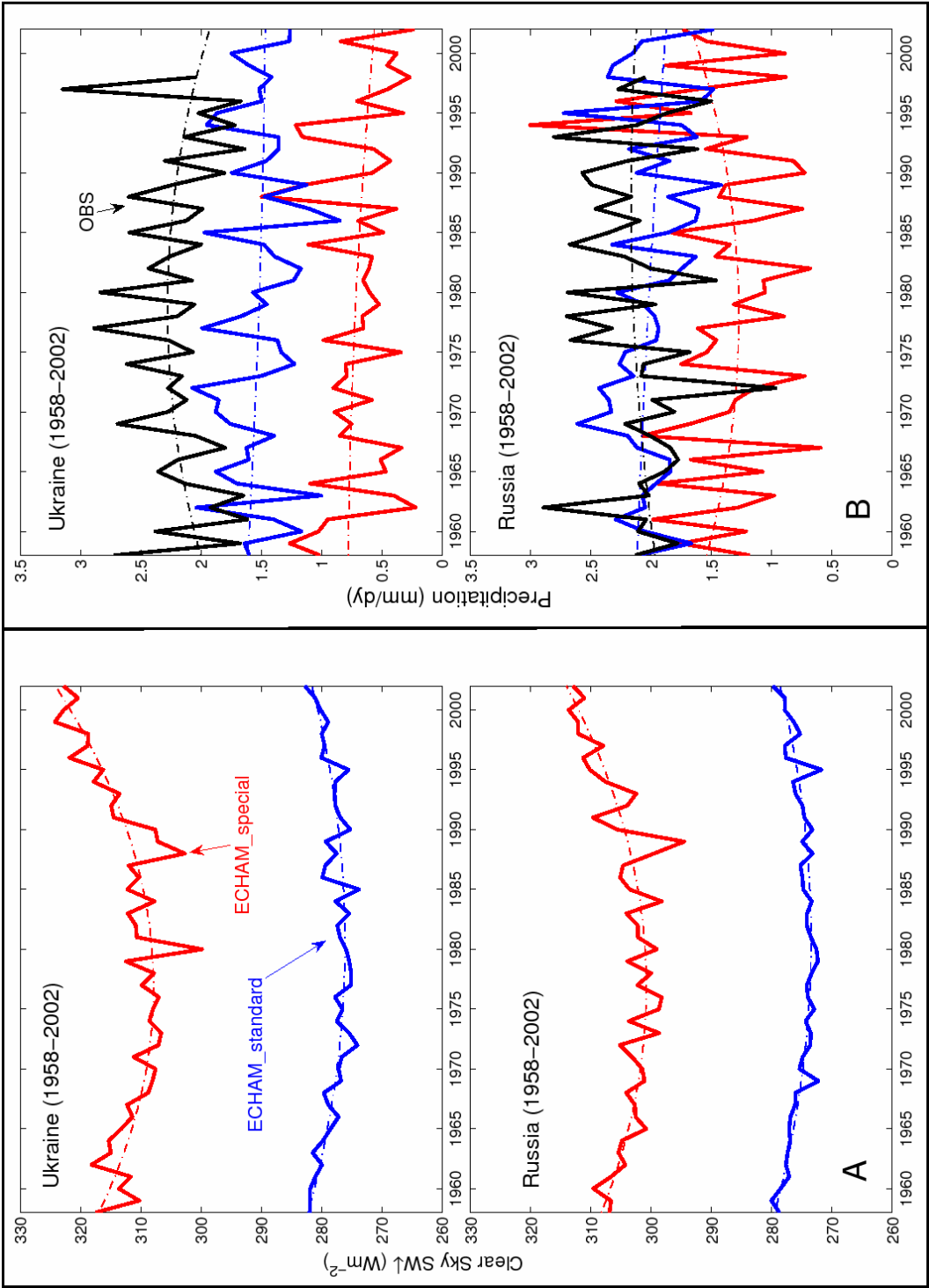
Figure 3.15. Same as Figure 10 but for clear sky downward shortwave radiation (A) and precipitation (B).
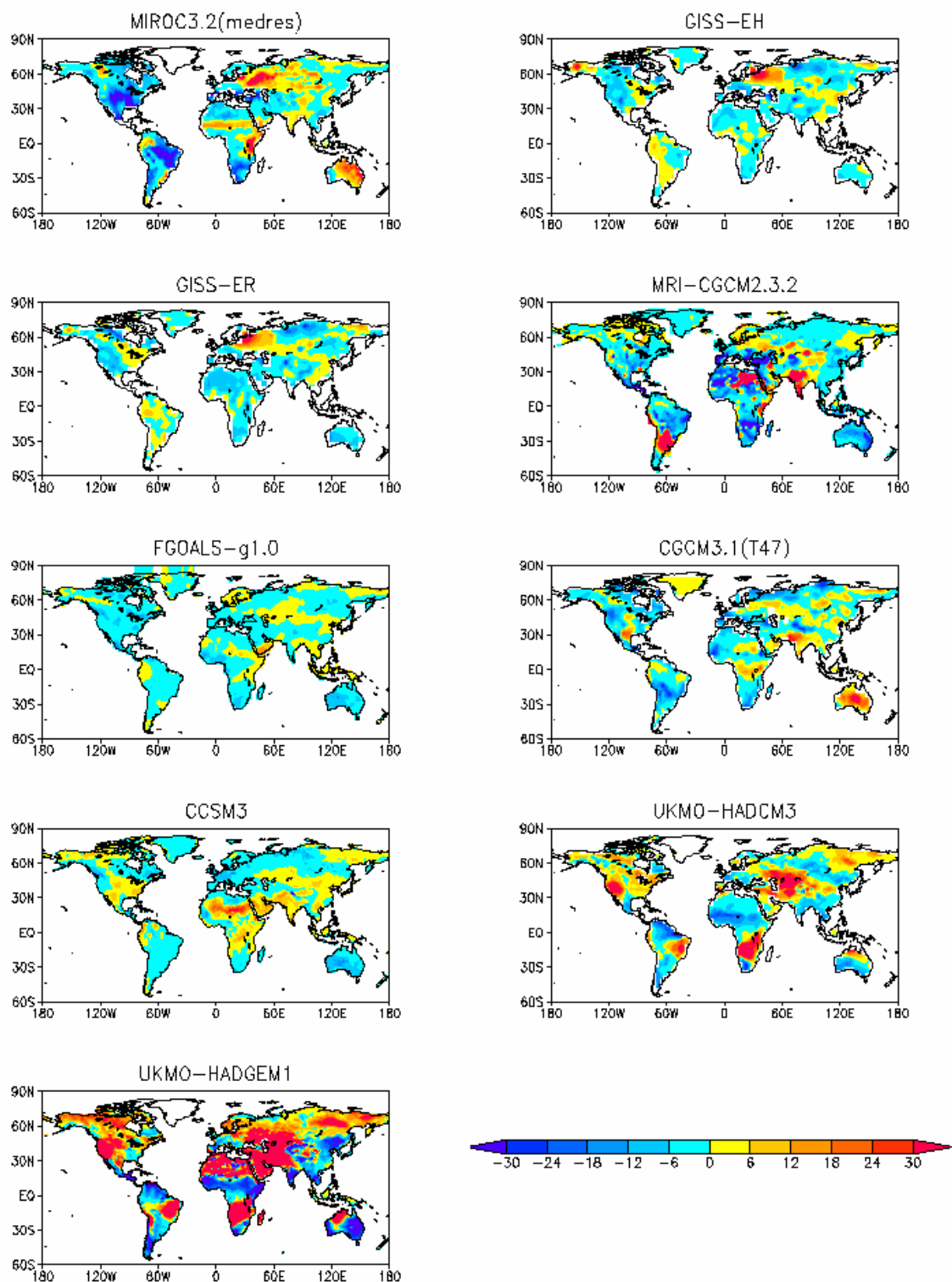
Figure 3.16. Relative change of soil moisture in summer (JJA) between 2060-2999 and 1960-1999 for models forced with the SRES A1B scenario, normalized by the average of 1960-1999. Units are in percent.
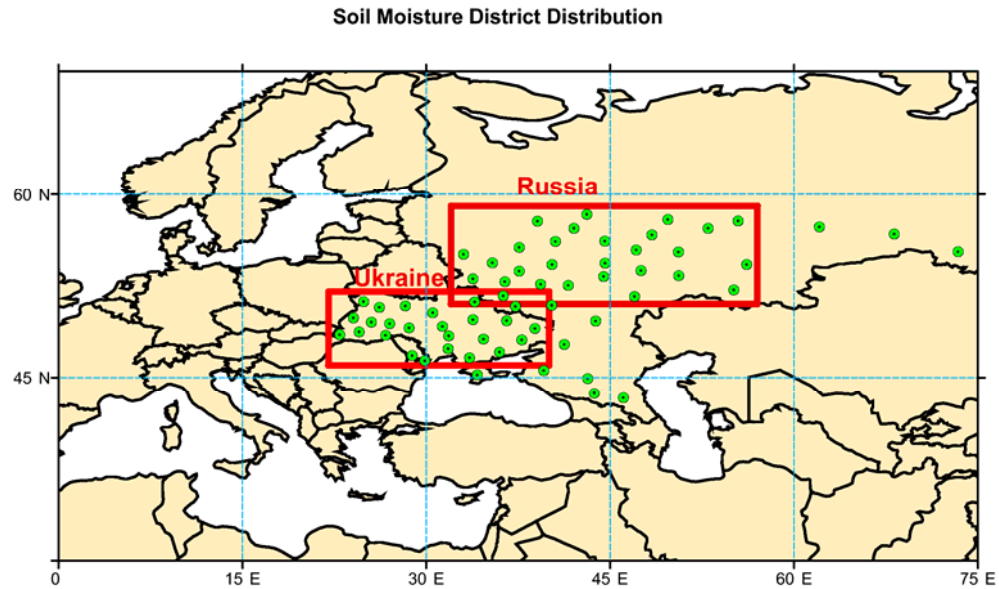
Figure 4.1. Soil moisture district distribution. Each district is an average of 3-6 stations. Red rectangles represent the modeling domain for Ukraine (22-40E, 46-52N) and Russia (32-57E, 51-59N). The observed soil moisture for Ukraine spans from 1958-2002 and covers 1958-1998 for Russia. The measurements are taken gravimetrically two to three times per month during growing seasons for top 0-20 cm and 0-100 cm.

Biogeophysics
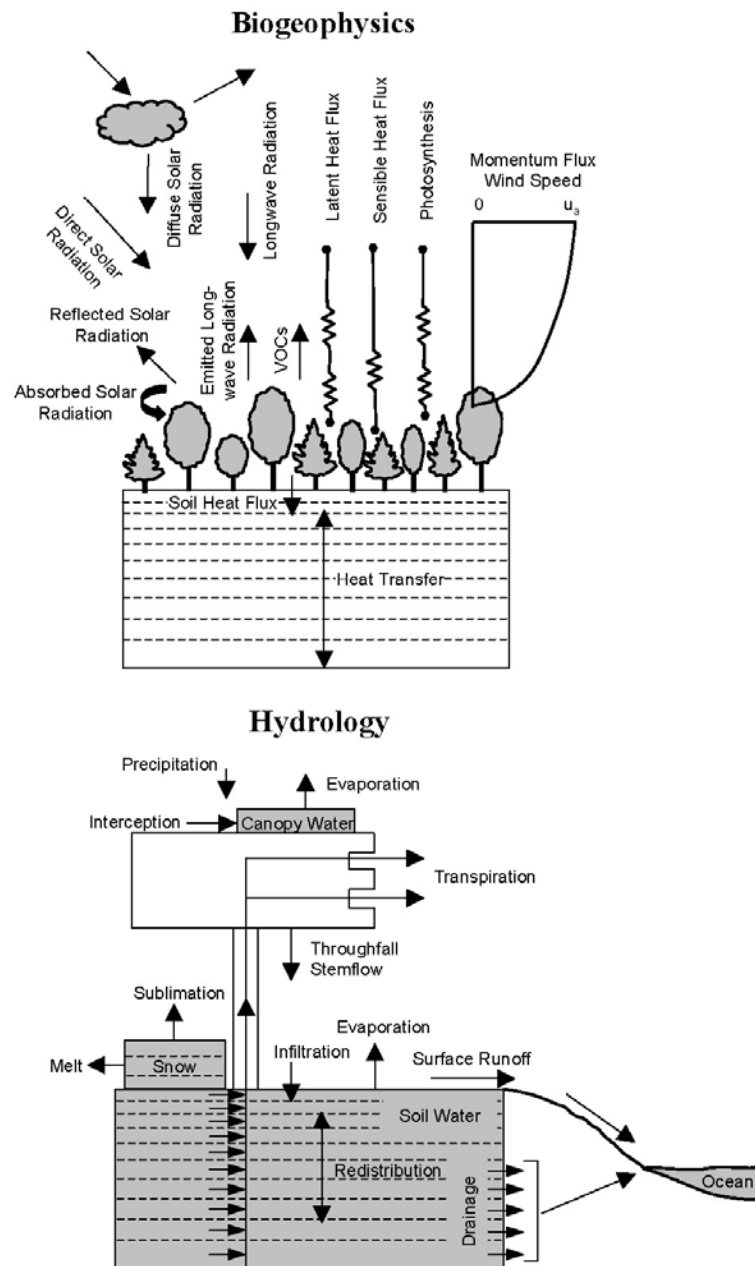
Hydrology

Figure 4.2. Land biogeophysical and hydrologic processes simulated by CLM (adapted from *Bonan et al.* [2002])
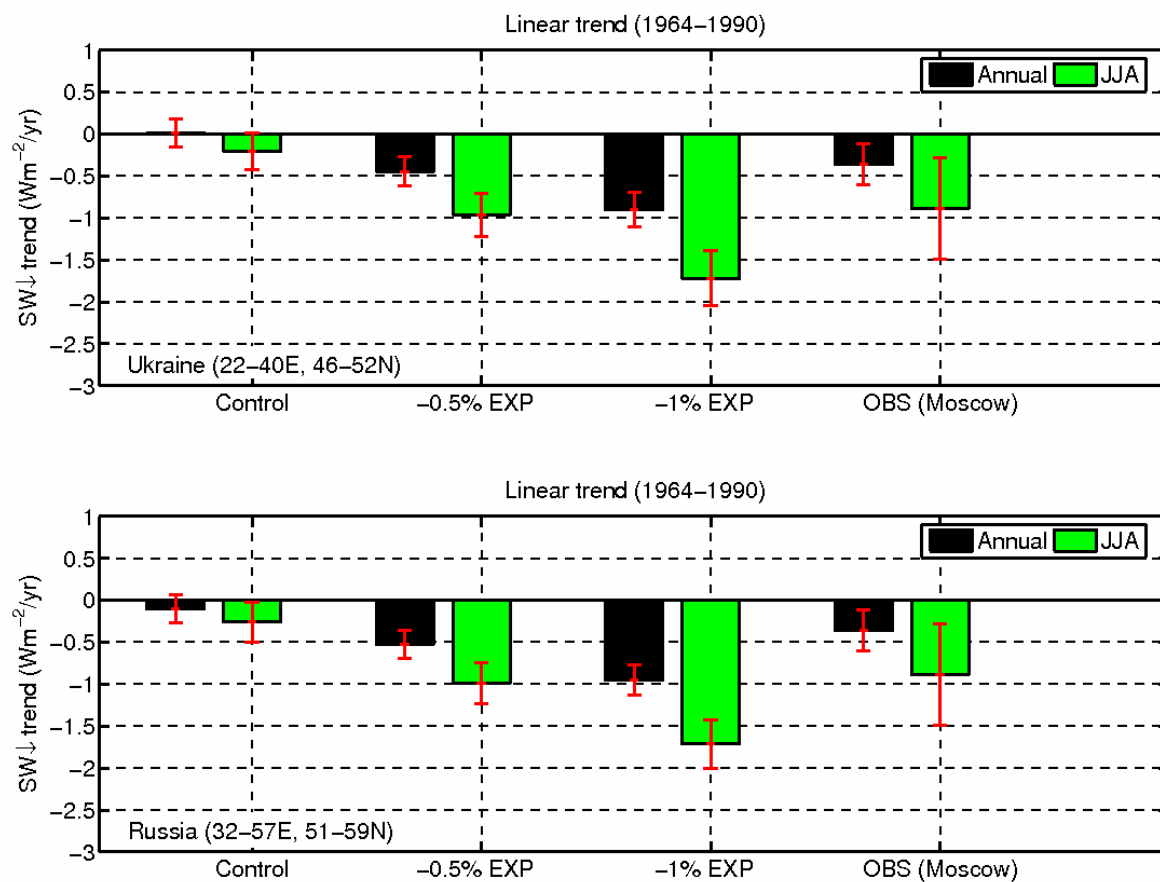
Figure 4.3. Estimated linear trends for shortwave radiation field for Ukraine (top panel) and Russia (bottom panel). Error bar represents the 95% confidence interval for the estimated trends based on linear regression. There is no significant decrease for the controls, neither NCEP/NCAR reanalysis. Also shown are the trends estimated from nearby station-based observations (Moscow).
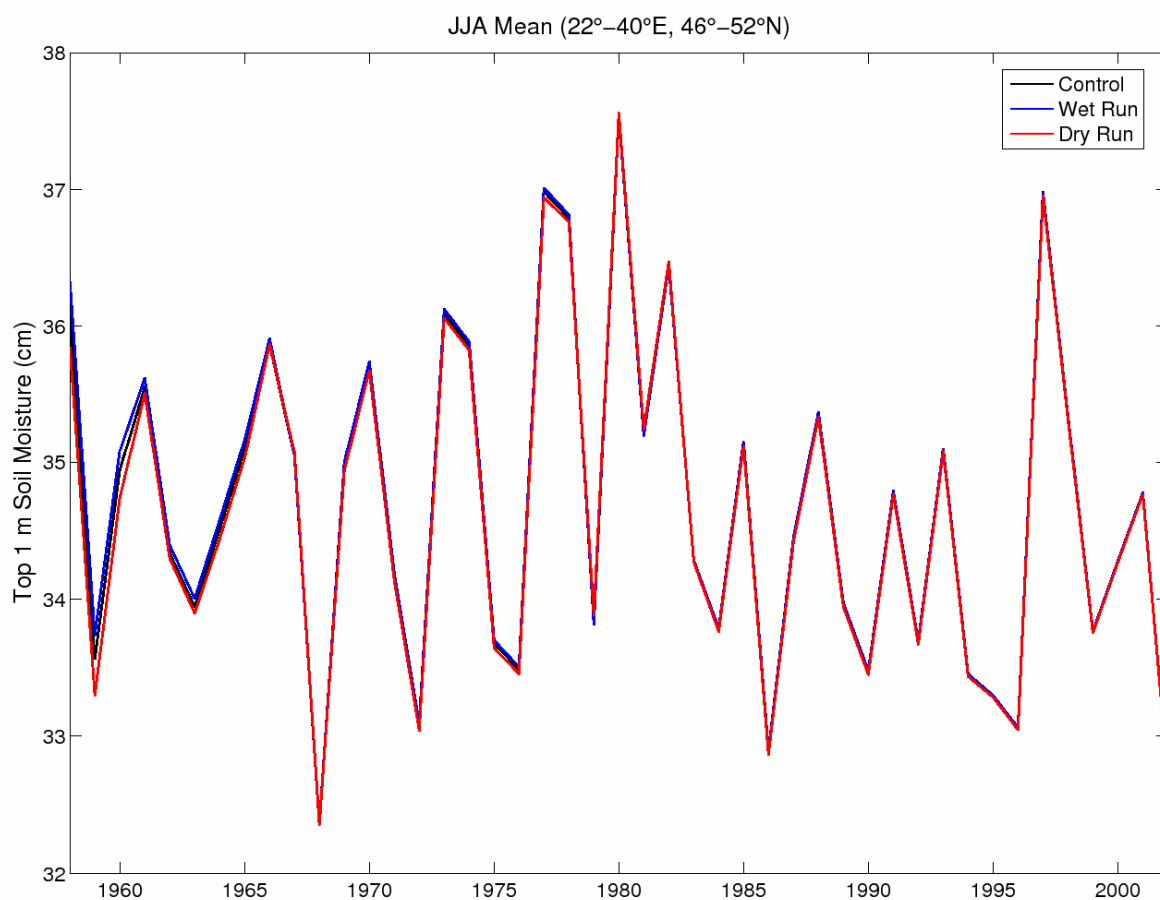
Figure 4.4. Top 1 m soil moisture from different spin-up conditions. The almost identical curves suggest that the simulated results are independent from the spin-up conditions.
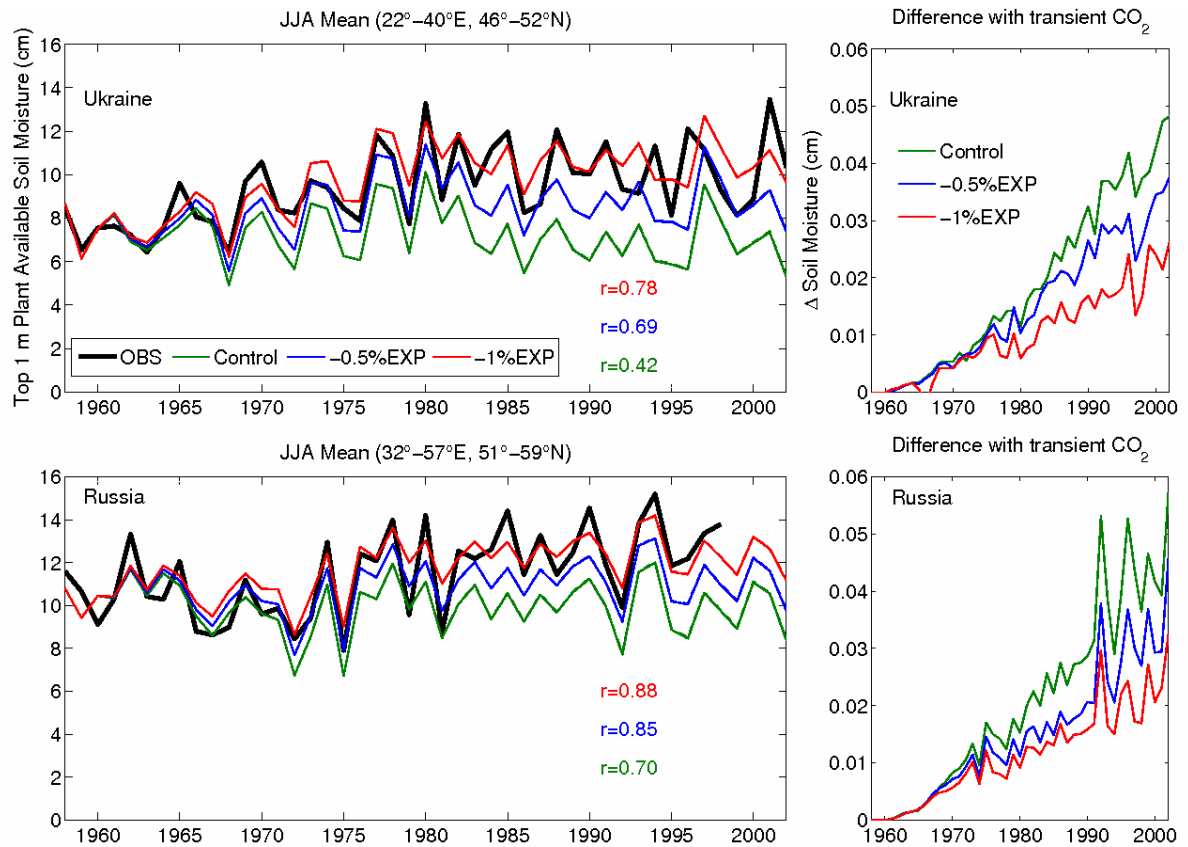
Figure 4.5. Observed and simulated JJA plant available soil moisture for 1958-2002. The model simulated soil moisture is adjusted to the mean of 1958-1960 observations. Top panels are for Ukraine box in Fig. 1 and bottom panels are for Russia box. For left panels, solid lines are simulations with constant CO_2 and dashed lines (barely visible) are simulations with time-dependent CO_2 increase. Also shown are the correlation coefficients between simulations and observations for the time period of the observations. Right panels show soil moisture increases due to elevated CO_2, plotted as the differences between the dashed and solid lines on an expanded vertical axis. The effects of solar dimming are large while the effects of increasing CO_2 on soil moisture are negligible in this model.
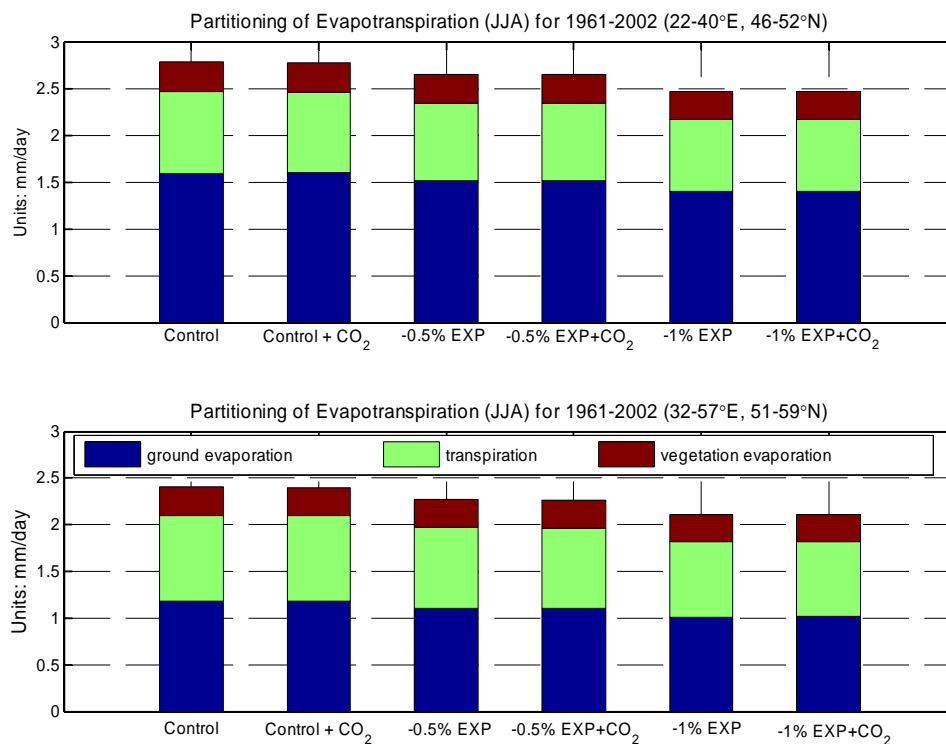
Figure 4.6. Partitioning of evapotranspiration (JJA) for 1961-2002. Ground evaporation accounts for about 50% of total evapotranspiration, followed by transpiration about 30%. CO2 induced reductions in evapotranspiration are negligible compared to the dimming effects.
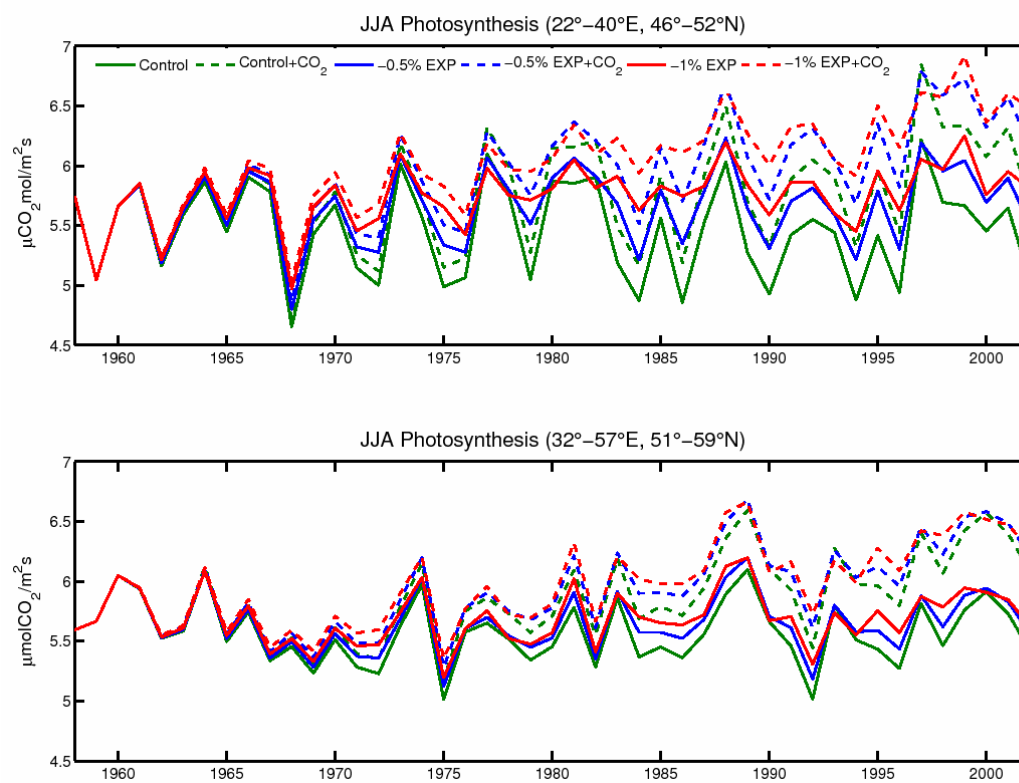
Figure 4.7. Same as Figure 4.5 but for photosynthesis.
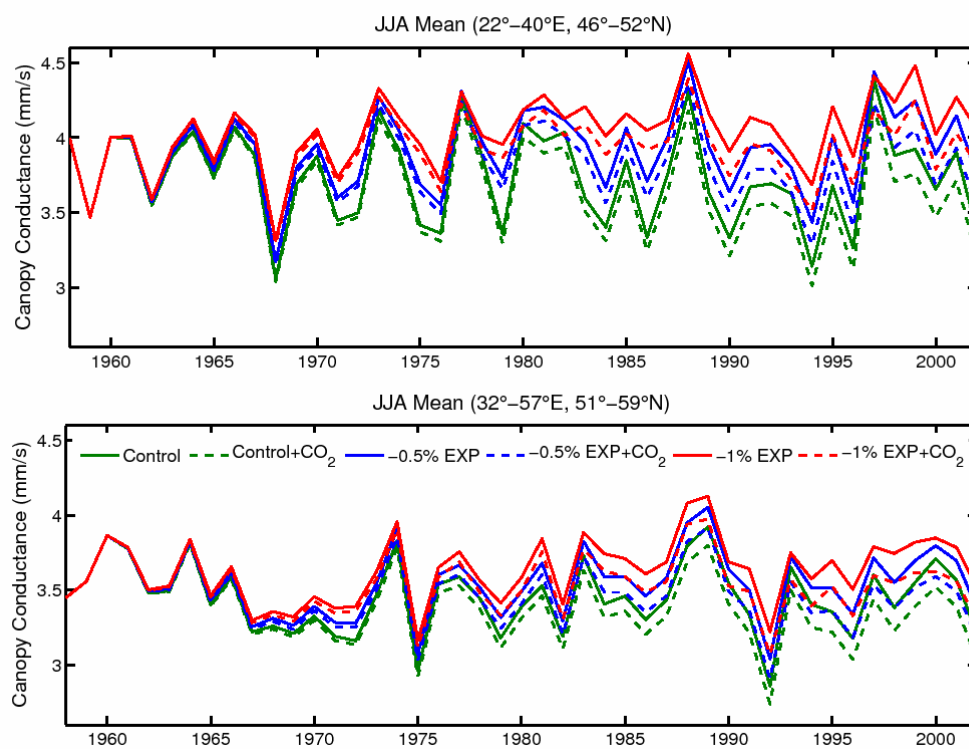
Figure 4.8. Same as Figure 4.5 but for canopy conductance.
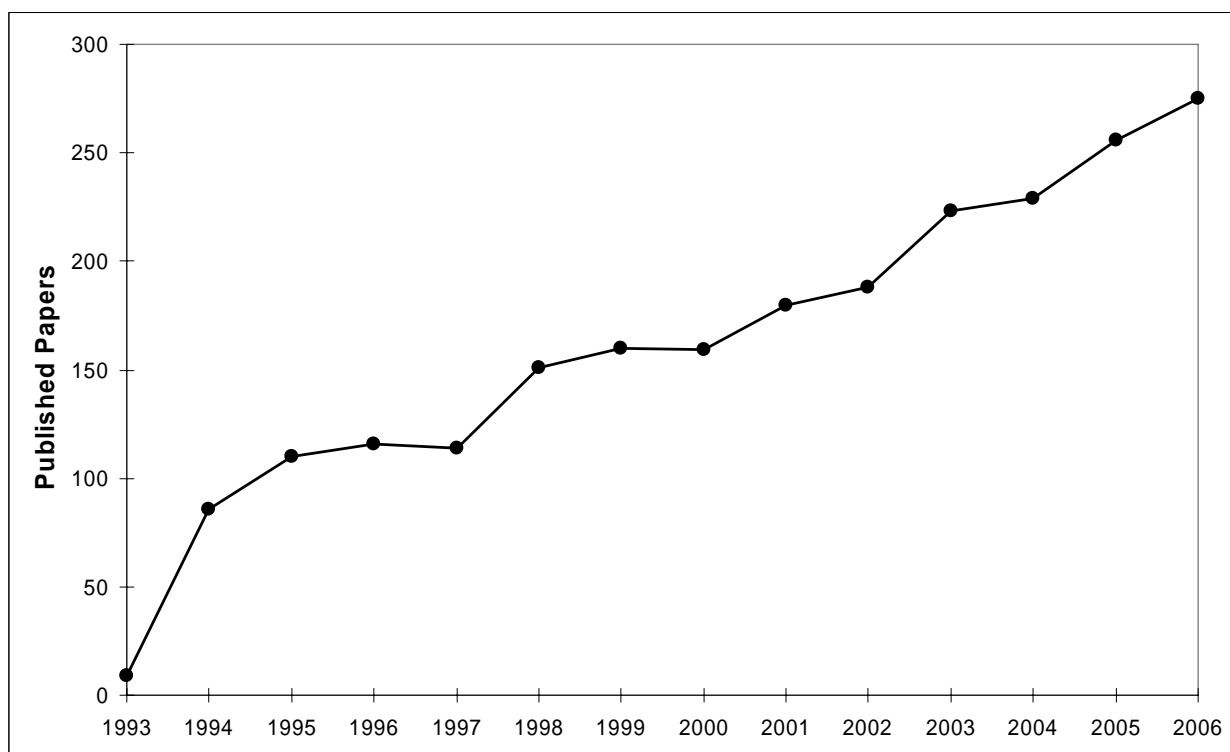
Figure 5.1. Papers published in the subject of soil moisture and climate. Y axis shows the number of papers published each year. The figure is created based on statistics from www.isiknowledge.com. The projected number for 2006 is based on the daily publication information as of July 21, 2006. Only papers published in science citation index journals are included.
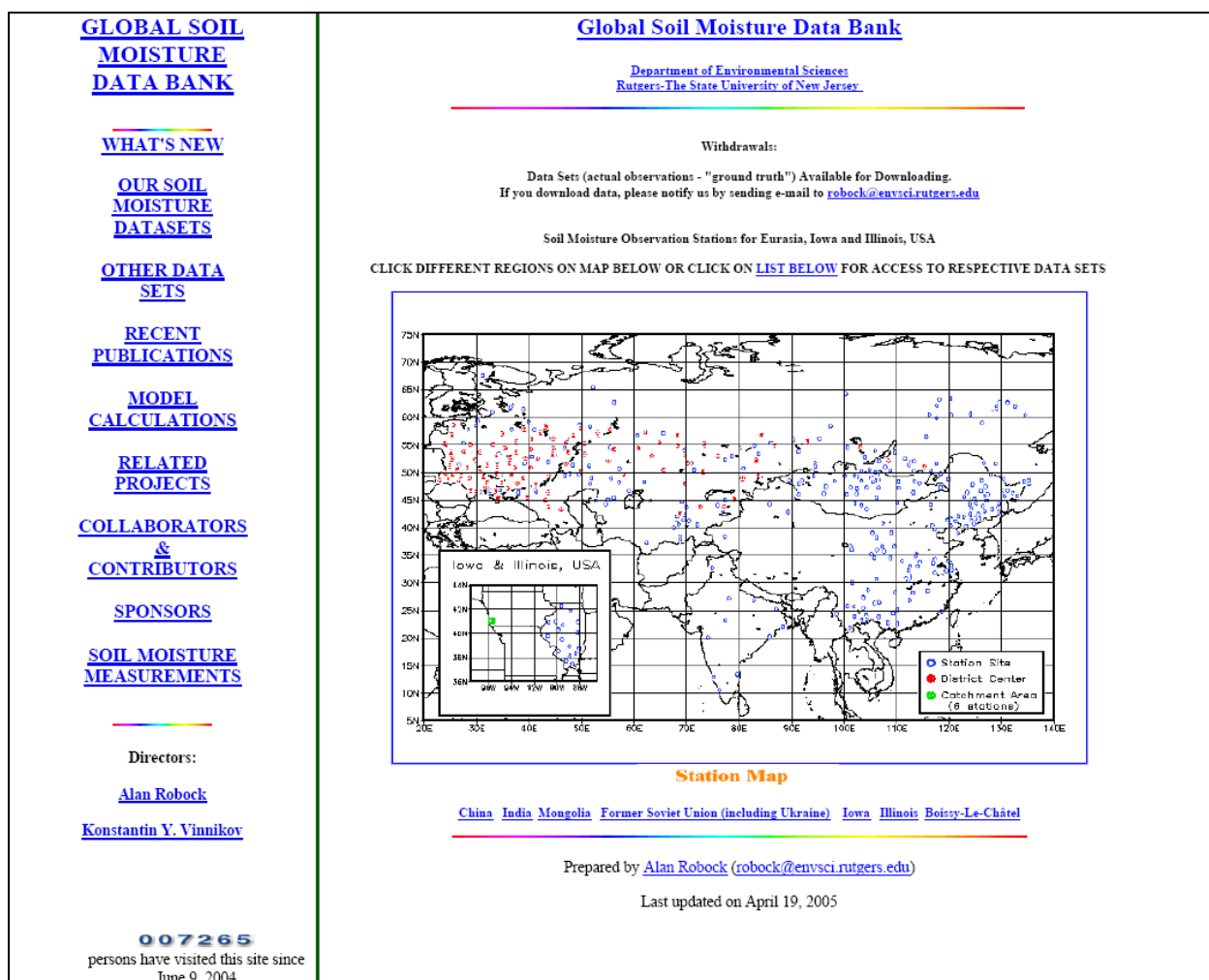
Figure 5.2. A snapshot of Global Soil Moisture Data Bank web interface.

Curriculum Vitae

Haibin Li

EDUCATION

1999   B.S., Environmental Sciences
Peking University, P. R. China

2002   M.S., Physical Geography (Hydrology and Water resources)
Chinese Academy of Sciences, P. R. China

2005   M.S., Environmental Sciences (Atmospheric Sciences Option)
Rutgers University

2007   Ph.D., Environmental Sciences (Atmospheric Sciences Option)
Rutgers University

RESEARCH EXPERIENCE

Graduate Research Assistant, Center for Environmental Prediction, Department of Environmental Sciences, Rutgers University, 2003-present

Graduate Research Assistant, Institute of Geographic Sciences and Natural Resources Research, Chinese Academy of Sciences, P. R. China, 1999-2002

PEER-REVIEWED PUBLICATIONS

Li, Haibin, Alan Robock, and Martin Wild, 2007: Evaluation of IPCC AR4 Soil Moisture Simulations for the Second Half of the 20th Century. *J. Geophys. Res. (in press)*

Robock, Alan and **Haibin Li,** 2006: Solar dimming and CO_2 effects on soil moisture trends, *Geophys. Res. Lett.*, *33*, L20708, doi:10.1029/2006GL027585.

Li, Haibin, Alan Robock, Suxia Liu, Xingguo Mo, and Pedro Viterbo, 2005: Evaluation of reanalysis soil moisture simulations using updated Chinese soil moisture observations. *J. Hydrometeorol., 6*, 180-193.

Lin, Zhonghui, Xingguo Mo, Hongjuan Li, and **Haibin Li**, 2002: Comparison of Three Spatial interpolation Methods for Climate Variables in China. *Acta Geographica Sinica*, *57 (1)*, 47-56.

Li, Lijuan, **Haibin Li**, and Juan Wang, 2002: Analysis on Hydrological and Water Quality Character and Their Spatial and Temporal Distribution in Lancangjiang River. *Scientia Geographica Sinica*, *22 (1)*, 49-56.

Li, Lijuan, **Haibin Li**, and Juan Wang, 2002: Study on the water requirements outside riverways in Haihe River Basin. *Haihe Water Resources*, *4*, 9-11.

Li, Lijuan, Juan Wang, and **Haibin Li**, 2002: Analysis of the spatial variability of rainfall in Wuding River Basin. *Geographical Research, 21 (4)*, 434-440.

Liu, Suxia, Xingguo Mo, **Haibin Li**, GongBing Peng, and Alan Robock, 2001:Spatial variation of Soil Moisture in China: Geostatistical Characterization. *Journal of the Meteorological Society of Japan, 79*, 555-574.

Li, Haibin, Zhonghui Lin, and Suxia Liu, 2001: Application of Kriging Technique in estimating soil moisture in China. *Geographical Research*, *20 (4)*, 446-452.